

University of Vermont

ScholarWorks @ UVM

UVM College of Arts and Sciences College
Honors Theses

Undergraduate Theses

2018

Iterative Exponential Growth through Manipulation of Sulfide Oxidation States

Tyler Jacob Jaynes

Follow this and additional works at: <https://scholarworks.uvm.edu/castheses>

Recommended Citation

Jaynes, Tyler Jacob, "Iterative Exponential Growth through Manipulation of Sulfide Oxidation States" (2018). *UVM College of Arts and Sciences College Honors Theses*. 53.
<https://scholarworks.uvm.edu/castheses/53>

This Undergraduate Thesis is brought to you for free and open access by the Undergraduate Theses at ScholarWorks @ UVM. It has been accepted for inclusion in UVM College of Arts and Sciences College Honors Theses by an authorized administrator of ScholarWorks @ UVM. For more information, please contact donna.omalley@uvm.edu.

Iterative Exponential Growth through Manipulation of Sulfide Oxidation States

A Dissertation Presented by

Tyler J. Jaynes

to The College of Arts and Sciences

of

The University of Vermont

In Partial Fulfillment of the Requirements for the Degree of Bachelor of
Science Specializing in Chemistry

April 26, 2018

Defense Date: May 3, 2018

Dissertation Examination Committee:

Dr. Severin T. Schneebeli, Advisor

Dr. Jay R. Silveira, Chair

Dr. Adam C. Whalley

Abstract:

Discovering methods to produce polymers of precisely defined length and sequence has been an age-old vexation for synthetic chemists. Classical polymerization techniques such as step growth and chain growth tend to produce inexact polymer sequences with broad ranges of molecular weights. Other techniques, such as solid state peptide synthesis, that allow construction of sequence defined oligomers, grow at a sluggish, linear rate. This research aims to explore a contemporary technique, iterative exponential growth (IEG), which utilizes a convergent/divergent strategy to grow oligomers of exact sequence and size in an exponential fashion. Specifically, we aim to use nucleophilic aromatic substitutions as a coupling strategy to drive the IEG. With our strategy, methyl sulfide substituents will be used to mask leaving groups, which can be accessed through oxidation. Six distinct evolutions of our approach have been studied, in pursuit of discovery of an ideal system which should couple in high yields.

Acknowledgements:

I would like to thank my parents for their endless support throughout this journey, as I follow in their footsteps and pursue a career in chemistry. In addition, I would like to thank Dr. Severin Schneebeil for his contagious enthusiasm in chemistry and science. This work was supported in part by the National Science Foundation (Grant CHE-1609137).

Table of Contents

Abstract.....	1
Acknowledgements.....	2
Table of Schemes.....	4
Table of Figures.....	5
Introduction.....	6
Experimental.....	11
Materials.....	11
Instrumentation.....	12
Procedures.....	12
Results and Discussion.....	22
1st Generation IEG Scheme with Methyl Protection.....	22
1st Generation IEG Scheme with TIPS Protection.....	24
1st Generation IEG Scheme with Benzyl Protection.....	25
2nd Generation IEG Scheme with Phenol Nucleophile.....	27
2nd Generation IEG Scheme with Short Chain Amino Nucleophile.....	28
2nd Generation IEG Scheme with Long Chain Amino Nucleophile.....	30
Conclusion.....	31
References.....	32

Table of Schemes

Scheme 1.....	8
Scheme 2.....	10
Scheme 3.....	11
Scheme 4.....	22
Scheme 5.....	23
Scheme 6.....	23
Scheme 7.....	23
Scheme 8.....	25
Scheme 9.....	25
Scheme 10.....	26
Scheme 11.....	26
Scheme 12.....	26
Scheme 13.....	27
Scheme 14.....	27
Scheme 15.....	28
Scheme 16.....	28
Scheme 17.....	29
Scheme 18.....	29
Scheme 19.....	30
Scheme 20.....	31

Table of Figures

Figure 1.....	34
Figure 2.....	35
Figure 3.....	36
Figure 4.....	37
Figure 5.....	38
Figure 6.....	39
Figure 7.....	40
Figure 8.....	41
Figure 9.....	42
Figure 10.....	43
Figure 11.....	44
Figure 12.....	45
Figure 13.....	46
Figure 14.....	47
Figure 15.....	48
Figure 16.....	49
Figure 17.....	50
Figure 18.....	51
Figure 19.....	52
Figure 20.....	53
Figure 21.....	54
Figure 22.....	55
Figure 23.....	56
Figure 24.....	57
Figure 25.....	58
Figure 26.....	59
Figure 27.....	60
Figure 28.....	61
Figure 29.....	62
Figure 30.....	63
Figure 31.....	64
Figure 32.....	65
Figure 33.....	66
Figure 34.....	67
Figure 35.....	68
Figure 36.....	69
Figure 37.....	70

Introduction:

To realize the full potential of polymers, it is imperative to gain full command over the properties and functionalities of the synthetic chains. Fundamental control can be gained only through strict dictation of MW, sequence and geometric character. Over millennia, nature has accessed the limitless capacity of polymers to procure nearly infinite biological applications by manipulation of these properties. The genetic information storage system for eukaryotes, DNA, contains just four base pairs, or monomers, which are organized in a shape- and sequence-defined fashion. However, these four distinct monomers are estimated to store a maximum of 455 billion gigabytes in a single gram of material¹. With this in mind, it is understandable why the pursuit of well-defined polymers has been a priority for polymer chemists.

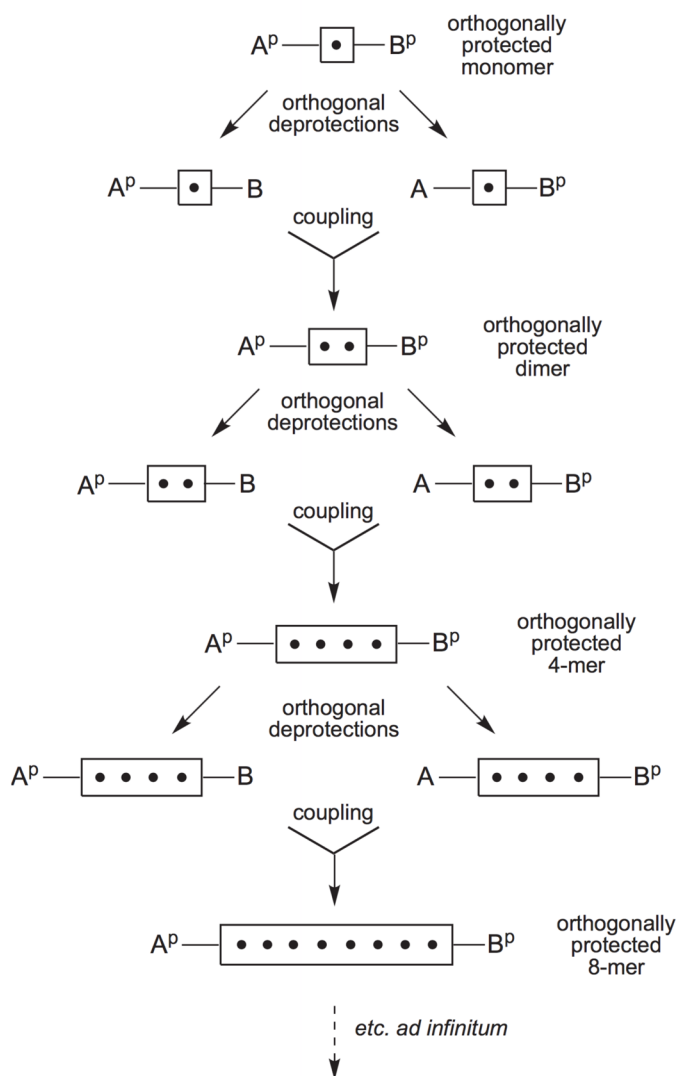
Classically, polymers have been synthesized in one of two ways, either through step growth polymerization or chain growth polymerization. The difference between step polymerization and chain polymerization can be attributed to the mechanism by which they are constructed. Step growth involves the stepwise addition of the functional groups of reactants such that any two growing chains can combine, i.e. monomer + monomer, monomer + dimer, dimer + dimer, dimer + trimer, etc. However, this generally leads to an overall sluggishness in the increase in MW of polymers. Oftentimes, step polymerization reactions are driven by some condensation product, where a small molecule is lost. It is imperative that the small molecule produced is removed to prevent unwanted side reactions to maximize the reaction conversion (P). In step polymerization, the reaction conversion, or the total percent of monomer consumed, is of utmost importance to generate long chains. For a polymerization with 1:1 stoichiometry of reactants, the average chain length (X_n) is directly related to P through the Carother's Equation², in which $X_n = 1/(1-P)$. This research aimed to create oligomers consisting of $X_n = 32$, or a 32-mer.

If this degree of polymerization was performed using step growth polymerization, it would require P to be 31/32 or 96.9% conversion of monomer. Therefore, step polymerization is limited to a select number of functional groups that engender a highly efficient reaction².

The arduous generation of chain length found in step polymerization can be avoided by utilizing chain polymerization². The chain growth mechanism requires an initiator that forms some reactive species, which then undergoes polymerization. This initiation can be cationic, anionic, or radical, and therefore tolerates a wider range of functional groups than step polymerization. Once a chain is initiated, it can then begin to grow through the addition of monomers. Unlike step polymerization, monomer can only react with a growing chain, it cannot react with other monomers, and growing chains can only react with monomer. This reactive specificity reduces the number of growing chains overall, and promotes a rapid increase in X_n , chain polymerizations produce high molecular weight species even if the reactions are stopped at just 1% conversion².

Both step and chain polymerizations yield a distribution of molecular weights. This results from the statistical variation observed while synthesizing polymers². This distribution of chain sizes can be classified by the polydispersity index (PDI) of a sample, which relates the weight average molecular weight (M_w) and the number average the molecular weight (M_n) through the equation $PDI = M_w/M_n$. As the M_w of a polymer can never be less than the M_n , the PDI is minimized at 1.0. A polymer with a PDI of 1.0 is referred to as monodisperse. However, one cannot generate monodisperse polymers using the standard step and chain growth mechanisms. In fact, the PDI 's of step and chain growth polymers are minimized at 2.0 and 1.5, respectively².

The aim of this research is to develop discrete monodisperse polymers, or oligomers, using a technique called iterative exponential growth (IEG)³. IEG can be described as a convergent/divergent approach, beginning with a dormant monomer that includes two distinct functionalities, which are orthogonally deprotected, affording two reactive species. These two reactive species are then combined in a chemoselective manner, resulting in a dormant dimer, which has identical protected



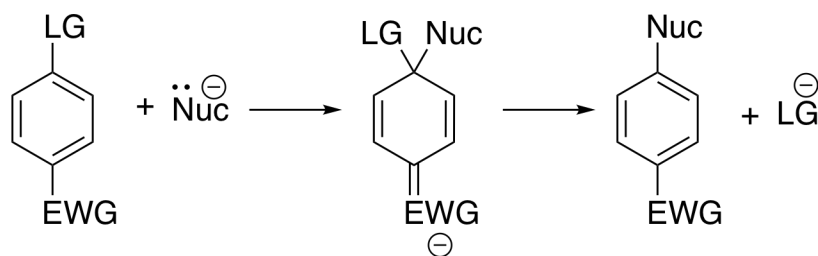
Scheme 1. Conceptual scheme of Iterative Exponential Growth (IEG)³.

functionalities to the dormant monomer. The dormant dimer can then undergo a deprotection/coupling cycle analogous to the monomer to generate a tetramer, etc. Once the desired size oligomer has been generated, the resulting macromolecule will contain a precisely defined sequence, and a chain length of 2^n , where n is the number of couplings that were performed on a given system. The IEG technique allows for rapid growth of size while maintaining a monodisperse system.

This system offers advantages over other methods of generating monodisperse oligomers such as solid-state peptide synthesis developed by Merrifield *et al.*⁴. Merrifield identified a method of producing specific peptide sequences by attaching a peptide covalently to a solid surface, and then adding subsequent peptide residues, one at a time, until the chain is completed, and the resulting polypeptide is cleaved from the solid support. Although this technique offers full sequential control, the chain length increases in a linear fashion, in contrast to IEG which increases chain length exponentially, while still supplying a monodisperse, sequence defined macromolecules.

The goal of this research aims to use IEG to fabricate novel oligoethers and oligoamines through nucleophilic aromatic substitutions (S_NAr). Oligoethers have been produced previously using IEG in previous studies. Hawker *et al.* produced polyethers by coupling phenoxide ions with a benzyl bromide derivative which proceeded through an S_N2 mechanism⁵. The group afforded oligomers with up to 32 monomers with a polydispersity index (PDI) of less than 1.01. This research will attempt to create uniform polymers similar in length and dispersity to the ones constructed by Hawker *et al.*

This research outlines a new strategy towards synthesizing oligomers of definite size by applying S_NAr as the coupling mechanism for IEG, which has not yet been reported in the literature. S_NAr involves the substitution of a leaving group by a nucleophile on an aromatic ring that is activated by an electron withdrawing group⁶. The mechanism begins (Scheme 2) through the addition of a nucleophile to the carbon atom at which the leaving group is tethered. This nucleophile adds electrons to the π^* orbital, subsequently breaking the π bond at the carbon atom and pushing electrons onto the electron withdrawing group, forming a tetrahedral



Scheme 2. Diagram outlining the Nucleophilic Aromatic Substitution (S_NAr) mechanism with an anionic nucleophile.

intermediate, known as a Meisenheimer complex⁶.

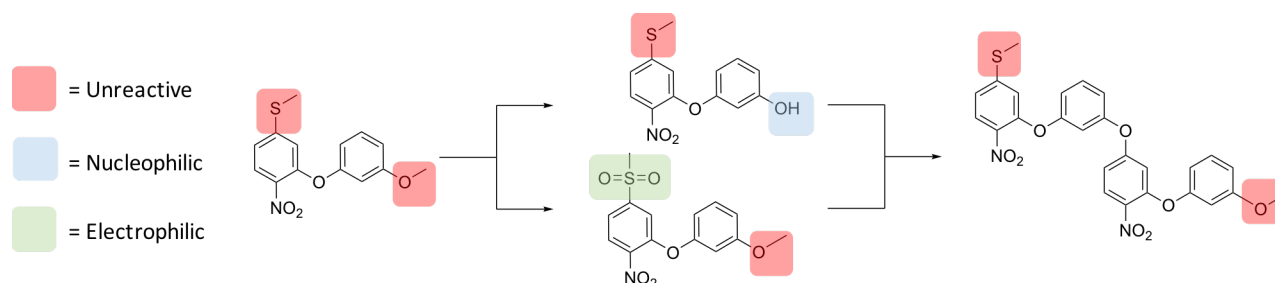
This first addition is recognized as the rate-limiting step due to the

dearomatization of the substrate, a kinetically slow process⁷. Halide atoms are common leaving groups for S_NAr , however, it should be noted that the activity of halides is reverse of that observed for S_N2 -type reactions. In S_N2 , the order of reactivity is $I > Br > Cl > F$, which is related to the carbon-halogen bond strength⁶. When studying S_NAr , it should be noted that fluorine shows increased reactivity compared to the remaining halides such that $F \gg Cl > Br > I$. The carbon-halogen bond strength is less important in S_NAr than in S_N2 , as this bond is not broken in the rate determining step. The increase in reactivity seen in fluorine is likely due to its highly electronegative nature⁶, as well as its minimal radius, which allows greater access to the π^* orbital of the aromatic ring.

To devise an IEG strategy that would utilize S_NAr reactivity, a monomer must have both nucleophilic and electrophilic functionality built-in. Each of these functionalities must be protected to prepare a dormant monomer. In this research, the nucleophile has been protected with methyl, benzyl, silyl, and *tert*-butyloxycarbonyl (boc) protecting groups⁸. The protection of the electrophilic portion requires more creativity, as aryl halides have limited protection strategies. In this case, methyl sulfone is employed as a leaving group, as it can be protected as an electron rich sulfide. This strategy of masking a sulfone to prevent S_NAr reactivity has been seen in the generation of macromolecules in the literature. Dehaen *et al.* successfully used

methyl sulfone as an S_NAr leaving group to functionalize pyrimidine substituents of macrocycles known as oxacalix[2]arene[2]-pyrimidines⁹. In addition, methyl sulfide was used by Zhao *et al.* to protect an electrophilic site in the generation of hyperbranched polyethers¹⁰. Yet, there has been no evidence of methyl sulfone as a leaving group in S_NAr to produce well-defined oligomers. This lack of research was the basis for this project.

The original blueprint for our work involved the generation of a dormant monomer centered around nitrobenzene, which was tethered to both the nucleophilic and electrophilic substituents (Scheme 3). The design has varied as different experimental challenges have become apparent.



Scheme 3. Original plan for IEG using S_NAr .

Experimental:

Materials. All commercially available starting materials were purchased from *Sigma Aldrich*, *Fisher Scientific*, *AK Scientific*, or *Oakwood Chemical*. All reagents were used as received without further purification. When needed, tetrahydrofuran (THF), diethyl ether, dichloromethane (DCM), dimethylformamide (DMF), and toluene were dried using a Glass Contour solvent purification system by SG Water USA, LLC. If necessary, air or moisture sensitive reactions were carried out under an inert atmosphere of nitrogen or argon.

Instrumentation. Removal of solvents was accomplished on a Büchi R-210 rotary evaporator and further concentration was done under a Fisher Scientific Maxima C-Plus vacuum line. Column chromatography was performed manually with Sorbent grade 60 silica with a mesh size between 230–400 using a forced flow of indicated solvents, or automatically with a Teledyne CombiFlash® chromatography system. Analytical thin layer chromatography (TLC) plates were purchased from Fisher Scientific (EMD Millipore TLC Silica Gel 60 F254). Visualization was accomplished by irradiation under UV light (254 nm). All ^1H NMR spectra were recorded at 298 K on a Varian Unity Inova 500 (500 MHz) or a Bruker ARX 500 (500 MHz) spectrometer. ^{13}C NMR spectra were recorded on a Bruker ARX 500 (125 MHz) spectrometer. Samples were dissolved in CDCl_3 . The spectra were referenced to the residual solvent peak (CDCl_3 : 7.26 ppm for ^1H NMR and 77.16 ppm for ^{13}C), or to tetramethylsilane (TMS) as the internal standard. Chemical shift values were recorded in parts per million (ppm). Data are reported as follows: chemical shift, multiplicity (s = singlet, d = doublet, t = triplet, q = quartet, m = multiplet), coupling constants (Hz), and number of protons. High resolution mass spectrometry data were obtained on Waters XEVO G2- XS QToF in positive ESI mode. All other mass spectrometry data was obtained on a Varian 2100T ion trap gas chromatograph-mass spectrometer in positive CI mode coupled with a Varian 3900 GC.

Procedures.

Synthesis of 1a. 3-Methoxyphenol (5.46 g, 44.03 mmol) and K_2CO_3 (7.83 g, 56.70 mmol) were dissolved in 50 mL of toluene. The solution was allowed to stir for 20 minutes, then, 2,4-difluoronitrobenzene (7.0 g, 44.03 mmol) was added. After stirring for 16 hours under N_2 , the mixture was cooled, and diluted with 50 mL of ethyl acetate before being washed with H_2O (1 x

50 mL), dried with anhydrous Na₂SO₄, and evaporated under reduced pressure to afford the crude product. The crude product obtained was purified by flash column chromatography (10% EtOAc in hexanes) to afford 10.50 g of **1a** in 90% yield.

Characterization Data for 1a. ¹H NMR (500 MHz, CDCl₃) δ 8.04 (dd, *J* = 9.1, 5.8 Hz, 1H, Ar–H), 7.31 (t, *J* = 8.1 Hz, 1H, Ar–H), 6.86 (ddd, *J* = 9.4, 7.1, 2.6 Hz, 1H, Ar–H), 6.81 – 6.77 (m, 1H, Ar–H), 6.70 – 6.62 (m, 3H, Ar–H), 3.81 (s, 3H, O–CH₃); ¹³C NMR (126 MHz, CDCl₃) δ 166.51, 164.46, 161.44, 155.82, 153.43, 130.87, 128.18, 111.95, 111.37, 110.09, 107.25, 106.14, 77.16, 55.66. (153.43, 110.09, and 107.25 are split by fluorine coupling); ¹⁹F NMR (471 MHz, CDCl₃) δ -99.06. MS (CI) calcd. for C₁₃H₁₀FNO₄: *m z*⁻¹ = 264.0 [M + H]⁺; Found 264.0.

Synthesis of 2. 1a (0.663 g, 2.52 mmol) and K₂CO₃ (0.695 g, 5.04 mmol) were dissolved in 10 mL of DMF. Then, sodium methanethiolate was added (0.544 g, 10.08 mmol). After stirring for 2 hours at room temperature, the solution was diluted with 25 mL of ethyl acetate, washed with H₂O (3 x 25 mL), brine (1 x 25 mL), dried with anhydrous Na₂SO₄, and evaporated under reduced pressure to afford 0.733 g of **2** in 100% yield.

Characterization Data for 2. ¹H NMR (500 MHz, CDCl₃) δ 7.97 (d, *J* = 8.7 Hz, 1H, Ar–H), 7.26 (t, 1H, Ar–H), 6.98 (dd, *J* = 8.7, 2.0 Hz, 1H, Ar–H), 6.81 (d, *J* = 2.0 Hz, 1H, Ar–H), 6.73 (dt, *J* = 8.4, 1.3 Hz, 1H, Ar–H), 6.62 – 6.57 (m, 2H, Ar–H), 3.80 (s, 3H, O–CH₃), 2.43 (s, 3H, S–CH₃). MS (CI) calcd. for C₁₄H₁₃NO₄S: *m z*⁻¹ = 292.0 [M + H]⁺; Found 292.0.

Synthesis of 2a. Methyl sulfide **2** (0.08 g, 0.28 mmol) and mCPBA (0.19 g, 0.770 mmol) were dissolved in 5 mL of ethyl acetate. After stirring for 16 hours under N₂ at room temperature, the solution was diluted with 15 mL of ethyl acetate, washed with saturated NaHCO₃ (1 x 15 mL), saturated Na₂SO₄ (1 x 15 mL), brine (1 x 15 mL), dried with anhydrous Na₂SO₄, and evaporated

under reduced pressure to afford the crude product. The crude product obtained was purified by flash column chromatography (10% EtOAc in hexanes) to afford 0.077 g of **2a** in 85% yield.

Synthesis of 3a. Resorcinol (3.0 g, 27.25 mmol), Imidazole (2.22 g, 32.65 mmol), and TIPS-Cl (5.23 g, 27.25 mmol) were dissolved in 50 mL of anhydrous THF. After stirring for 5 hours at 80°C, the mixture was quenched with 50 mL of 0.5 M HCl and washed with H₂O (1 x 50 mL). The aqueous layers were then combined and extracted from with DCM (3 x 50 mL), dried with MgSO₄, and concentrated to afford the crude product. The crude product was purified by flash column chromatography (0 to 20% EtOAc in hexanes) to afford 3.19 g of **3a** in 47% yield.

Characterization Data for 3a. ¹H NMR (500 MHz, CDCl₃) δ 7.05 (t, *J* = 8.0 Hz, 1H, Ar-H), 6.47 (dd, *J* = 8.2, 2.2 Hz, 1H, Ar-H), 6.43 – 6.38 (m, 2H, Ar-H), 4.67 (s, *J* = 6.2 Hz, 1H, Ar-OH), 1.29 – 1.20 (m, 3H, Si-CH), 1.10 (d, *J* = 7.5 Hz, 18H, C-CH₃).

Synthesis of 4. Siloxyphenol **3a** (0.41 g, 1.63 mmol) and K₂CO₃ (0.292 g, 2.12 mmol) were dissolved in 5 mL of toluene. The solution was allowed to stir for 20 minutes, then, 2,4-difluoronitrobenzene (0.26 g, 1.63 mmol) was added. After stirring at 60°C for 18 hours, the mixture was cooled, and diluted with 15 mL of ethyl acetate before being washed with H₂O (1 x 25 mL), dried with anhydrous Na₂SO₄, and evaporated under reduced pressure to afford the crude product. The crude product was purified by flash column chromatography (0 to 5% EtOAc in hexanes) to afford 0.50 g of **4** in 76% yield.

Characterization Data for 4. ¹H NMR (500 MHz, CDCl₃) δ 8.04 (dd, *J* = 9.1, 5.8 Hz, 1H, Ar-H), 7.26 (t, 1H, Ar-H), 6.84 (ddd, *J* = 9.4, 7.1, 2.6 Hz, 1H, Ar-H), 6.78 (dd, *J* = 8.2, 2.2 Hz, 1H, Ar-H), 6.69 – 6.59 (m, 3H, Ar-H), 1.25 (h, *J* = 7.3 Hz, 3H, Si-CH), 1.09 (d, *J* = 7.5 Hz, 18H, C-CH₃). MS (CI) calcd. for C₂₁H₂₈FNO₄Si: *m z*⁻¹ = 406.2 [M+H]⁺; found 406.2.

Synthesis of 5b. **4** (0.50 g, 1.23 mmol), K₂CO₃ (0.25 g, 1.81 mmol), and sodium methanethiolate (0.26 g, 4.90 mmol) were dissolved in 8 mL of DMF. After stirring for 2 hours at room temperature, the solution was diluted with 25 mL of ethyl acetate, washed with H₂O (3 x 25 mL), brine (1 x 25 mL), dried with anhydrous Na₂SO₄, and evaporated under reduced pressure to afford the crude product. The crude product was purified by flash column chromatography (15 to 45% EtOAc in hexanes) to afford 0.337 g of **5b** in 100% yield.

Characterization Data for 5b. ¹H NMR (500 MHz, CDCl₃) δ 7.97 (d, *J* = 8.7 Hz, 1H, Ar-H), 7.22 (t, *J* = 8.2 Hz, 1H, Ar-H), 7.00 (dd, *J* = 8.7, 2.0 Hz, 1H, Ar-H), 6.83 (d, *J* = 2.0 Hz, 1H, Ar-H), 6.62 (dddd, *J* = 24.5, 8.2, 2.4, 0.8 Hz, 2H, Ar-H), 6.53 (t, *J* = 2.4 Hz, 1H, Ar-H), 4.88 (s, 1H, Ar-OH), 2.45 (s, 3H, S-CH₃).

Synthesis of 7. 3-(Benzyloxy)phenol (0.69 g, 3.45 mmol) and K₂CO₃ (0.953 g, 6.9 mmol) were dissolved in 10 mL of toluene. The solution was allowed to stir for 20 minutes, then, 2,4-difluoronitrobenzene (0.494 g, 3.10 mmol) was added. After stirring at 60°C for 18 hours, the mixture was cooled, and diluted with 50 mL of ethyl acetate before being washed with H₂O (1 x 50 mL), dried with anhydrous Na₂SO₄, and evaporated under reduced pressure to afford the crude product. The crude product was purified by flash column chromatography (0 to 5% EtOAc in hexanes) to afford 0.95 g of **7** in 90% yield.

Characterization Data for 7. ¹H NMR (500 MHz, CDCl₃) δ 8.04 (dd, *J* = 9.1, 5.8 Hz, 1H, Ar-H), 7.48 – 7.29 (m, 6H, Ar-H), 6.91 – 6.83 (m, 2H, Ar-H), 6.75 – 6.64 (m, 3H, Ar-H), 5.06 (s, 2H, Ar-CH₂); ¹³C NMR (126 MHz, CDCl₃) δ 166.50, 164.45, 160.51, 155.88, 153.41, 136.45, 130.93, 128.80, 128.33, 128.18, 127.67, 112.23, 110.18, 107.21, 107.01, 77.16, 70.46. (153.41, 128.18, 110.18, 107.21 are split by fluorine coupling).

Synthesis of 8. Electrophile **7** (3.24 g, 9.55 mmol), K₂CO₃ (2.6 g, 19.1 mmol) and sodium methanethiolate (3.1 g, 57.3 mmol) were dissolved in 25 mL of DMF. After stirring for 2 hours at room temperature, the solution was diluted with 50 mL of ethyl acetate, washed with H₂O (3 x 50 mL), brine (1 x 50 mL), dried with anhydrous Na₂SO₄, and evaporated under reduced pressure to afford 3.47 g of **8** in 99% yield.

Characterization Data for 8. ¹H NMR (500 MHz, CDCl₃) δ 7.97 (d, *J* = 8.7 Hz, 1H, Ar-H), 7.43 – 7.31 (m, 5H, Ar-H), 7.26 (t, 1H, Ar-H), 6.99 (dd, *J* = 8.8, 2.0 Hz, 1H, Ar-H), 6.80 (tt, *J* = 4.0, 2.1 Hz, 2H, Ar-H), 6.66 (t, *J* = 2.3 Hz, 1H, Ar-H), 6.63 (ddd, *J* = 8.1, 2.3, 0.8 Hz, 1H, Ar-H), 5.05 (s, 2H, Ar-CH₂), 2.43 (s, 3H, S-CH₃); ¹³C NMR (126 MHz, CDCl₃) δ 160.40, 157.01, 151.05, 148.91, 136.58, 130.64, 128.77, 128.28, 127.71, 126.55, 119.73, 116.99, 111.34, 111.08, 106.08, 77.16, 70.40, 15.01.

Synthesis of 8b. Sulfide **8** (0.50 g, 1.36 mmol) was dissolved in 20 mL of anhydrous DCM. The mixture was then cooled to -78°C, and placed under N₂. 1M BCl₃ (7.5 mL, 7.5 mmol) was then added dropwise via syringe into the stirring solution. After 1 hour, the mixture was quenched by adding 2 mL of MeOH. Product was deprotonated and extracted from the organic layer with 0.5 NaOH (5 x 50 mL). The aqueous layer was then neutralized with 1M HCl until the pH reached 1. Product was then extracted using Et₂O, dried with Na₂SO₄, and evaporated under reduced pressure to afford the crude product. The crude product was purified by flash column chromatography (0 to 5% EtOAc in hexanes) to afford 0.25g of **8b** in 67% yield.

Characterization Data for 8b. ¹H NMR (500 MHz, CDCl₃) δ 7.96 (d, *J* = 8.7 Hz, 1H, Ar-H), 7.20 (t, *J* = 8.1 Hz, 1H, Ar-H), 6.99 (dd, *J* = 8.7, 2.0 Hz, 1H, Ar-H), 6.81 (d, *J* = 2.0 Hz, 1H, Ar-H),

6.65 (ddd, $J = 8.2, 2.4, 0.8$ Hz, 1H, Ar–H), 6.58 (ddd, $J = 8.2, 2.4, 1.0$ Hz, 1H, Ar–H), 6.53 (t, $J = 2.3$ Hz, 1H, Ar–H), 5.41 (s, 1H, Ar–OH), 2.43 (s, 3H, S–CH₃).

Synthesis of 9. Phenol **8b** (0.03 g, 0.108 mmol), electrophile **7** (0.036, 0.108 mmol), and K₂CO₃ (0.04 g, 0.324 mmol) were dissolved in 3 mL of DMF. After stirring for 18 hours at 60°C, the solution was diluted with 25 mL of Et₂O, washed with H₂O (3 x 25 mL), brine (1 x 25 mL), dried with anhydrous Na₂SO₄, and evaporated under reduced pressure to afford the crude product. The crude product was purified by flash column chromatography (20% EtOAc in hexanes) to afford 0.0525 g of **9** in 81% yield.

Characterization Data for 9. ¹H NMR (500 MHz, CDCl₃) δ 8.03 (d, $J = 9.1$ Hz, 1H, Ar–H), 7.98 (d, $J = 8.7$ Hz, 1H, Ar–H), 7.43 – 7.30 (m, 6H, Ar–H), 7.28 (t, 1H, Ar–H), 7.04 (dd, $J = 8.7, 2.0$ Hz, 1H, Ar–H), 6.85 (d, $J = 2.0$ Hz, 1H, Ar–H), 6.85 – 6.79 (m, 3H, Ar–H), 6.71 – 6.67 (m, 3H, Ar–H), 6.65 (dd, $J = 2.3, 0.8$ Hz, 1H, Ar–H), 6.63 (t, $J = 2.3$ Hz, 1H, Ar–H), 5.04 (s, 2H, Ar–CH₂), 2.46 (s, 3H, S–CH₃). MS (ESI) calcd. for C₃₂H₂₄N₂O₈S: m/z = 597.13 [M+H]⁺; found 597.3.

Synthesis of 9a. Methyl sulfide dimer **9** (0.110 g, 0.18 mmol) and mCPBA (0.18 g, 0.72 mmol) were dissolved in 5 mL of ethyl acetate. After stirring for 16 hours under N₂ at room temperature, the solution was diluted with 15 mL of ethyl acetate, washed with saturated NaHCO₃ (1 x 15 mL), saturated Na₂SO₄ (1 x 15 mL), brine (1 x 15 mL), dried with anhydrous Na₂SO₄, and evaporated under reduced pressure to afford the crude product. The crude product obtained was purified by flash column chromatography (10% EtOAc in hexanes) to afford 0.113 g of **9a** in 100% yield.

Characterization Data for 9a. ¹H NMR (500 MHz, CDCl₃) δ 8.04 (t, $J = 9.2$ Hz, 2H, Ar–H), 7.77 (dd, $J = 8.4, 1.7$ Hz, 1H, Ar–H), 7.61 (d, $J = 1.7$ Hz, 1H, Ar–H), 7.45 – 7.27 (m, 7H, Ar–H), 6.92

(ddd, $J = 15.5, 8.2, 2.3$ Hz, 2H, Ar-H), 6.83 – 6.77 (m, 2H, Ar-H), 6.73 – 6.61 (m, 4H, Ar-H), 5.04 (s, 2H, Ar-CH₂), 3.04 (s, 3H, S-CH₃).

Synthesis of 9b. Methyl sulfide dimer **9** (0.50 g, 0.84 mmol) was dissolved in 2 mL of anhydrous DCM. The mixture was then cooled to -78°C, and placed under N₂. 1 M BCl₃ (0.33 mL, 0.33 mmol) was then added dropwise via syringe into the stirring solution. After 1 hour, the mixture was quenched by adding 0.5 mL of MeOH. Product was deprotonated and extracted from the organic layer with 0.5 NaOH (5 x 25 mL). The aqueous layer was then neutralized with 1M HCl until the pH reached 1. Product was then extracted using Et₂O, dried with Na₂SO₄, and evaporated under reduced pressure to afford the crude product. The crude product was purified by flash column chromatography (0 to 5% EtOAc in hexanes) to afford 0.012 g of **9b** in 28% yield.

Characterization Data for 9b. : ¹H NMR (500 MHz, CDCl₃) δ 7.98 (d, $J = 9.1$ Hz, 1H, Ar-H), 7.94 (d, $J = 8.7$ Hz, 1H, Ar-H), 7.32 (t, $J = 8.2$ Hz, 1H, Ar-H), 7.16 (t, $J = 8.1$ Hz, 1H, Ar-H), 7.02 (dd, $J = 8.8, 2.1$ Hz, 1H, Ar-H), 6.84 (d, $J = 2.1$ Hz, 1H, Ar-H), 6.80 (dd, $J = 8.4, 2.3$ Hz, 2H, Ar-H), 6.69 – 6.63 (m, 3H, Ar-H), 6.60 – 6.53 (m, 3H, Ar-H), 6.25 – 6.17 (m, 1H), 2.43 (s, 3H, S-CH₃).

Synthesis of 11. 3-(Benzyloxy)phenol (0.625 g, 3.125 mmol), 4-chloro-6-(methylthio)-pyrimidine (0.500 g, 3.125 mmol), and K₂CO₃ (0.813 g, 6.25 mmol) were dissolved in 50 mL of DMF. After stirring at 60°C for 18 hours, the mixture was cooled, and diluted with 50 mL of ethyl acetate before being washed with 1 M HCl (1 x 50 mL), H₂O (1 x 50 mL), dried with anhydrous Na₂SO₄, and evaporated under reduced pressure to afford the crude product. The crude product was purified by flash column chromatography (0 to 5% EtOAc in hexanes) to afford 0.4474 g of **11** in 44% yield.

Characterization Data for 11. ^1H NMR (500 MHz, CDCl_3) δ 7.98 (d, J = 9.1 Hz, 1H, Ar-H), 7.94 (d, J = 8.7 Hz, 1H, Ar-H), 7.32 (t, J = 8.2 Hz, 1H, Ar-H), 7.16 (t, J = 8.1 Hz, 1H, Ar-H), 7.02 (dd, J = 8.8, 2.1 Hz, 1H, Ar-H), 6.84 (d, J = 2.1 Hz, 1H, Ar-H), 6.80 (dd, J = 8.4, 2.3 Hz, 2H, Ar-H), 6.69 – 6.63 (m, 3H, Ar-H), 6.60 – 6.53 (m, 3H, Ar-H), 6.25 – 6.17 (m, 1H, Ar-H), 5.07 (s, 2H, Ar-CH₂) 2.43 (s, 3H, S-CH₃); ^{13}C NMR (126 MHz, CDCl_3) δ 172.57, 168.58, 160.10, 157.96, 153.40, 136.55, 130.39, 128.70, 128.19, 127.62, 113.96, 112.52, 108.55, 103.37, 70.30, 12.94. MS (CI) calcd. for $\text{C}_{18}\text{H}_{16}\text{N}_2\text{O}_2\text{S}$: $m/z = 325.1$ $[\text{M}+\text{H}]^+$; found 325.1.

Synthesis of 11a. Sulfide **11** (0.04 g, 0.123 mmol) and mCPBA (0.12 g, 0.49 mmol) were dissolved in 2 mL of ethyl acetate. After stirring for 16 hours under N_2 at room temperature, the solution was diluted with 10 mL of ethyl acetate, washed with saturated NaHCO_3 (1 x 10 mL), saturated Na_2SO_4 (1 x 10 mL), brine (1 x 10 mL), dried with anhydrous Na_2SO_4 , and evaporated under reduced pressure to afford the crude product. The crude product obtained was purified by flash column chromatography (10% EtOAc in hexanes) to afford 0.0073 g of **11a** in 16% yield.

Characterization Data for 11a. ^1H NMR (500 MHz, CDCl_3) δ 8.89 (d, J = 1.0 Hz, 1H, Ar-H), 7.56 (d, J = 1.0 Hz, 1H, Ar-H), 7.44 – 7.39 (m, 4H, Ar-H), 7.38 – 7.32 (m, 2H, Ar-H), 6.96 (ddd, J = 8.5, 2.5, 0.9 Hz, 1H, Ar-H), 6.79 (t, J = 2.3 Hz, 1H, Ar-H), 6.76 (ddd, J = 7.8, 2.3, 0.9 Hz, 1H, Ar-H), 5.07 (s, 2H, Ar-CH₂), 3.25 (s, 3H, S-CH₃).

Synthesis of 11c. Sulfide **11** (0.04 g, 0.123 mmol) was dissolved in 3 mL of EtOAc. To this solution, a spatula tip of 10% Pd/C was added, and placed into a reactor with 1 ATM of H_2 . After stirring at room temperature for 2 days, the solution was filtered through a pad of Celite and concentrated to afford **11c**.

Characterization Data for 11c. ^1H NMR (500 MHz, CDCl_3) δ 8.81 (s, 1H, Ar-H), 8.56 (d, J = 5.8, 0.7 Hz, 1H, Ar-H), 7.46 – 7.37 (m, 4H, Ar-H), 7.37 – 7.31 (m, 2H, Ar-H), 6.91 (ddt, J = 8.4, 2.4, 1.0 Hz, 1H, Ar-H), 6.87 (dt, J = 5.8, 1.2 Hz, 1H, Ar-H), 6.80 – 6.75 (m, 2H, Ar-H), 5.06 (s, 2H, Ar- CH_2).

Synthesis of 13. 3-(Boc-Amino)-1-propanol (1.24 g, 7.06 mmol) and NaH (60% in mineral oil) (0.565 g, 14.13 mmol) were dissolved in 30 mL of THF. After the mixture was stirred for 30 minutes, 4-chloro-6-(methylthio)-pyrimidine (1.13 g, 7.06 mmol) dissolved in 10 mL of THF was added via syringe and allowed to stir for 2 hours. Once the reaction was complete, the mixture was diluted with 50 mL of ethyl acetate, washed with H_2O (1 x 50 mL), brine (1 x 50 mL), dried with Na_2SO_4 to afford 1.08 g of **13** in 51% yield.

Characterization Data for 13. ^1H NMR (500 MHz, CDCl_3) δ 8.50 (d, J = 1.0 Hz, 1H, Ar-H), 6.52 (d, J = 1.0 Hz, 1H, Ar-H), 4.81 (s, 1H, N-H), 4.37 (t, J = 6.1 Hz, 2H, O- CH_2), 3.24 (d, J = 6.6 Hz, 2H, N- CH_2), 2.50 (s, 3H, S- CH_3), 1.97 – 1.88 (m, 2H, C- CH_2), 1.41 (s, 9H, C- CH_3). ^{13}C NMR (126 MHz, CDCl_3) δ 171.07, 168.47, 157.43, 156.02, 103.20, 100.09, 79.31, 64.17, 37.60, 31.00, 29.40, 28.49, 12.94.

Synthesis of 13a. Methyl sulfide **13** (0.350 g, 1.17 mmol) and mCPBA (0.81 g, 4.68 mmol) were dissolved in 15 mL of ethyl acetate. After stirring for 16 hours under N_2 at room temperature, the solution was diluted with 50 mL of ethyl acetate, washed with saturated NaHCO_3 (1 x 25 mL), saturated Na_2SO_4 (1 x 25 mL), brine (1 x 25 mL), dried with anhydrous Na_2SO_4 , and evaporated under reduced pressure to afford the crude product. The crude product obtained was purified by flash column chromatography (30 to 50% EtOAc in hexanes) to afford 0.28 g of **13a** in 72% yield.

Characterization Data for 13a. ^1H NMR (500 MHz, CDCl_3) δ 8.86 (d, $J = 1.0$ Hz, 1H, Ar-H), 7.40 (d, $J = 1.0$ Hz, 1H, Ar-H), 4.70 (s, 1H, N-H), 4.53 (t, $J = 6.2$ Hz, 2H, O-CH₂), 3.29 (q, $J = 6.5$ Hz, 2H, N-CH₂), 3.21 (s, 3H, S-CH₃), 2.01 (p, $J = 6.5$ Hz, 2H, C-CH₂), 1.44 (s, 9H, C-CH₃).

Synthesis of 13b. Methyl Sulfide **13** (0.35 g, 1.17 mmol) was dissolved in 15 mL of DCM. To this stirring solution TFA (1.0 mL, 11.7 mmol) was added via syringe. After stirring for 1 hour at room temperature, the reaction mixture was concentrated under reduced pressure, re-dissolved in 50 mL of ethyl acetate, extracted with 1M HCl (3 x 50 mL), neutralized with 2M NaOH, extracted with ethyl acetate (5 x 50 mL), and concentrated to afford 0.20 g of **13b** in 86% yield.

Characterization Data for 13b. ^1H NMR (500 MHz, CDCl_3) δ 8.53 (d, $J = 1.1$ Hz, 1H, Ar-H), 6.54 (d, $J = 1.1$ Hz, 1H, Ar-H), 4.42 (t, $J = 6.3$ Hz, 2H), 2.85 (t, $J = 6.8$ Hz, 2H, N-CH₂), 2.52 (s, 3H, S-CH₃), 1.90 (t, $J = 6.5$ Hz, 2H, C-CH₂).

Characterization Data for 13c. ^1H NMR (500 MHz, CDCl_3) δ 8.55 (d, $J = 1.0$ Hz, 1H, Ar-H), 6.56 (d, $J = 1.0$ Hz, 1H, Ar-H), 4.49 (t, $J = 5.9$ Hz, 2H, O-CH₂), 3.60 – 3.55 (m, 2H, N-CH₂), 2.54 (s, 3H, S-CH₃), 2.18 – 2.12 (m, 2H, C-CH₂), 1.44 (s, 1H, O-H).

Synthesis of 16. N-Boc-1,6-Diaminohexane (1.00 g, 4.67 mmol) and 4-chloro-6-(methylthio)-pyrimidine (0.25, 1.56 mmol) were dissolved in 5 mL of 2-propanol. After stirring for 18 hours at 60°C, the mixture was concentrated under reduced pressure, redissolved in 50 mL DCM, washed with 1M NaOH (1 x 50 mL), brine (1 x 50 mL), dried with Na_2SO_4 , and evaporated under reduced pressure to afford 0.45 g of **16** in 78% yield.

Characterization Data for 16. ^1H NMR (500 MHz, CDCl_3) δ 8.34 (d, $J = 1.1$ Hz, 1H, Ar-H), 6.15 (d, $J = 1.2$ Hz, 1H, Ar-H), 5.00 (s, 1H, N-H), 4.53 (s, 1H, N-H), 3.23 (d, $J = 7.3$ Hz, 2H, N-CH₂), 3.10 (t, $J = 6.8$ Hz, 2H, N-CH₂), 2.50 (s, 3H, S-CH₃), 1.59 (h, $J = 6.5, 6.0$ Hz, 2H, C-CH₂), 1.50 – 1.45

(m, 2H, C-CH₂), 1.43 (s, 9H, C-CH₃), 1.42 – 1.28 (m, 4H, C-CH₂); ¹³C NMR (126 MHz, CDCl₃) δ 171.14, 161.26, 157.57, 156.04, 79.11, 76.77, 60.39, 41.19, 40.26, 30.03, 29.07, 28.43, 26.38, 26.25, 21.05, 14.20, 12.62. HRMS (ESI) calcd. for C₁₆H₂₈N₄O₂S: $m/z^{-1} = 341.2011$ [M+H]⁺; found 341.2014.

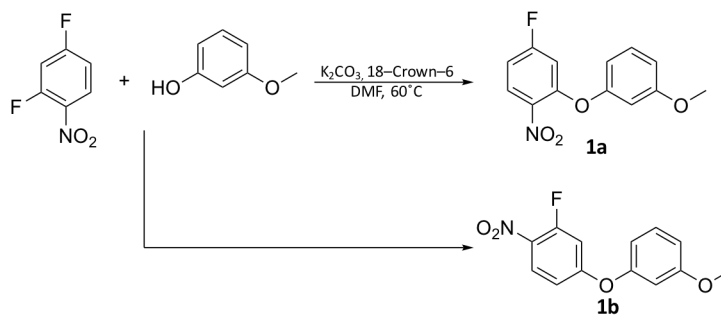
Synthesis of 16a. Methyl sulfide **16** (0.21 g, 0.60 mmol) and mCPBA (0.59, 2.40 mmol) were dissolved in 10 mL of ethyl acetate. After stirring for 16 hours under N₂ at room temperature, the solution was diluted with 50 mL of ethyl acetate, washed with saturated NaOH (1 x 25 mL), saturated Na₂SO₄ (1 x 25 mL), brine (1 x 25 mL), dried with anhydrous Na₂SO₄, and evaporated under reduced pressure to afford 0.11 g of **16b** in 50% yield.

Characterization Data for 16a. ¹H NMR (500 MHz, CDCl₃) δ 8.83 (s, 1H, Ar-H), 7.57 (s, 1H, Ar-H), 7.28 (s, 1H, Ar-H), 4.54 (s, 1H, N-H), 3.40 (q, *J* = 6.8 Hz, 2H, N-CH₂), 3.22 (s, 3H, S-CH₃), 3.12 (q, *J* = 7.2 Hz, 2H, N-CH₂), 1.73 (p, *J* = 7.2 Hz, 2H, C-CH₂), 1.53 – 1.47 (m, 3H, C-CH₂), 1.44 (s, 10H, C-CH₃), 1.41 – 1.35 (m, 2H, C-CH₂).

Results and Discussion:

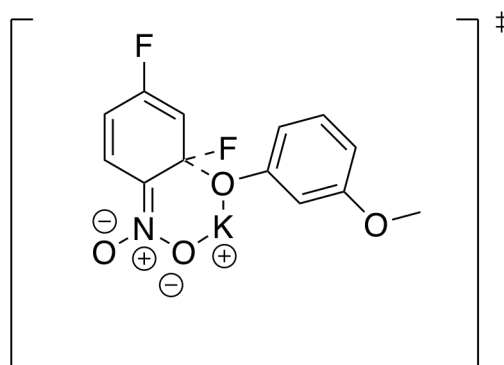
1st Generation IEG Scheme with Methyl Protection:

The synthesis of the 1st generation dormant monomer began with addition of the nucleophilic portion of the molecule, 3-methoxy phenol, combined with 2,4-difluorobenzene, to afford **1a** (Scheme 4). It was quickly realized, that the fluorine molecules of 2,4-difluorobenzene reacted with similar



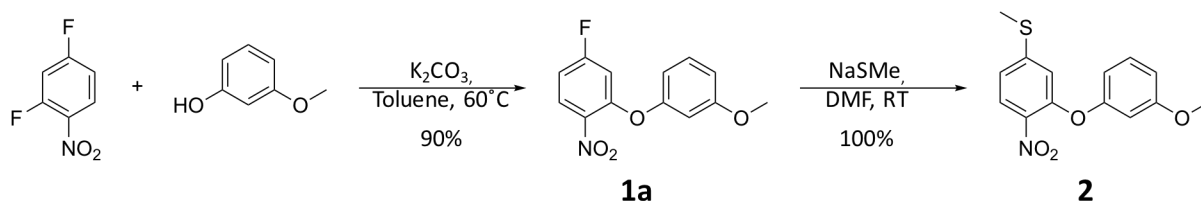
Scheme 4. Diagram displaying synthesis of regioisomers **1a** and **1b**.

rates, resulting in substitutions at both positions, confirmed by ^1H NMR (Figure 1). The two regioisomers **1a** and **1b** were inseparable through silica column chromatography, so the reaction had to be modified (Scheme 5). To engender an *ortho* regioselective $\text{S}_{\text{N}}\text{Ar}$ addition, a method pioneered by Bhagat *et al.* was introduced¹¹. This method optimizes the stabilization of the *ortho*-addition



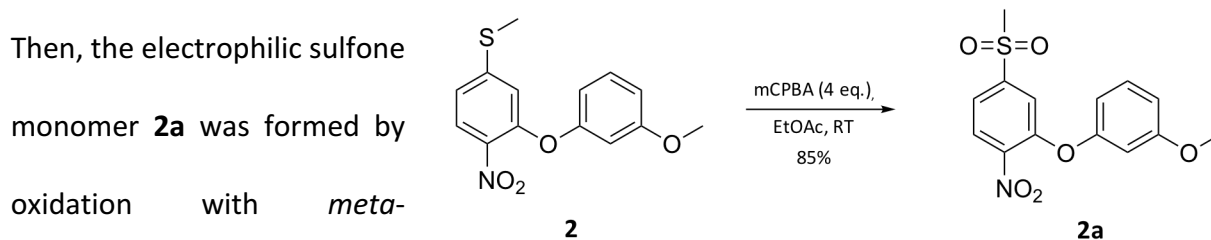
Scheme 5. Image of transition state responsible for *ortho* regioselectivity¹¹.

through the formation of a polar six-membered transition state complex (Scheme 6). As shown in the figure, the oxygen contained in the nitro group is stabilizing the potassium cation



Scheme 6. Regioselective synthesis of **1a**

associated with the phenoxide nucleophile. The key to forming this six-membered transition state complex is using a non-polar solvent, such as toluene, as polar solvents, like dimethyl formamide (DMF), would solvate the cation, disallowing such a transition state. Following this method, **1a** was formed regioselectively in 90% yield. From **1a**, the dormant monomer **2** was produced in quantitative yield (Scheme 6) through the addition of sodium methanethiolate¹².



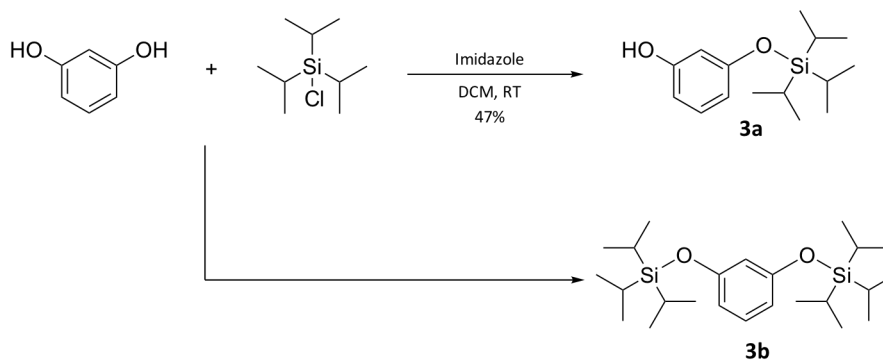
Scheme 7. Oxidation of **2**.

(mCPBA) (Scheme 7) with reasonable yield. However, the nucleophilic phenol monomer was unable to be synthesized, as the methyl protecting group could not be removed through a variety of deprotection strategies including Lewis acids BBr_3 ¹³, Bu_4NI ¹⁴, and BCl_3 ¹⁴. A new protection strategy was needed for the nucleophilic phenol portion of the molecule.

1st Generation IEG Scheme with TIPS Protection:

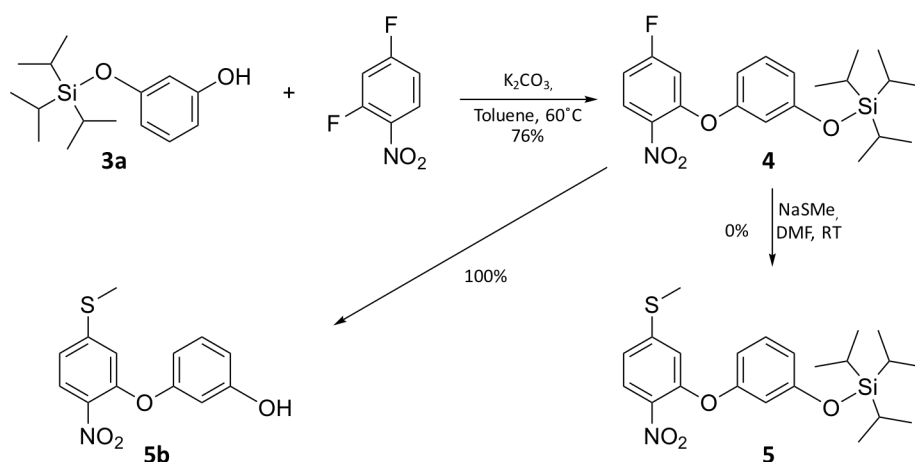
Due to inability to demethylate **2**, a new protection strategy was desired with a group that could be removed with relative ease. After careful consideration, the best option appeared to be a silyl-based protecting group, as it could be removed with refluxing methanol⁸. With a broad diversity of silyl protecting groups available, one had to be selected with both acid stability during oxidation, and base stability during coupling. Three common silyl protection groups were considered, triisopropylsilyl ether (TIPS), triethylsilyl ether (TES), and *tert*-butyldimethylsilyl ether (TBDMS). Both the acid and base stability of these groups have been previously reported⁸. The relative stability in 1% HCl at 25°C was observed to be TBDMS > TIPS >> TES, whereas the stability in 5% NaOH was found to be TIPS >> TBDMS > TES. TBDMS showed the greatest stability at low pH, however, was readily cleaved at high pH conditions, so TIPS was chosen as the nucleophilic protecting group due to its stability in both acidic and basic media⁸. Resorcinol was protected with triisopropylsilyl chloride to form **3a** in relatively low yields, as the disubstituted, **3b**, was also formed (Scheme 8). **3a** was then added to 2,4-difluoronitrobenzene, where it underwent a regioselective $\text{S}_{\text{N}}\text{Ar}$ to form **4**. Sodium thiomethylate was added in the hopes of forming **5**, however, the excess of thiomethylate added to the reaction likely cleaved the TIPS group as well, so only the formation of **5b** was observed (Scheme 9). Although this deprotection was

unintended, it actually was advantageous to the synthetic route, as it protected the electrophilic group and deprotected the nucleophilic group in



Scheme 8. Image depicting both mono- and di- protection of resorcinol with TIPS-Cl.

one step in quantitative yield. To form the respective dimer, electrophilic **4** and nucleophilic **5b**



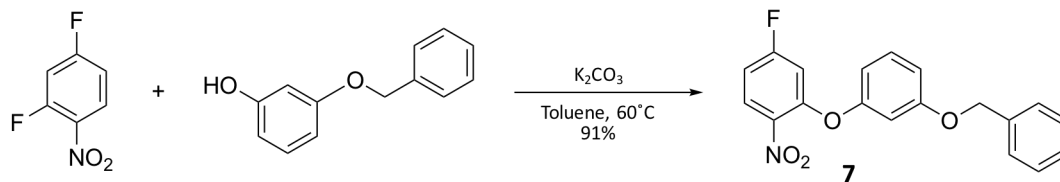
Scheme 9. Diagram showing formation of **5** and **5b**.

were combined in S_NAr conditions, but no product formation was seen, likely due to the nucleophilic lability of TIPS observed in the previous step. The

unstable nature of the TIPS group forced yet another change in protection strategy.

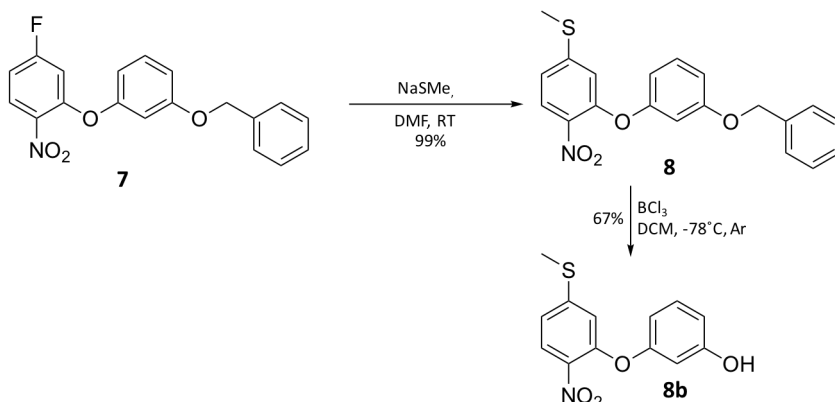
1st Generation IEG Scheme with Benzyl Protection:

Once the TIPS protection group failed under nucleophilic conditions, a more robust protecting group was desired that was less reactive than TIPS. The next phenol protection would be a benzyl protected resorcinol, as it was commercially available and could be removed under a variety of Lewis acidic and reductive conditions⁸. 3-(benzyloxy)phenol was added to the *ortho* position of 2,4-difluoronitrobenzene in a similar fashion to **4**, to form **7** (Scheme 10). The



Scheme 10. Figure displaying installation of benzyl protected resorcinol onto 2,4-difluorobenzene.

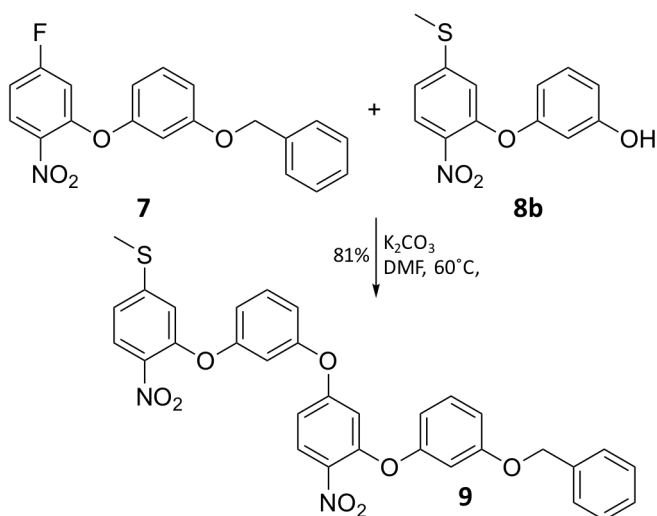
electrophilic portion of **7** was then protected with sodium methanethiolate to form **8**, with the benzyl protecting group intact (Scheme 11). The benzyl group was successfully deprotected using conditions reported by Carter *et al*¹⁵ using BCl_3 to afford **8b**.



To form dimer **9**, electrophile **7** and debenzylated **8b** were combined with K_2CO_3 in DMF (Scheme 12). Dimer **9** was successfully oxidized to the

Scheme 11. Scheme illustrating synthesis of **8**, followed by subsequent debenzylation to afford **8b**.

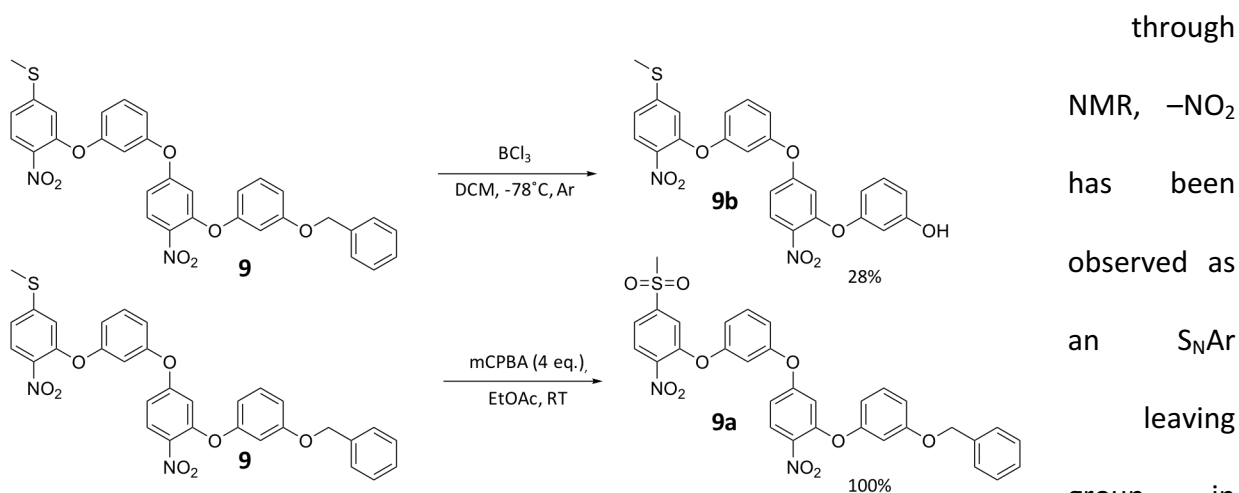
sulfone **9a** (Scheme 13), designated by the downfield shift of the $S-CH_3$ peak from 2.46 to 3.04



Scheme 12. Diagram outlining synthesis of dimer **9**.

ppm in the 1H NMR spectrum. Dimer **9** was also debenzylated following using BCl_3 (Scheme 13). The combination of **9a** and **9b** was a consequential step in the IEG strategy, as it was the first test of the efficacy of methyl sulfone as a leaving group. Although the use of sulfinate as a leaving group had been

previously reported in S_NAr ^{9,10}, this was the first test of a non-pyrimidine system. Unfortunately, the coupling test provided discouraging results, as the expected tetramer was not observed, only a variety of degradation products. To explain why the reaction did not proceed as anticipated, it was hypothesized that the π electron character of the $-SO_2Me$ group activated the $-NO_2$ group for S_NAr , which resulted in a disfavored product. Although this hypothesis was not confirmed

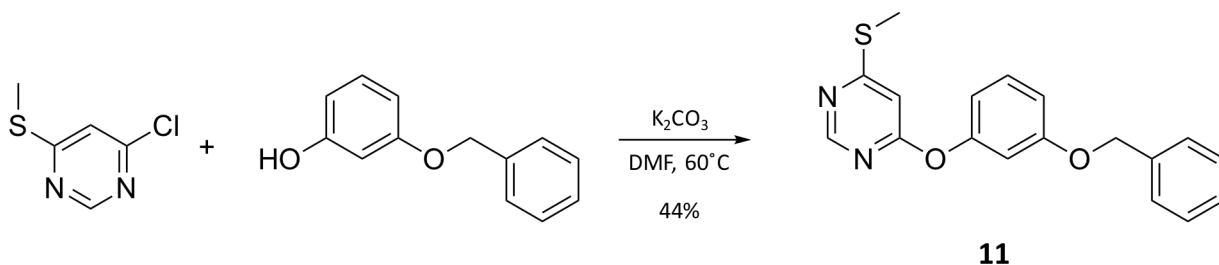


Scheme 13. Scheme outlining orthogonal deprotection of **9**.

Wu *et al*¹⁶. However, further analysis is necessary to confirm this prediction. To prevent the loss of $-NO_2$, a new iteration of IEG by utilizing a heterocycle in which the electron withdrawing nature was included within the ring to prevent the loss of an EWG.

2nd Generation IEG Scheme with Phenol Nucleophile:

Aromatic heterocycles containing nitrogen are reactive toward nucleophilic substitution,



Scheme 14. Synthesis of dormant monomer **11**.

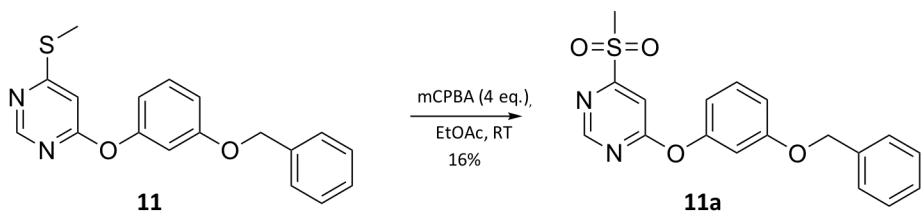
as the nitrogen atoms can stabilize the anionic intermediate similarly to how electron

withdrawing groups do when tethered to benzene rings⁶. Work performed by Zhao *et al.* showed that polymers could be produced through S_NAr with pyrimidine as a substrate¹⁰, which inspired this evolution of this IEG system. To produce the dormant monomer, 3-(benzyloxy)phenol was combined with 4-chloro-6-(methylthio)-pyrimidine to form **11** (Scheme 14). The dormant monomer was then successfully oxidized using mCPBA to afford **11a** (Scheme 15). The dormant monomer was unable to be debenzylated under Lewis acidic conditions, so reductive conditions were utilized,

specifically

hydrogenation

catalyzed by Pd/C⁸.

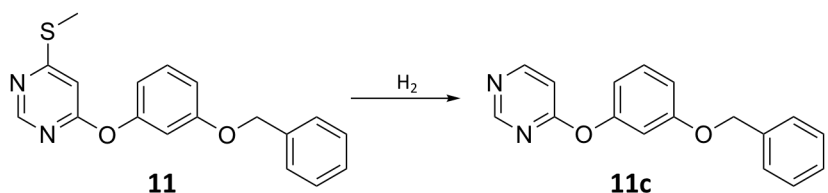


Scheme 15. Oxidation of dormant monomer **11** to sulfone **11a**.

Unfortunately, reductive conditions did not debenzylate the phenolic portion of **11**, but it in fact underwent reductive desulfurization, a transformation that has been previously described by Maulide *et al.*²⁰ resulting in **11c** (Scheme 16). This hypothesis is supported by the attenuation of

the S–CH₃ ¹H NMR peak at 2.43 ppm and the formation of a doublet at 8.56 ppm in

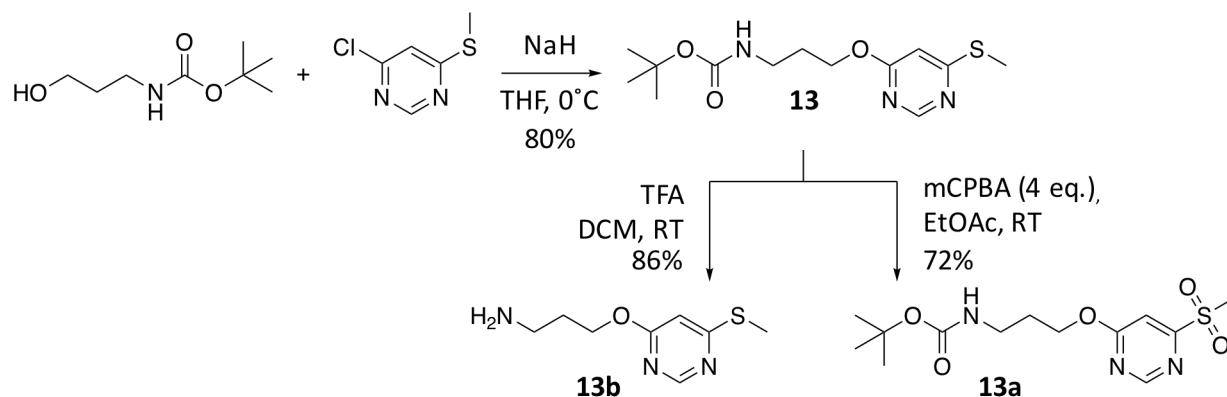
the **11c** ¹H NMR spectrum.



Scheme 16. Reductive desulfurization of **11**.

2nd Generation IEG Scheme with Short Chain Amine Nucleophile:

Once it became apparent that the debenzylation of **11** would not proceed under a wide variety of conditions, the nucleophile was adjusted to a primary alkyl amine. *Tert*-butyloxycarbonyl (boc) moieties are exceptional amine protecting group that can be cleaved in



Scheme 17. Formation of monomer and subsequent deprotection.

high yields using TFA¹³. In addition, amines have been well documented as nucleophiles in S_NAr reactions¹⁷, so this proved to be a feasible strategy. The synthesis began by adding 3-(Boc-Amino)-1-propanol to 4-chloro-6-(methylthio)-pyrimidine to form monomer **13**. Sulfide **13** was then orthogonally deprotected to form **13a** and **13b** (Scheme 17). The reactive species **13a** and **13b** were then combined under S_NAr conditions published by Smith *et al.*¹⁸ aiming to form the associated

dimer. After

24 hours, the

sulfone **13a**



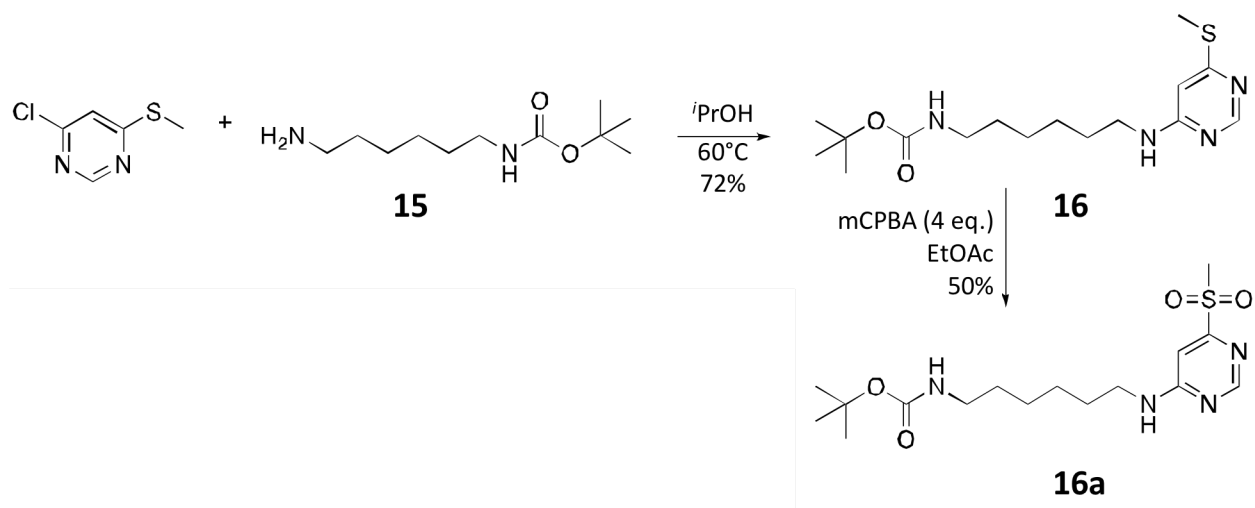
Scheme 18. Proposed Smiles degradation pathway, including spirocyclic intermediate.

was completely unreacted, whereas **13b** degraded to alcohol **13c** (Scheme 18). Product **13c** was isolated, and it appeared that **13b** had undergone a Smiles rearrangement¹⁹ (Scheme 18). The Smiles rearrangement is an intramolecular S_NAr transformation that proceeds via a spirocyclic intermediate in which the migration of an aromatic ring occurs¹⁹. Three conditions must be met in order for the Smiles rearrangement to take place. First of all, the aromatic ring must be activated, which is true for the pyrimidine ring in **13**, as it is primed for an S_NAr reaction. Secondly, the incoming group must be of greater nucleophilicity than the group leaving the aromatic ring.

This is true for **13b** as primary amines are greater nucleophiles than primary alcohols due to the decreased electronegativity of amines. This process is analogous to the relative thermodynamic advantage present in the aminolysis of a carboxylate compared to the hydrolysis of an amide. Finally, the ring formed in the spirocyclic intermediated must be thermodynamically accessible, so generally 5 and 6 membered rings are observed¹⁹. Compound **13b** fits all the criteria for a Smiles transformation, and the product **13c** was isolated, so there is reason to believe that Smiles was the observed degradation pathway.

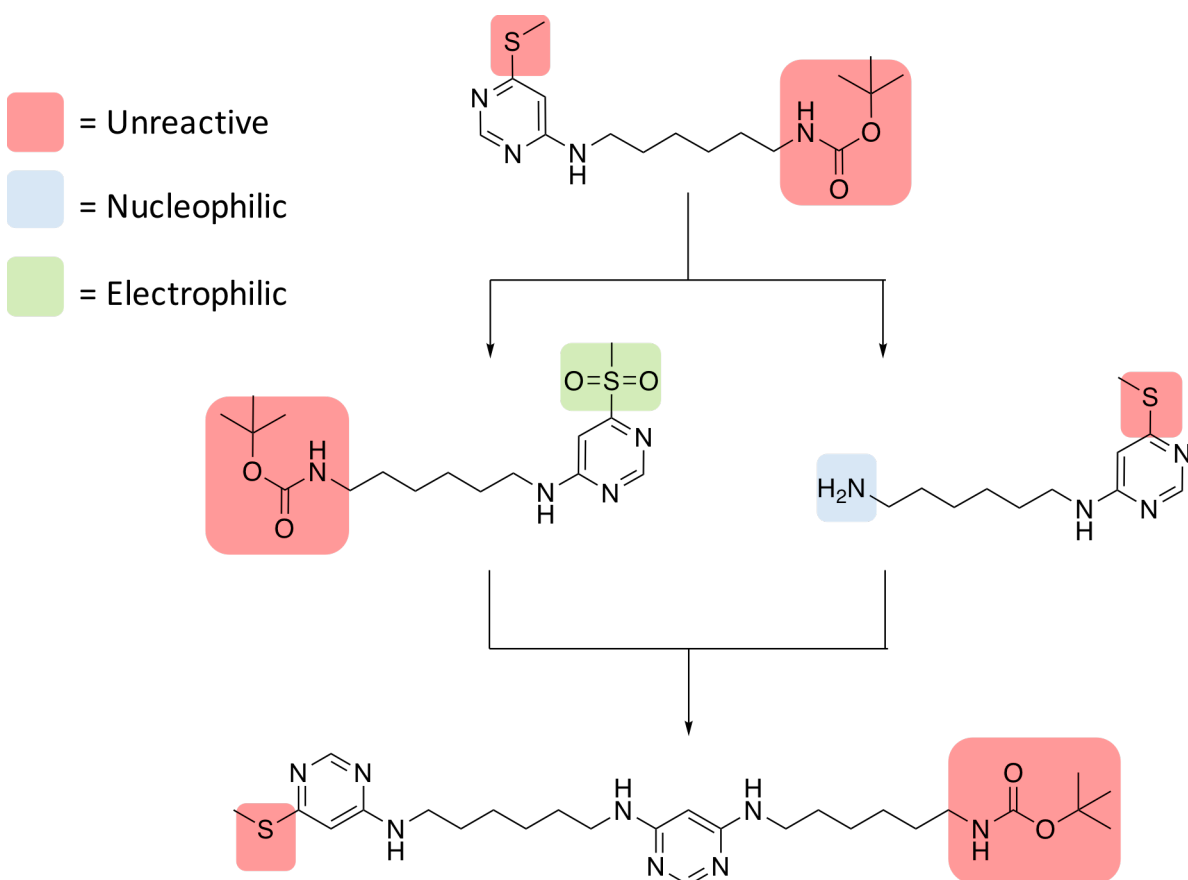
2nd Generation IEG Scheme with Long Chain Amine Nucleophile:

To prevent the observed Smiles rearrangement, the nucleophilic portion of the molecule was modified in two ways. To start, the aliphatic chain was increased from 3 to 6 carbons, in order to prevent the favorable 6-membered spirocyclic intermediate. In this iteration, if the spirocyclic intermediate were to form, it would proceed through a 9-membered ring, which has an increased entropic cost. Next, the group linking the alkyl amine to the pyrimidine ring was altered from an ether to a secondary amine. This way, if a spirocyclic intermediate is formed, and



Scheme 19. Synthesis of **16** and oxidation to **16a**.

an exchange occurs, the resulting molecule will be identical to the initial compound. Therefore, the system was modified to negate any effects of the Smiles rearrangement. The improved dormant monomer synthesis was formed by combining N-Boc-1,6-Diaminohexane **15** with 4-chloro-6-(methylthio)-pyrimidine to form dormant monomer **16**. In order to test the effectiveness of the current system, **16** was oxidized to the sulfone **16a** and combined with another equivalent of **15** to form **17**. Preliminary data has showed that **17** was successfully synthesized, however, further purification and data acquisition must be performed to verify this result.



Scheme 20. 2nd Generation IEG plan with long chain amine nucleophile.

Conclusion: In this work, a sulfone has been used as a leaving group in S_NAr to facilitate the construction of oligomers through iterative exponential growth. We have tested the efficacy of

6 distinct systems using different nucleophiles, and have concluded that pyrimidine offers advantages over NO₂– activated benzene rings. *Tert*-butyloxycarbonyl has been identified as an ideal protecting group for an amine nucleophile, as it does not have to be cleaved under reductive conditions, thereby keeping the masked sulfone intact. Finally, a long chain amine nucleophile connected via a 2° amine has proven to be the most promising nucleophile to date, as it prevents any degradation of monomer through the Smiles rearrangement.

References:

1. Church, G. M.; Gao, Y.; Kosuri, S., Next-Generation Digital Information Storage in DNA. *Science* **2012**, 337 (6102), 1628-1628.
2. Odian, G., *Principles of Polymerization*. Wiley: 2004.
3. Binauld, S.; Damiron, D.; Connal, L. A.; Hawker, C. J.; Drockenmuller, E., Precise Synthesis of Molecularly Defined Oligomers and Polymers by Orthogonal Iterative Divergent/Convergent Approaches. *Macromolecular Rapid Communications* **2011**, 32 (2), 147-168.
4. Merrifield, R. B., Solid Phase Peptide Synthesis. I. The Synthesis of a Tetrapeptide. *Journal of the American Chemical Society* **1963**, 85 (14), 2149-2154.
5. Hawker, C. J.; Malmström, E. E.; Frank, C. W.; Kampf, J. P., Exact Linear Analogs of Dendritic Polyether Macromolecules: Design, Synthesis, and Unique Properties. *Journal of the American Chemical Society* **1997**, 119 (41), 9903-9904.
6. Carey, F. A.; Sundberg, R. J., *Part B: Reactions and Synthesis*. Springer Berlin Heidelberg: 2013.
7. Błaziak, K.; Danikiewicz, W.; Małkosza, M., How Does Nucleophilic Aromatic Substitution Really Proceed in Nitroarenes? Computational Prediction and Experimental Verification. *Journal of the American Chemical Society* **2016**, 138 (23), 7276-7281.
8. Wuts, P. G. M., *Greene's Protective Groups in Organic Synthesis*. Wiley: 2014.
9. Van Rossom, W.; Caers, J.; Robeyns, K.; Van Meervelt, L.; Maes, W.; Dehaen, W., (Thio)ureido Anion Receptors Based on a 1,3-Alternate Oxacalix[2]arene[2]pyrimidine Scaffold. *The Journal of Organic Chemistry* **2012**, 77 (6), 2791-2797.
10. Guan, Y.; Wang, C.; Wang, D.; Dang, G.; Chen, C.; Zhou, H.; Zhao, X., Methylsulfone as a leaving group for synthesis of hyperbranched poly(arylene pyrimidine ether)s by nucleophilic aromatic substitution. *RSC Advances* **2015**, 5 (17), 12821-12823.
11. Sythana, S. K.; Naramreddy, S. R.; Kavitha, S.; Ch, V. K.; Bhagat, P. R., Nonpolar Solvent a Key for Highly Regioselective S_NAr Reaction in the Case of 2,4-Difluoronitrobenzene. *Organic Process Research & Development* **2014**, 18 (7), 912-918.
12. Ma, H. J.; Zhang, J. H.; Xia, X. D.; Kang, J.; Li, J. H., Design, synthesis and herbicidal evaluation of novel 4-(1H-pyrazol-1-yl)pyrimidine derivatives. *Pest Management Science* **2015**, 71 (8), 1189-1196.

13. Liu, X.; Weinert, Z. J.; Sharafi, M.; Liao, C.; Li, J.; Schneebeil, S. T., Regulating Molecular Recognition with C-Shaped Strips Attained by Chirality-Assisted Synthesis. *Angewandte Chemie International Edition* **2015**, 54 (43), 12772-12776.
14. Brooks, P. R.; Wirtz, M. C.; Vetelino, M. G.; Rescek, D. M.; Woodworth, G. F.; Morgan, B. P.; Coe, J. W., Boron Trichloride/Tetra-n-Butylammonium Iodide: A Mild, Selective Combination Reagent for the Cleavage of Primary Alkyl Aryl Ethers. *The Journal of Organic Chemistry* **1999**, 64 (26), 9719-9721.
15. Perkins, J. R.; Carter, R. G., Synthesis of Programmable Tetra-ortho-Substituted Biaryl Compounds Using Diels–Alder Cycloadditions/Cycloreversions of Disubstituted Alkynyl Stannanes. *Journal of the American Chemical Society* **2008**, 130 (11), 3290-3291.
16. Senger, N. A.; Bo, B.; Cheng, Q.; Keeffe, J. R.; Gronert, S.; Wu, W., The Element Effect Revisited: Factors Determining Leaving Group Ability in Activated Nucleophilic Aromatic Substitution Reactions. *The Journal of organic chemistry* **2012**, 77 (21), 9535-9540.
17. Ramil Baiazitov, W. D., Chang-Sun Lee, Seongwoo Hwang, Neil G. Almstead, Young-Choon Moon, Chemoselective Reactions of 4,6-Dichloro-2-(methylsulfonyl)pyrimidine and Related Electrophiles with Amines. *Synthesis* **2013**, 45 (13).
18. Armstrong, R. J.; Smith, M. D., Catalytic Enantioselective Synthesis of Atropisomeric Biaryls: A Cation-Directed Nucleophilic Aromatic Substitution Reaction. *Angewandte Chemie International Edition* **2014**, 53 (47), 12822-12826.
19. Plesniak, K.; Zarecki, A.; Wicha, J., The Smiles Rearrangement and the Julia–Kocienski Olefination Reaction. In *Sulfur-Mediated Rearrangements II*, Schaumann, E., Ed. Springer Berlin Heidelberg: Berlin, Heidelberg, 2007; pp 163-250.
20. Xie, L.-G.; Niyomchon, S.; Mota, A. J.; González, L.; Maulide, N., Metal-free intermolecular formal cycloadditions enable an orthogonal access to nitrogen heterocycles. *Nature Communications* **2016**, 7, 10914.

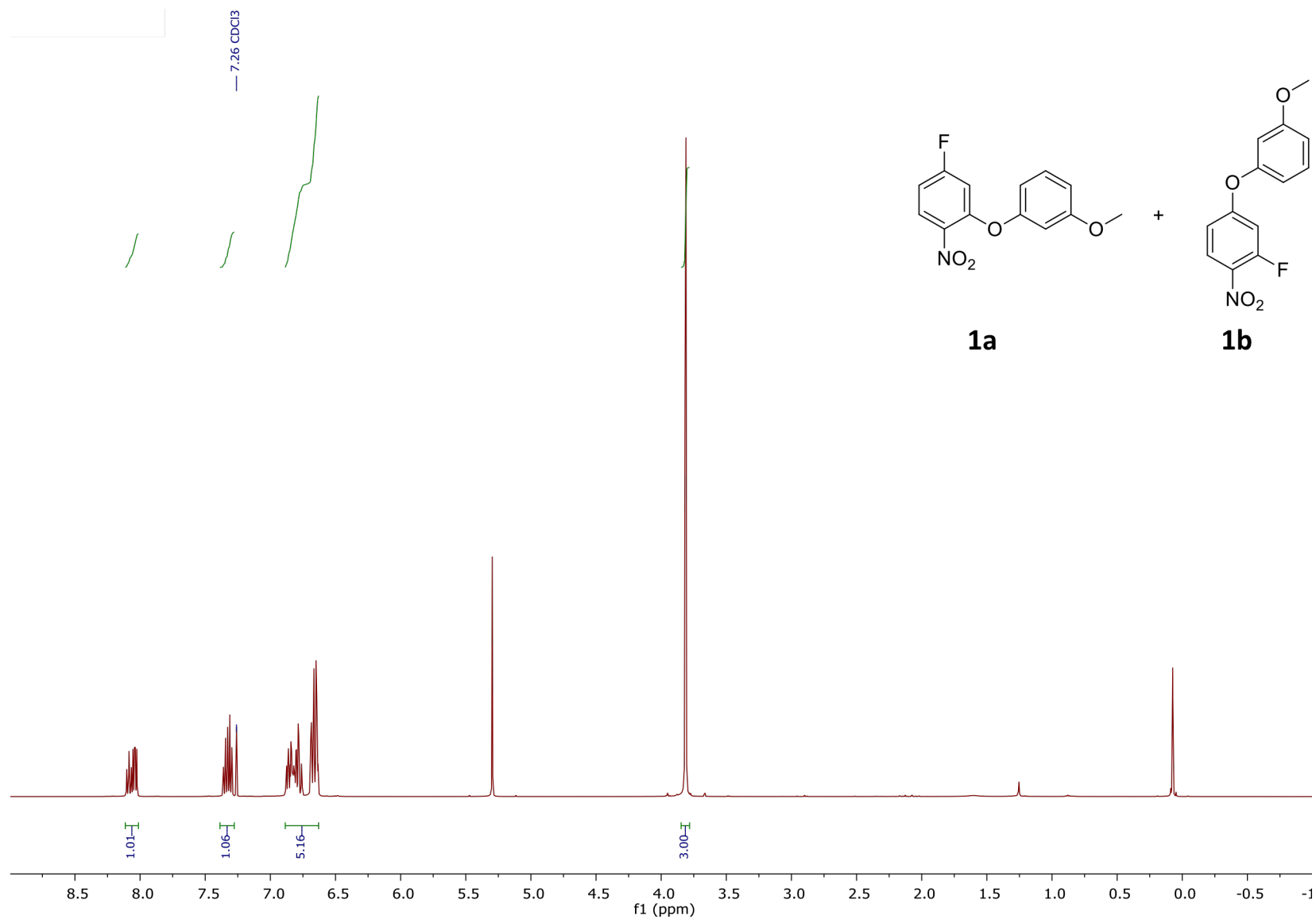


Figure 1. ^1H NMR spectrum of **1a** and **1b** mixture.

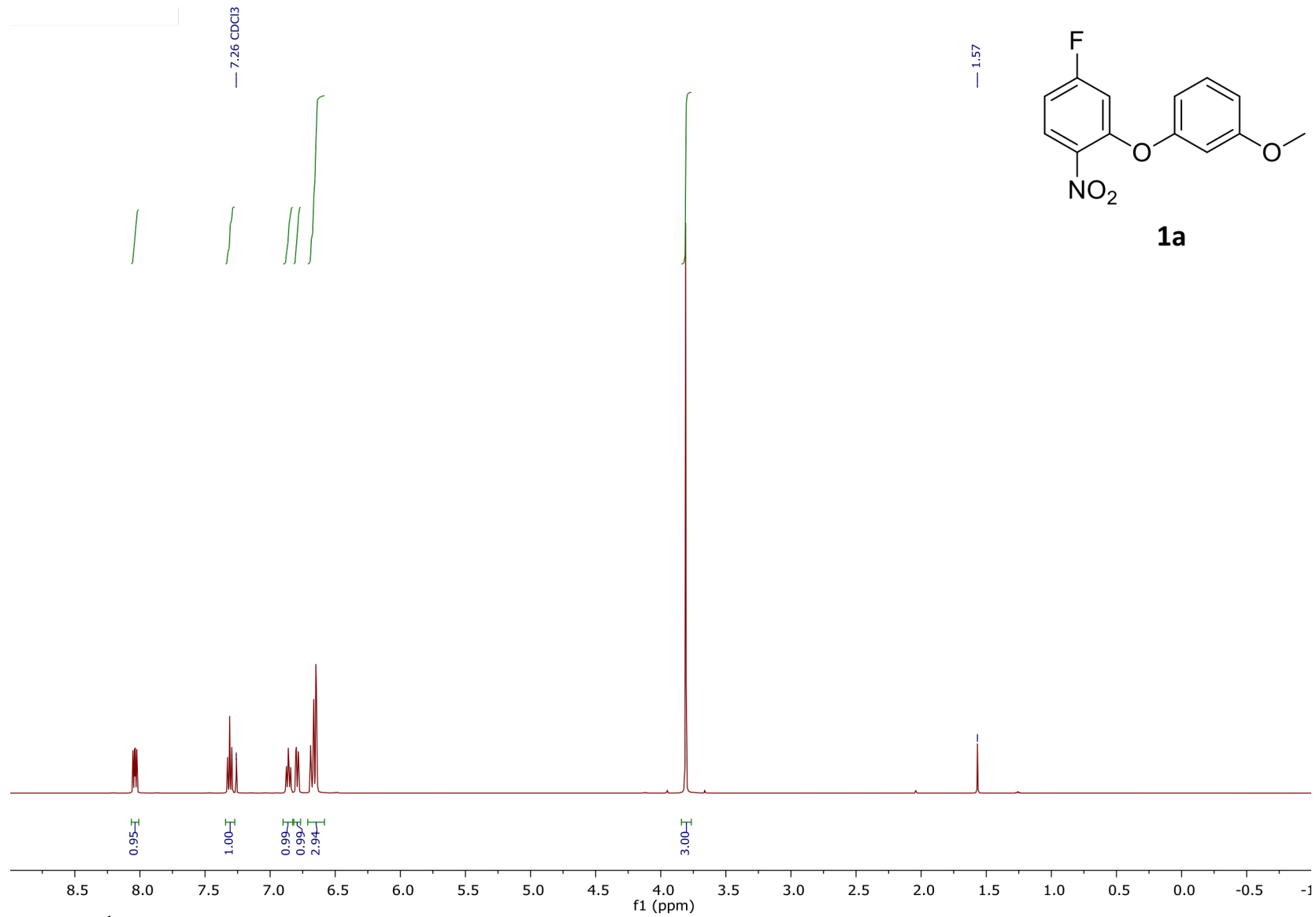


Figure 2. ¹H NMR spectrum of **1a**.

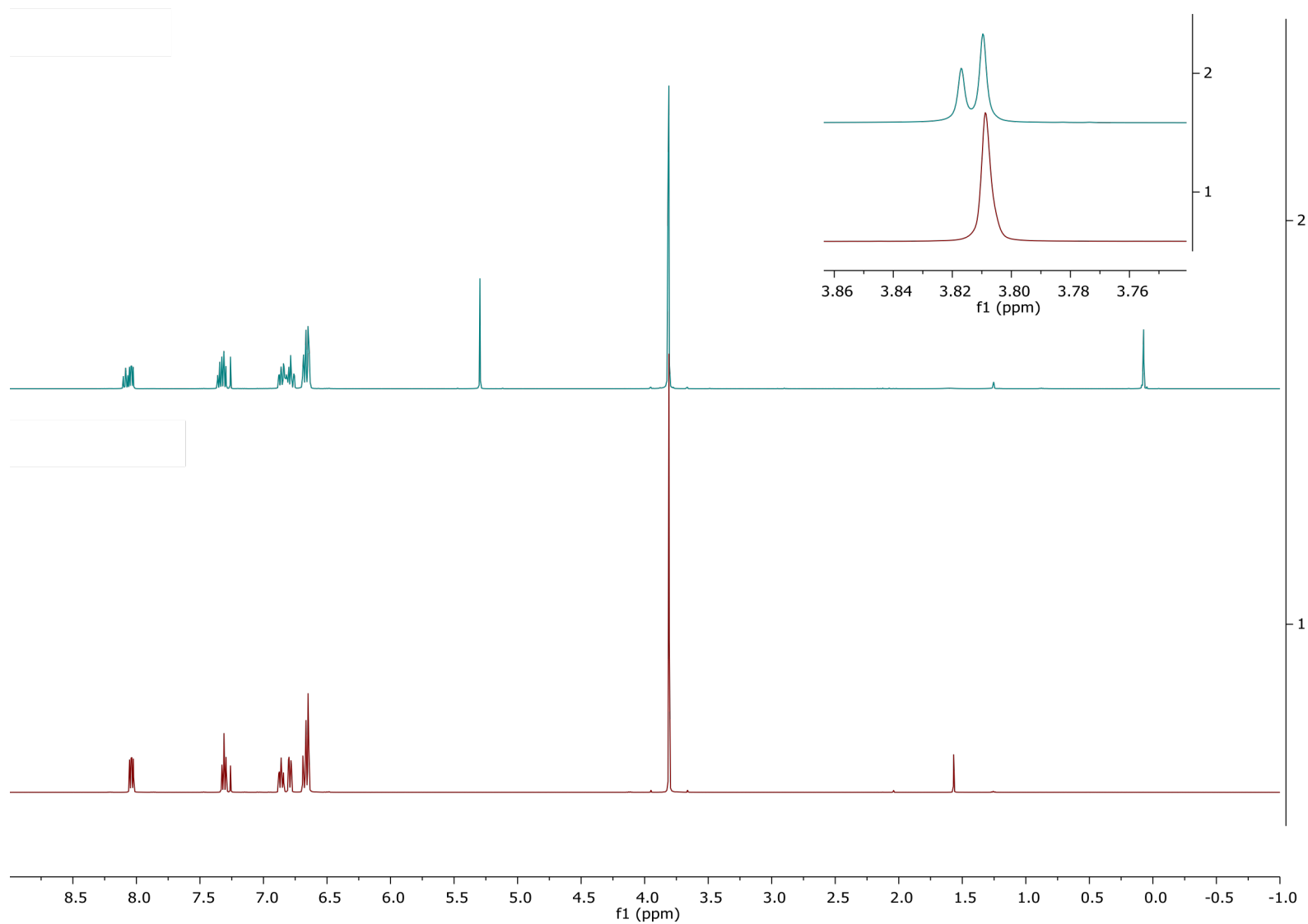


Figure 3. Stacked ^1H NMR spectra of **1a** and **1b** above pure **1a**.

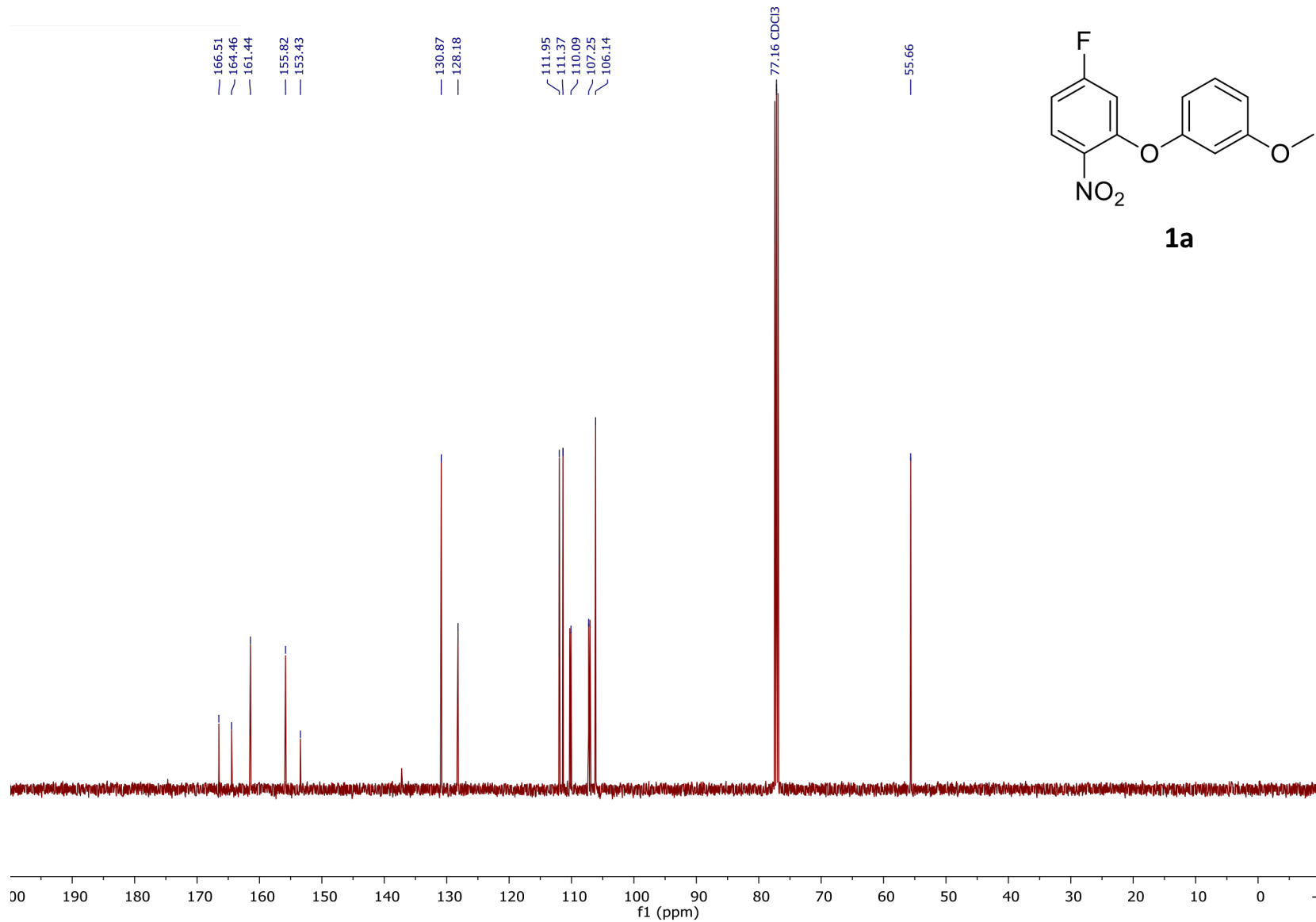


Figure 4. ¹³C NMR spectrum of **1a**.

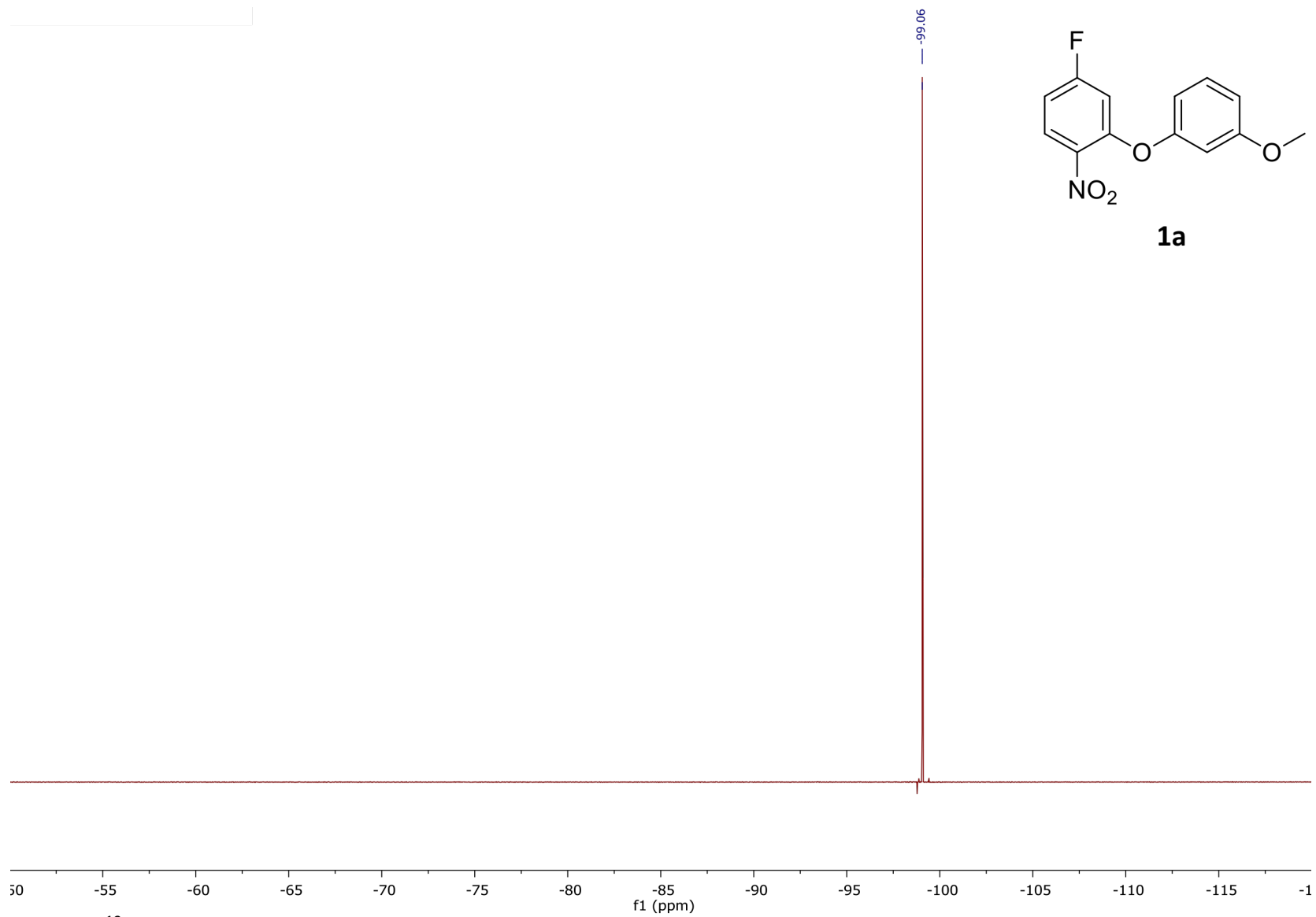


Figure 5. ^{19}F NMR spectrum of **1a**.

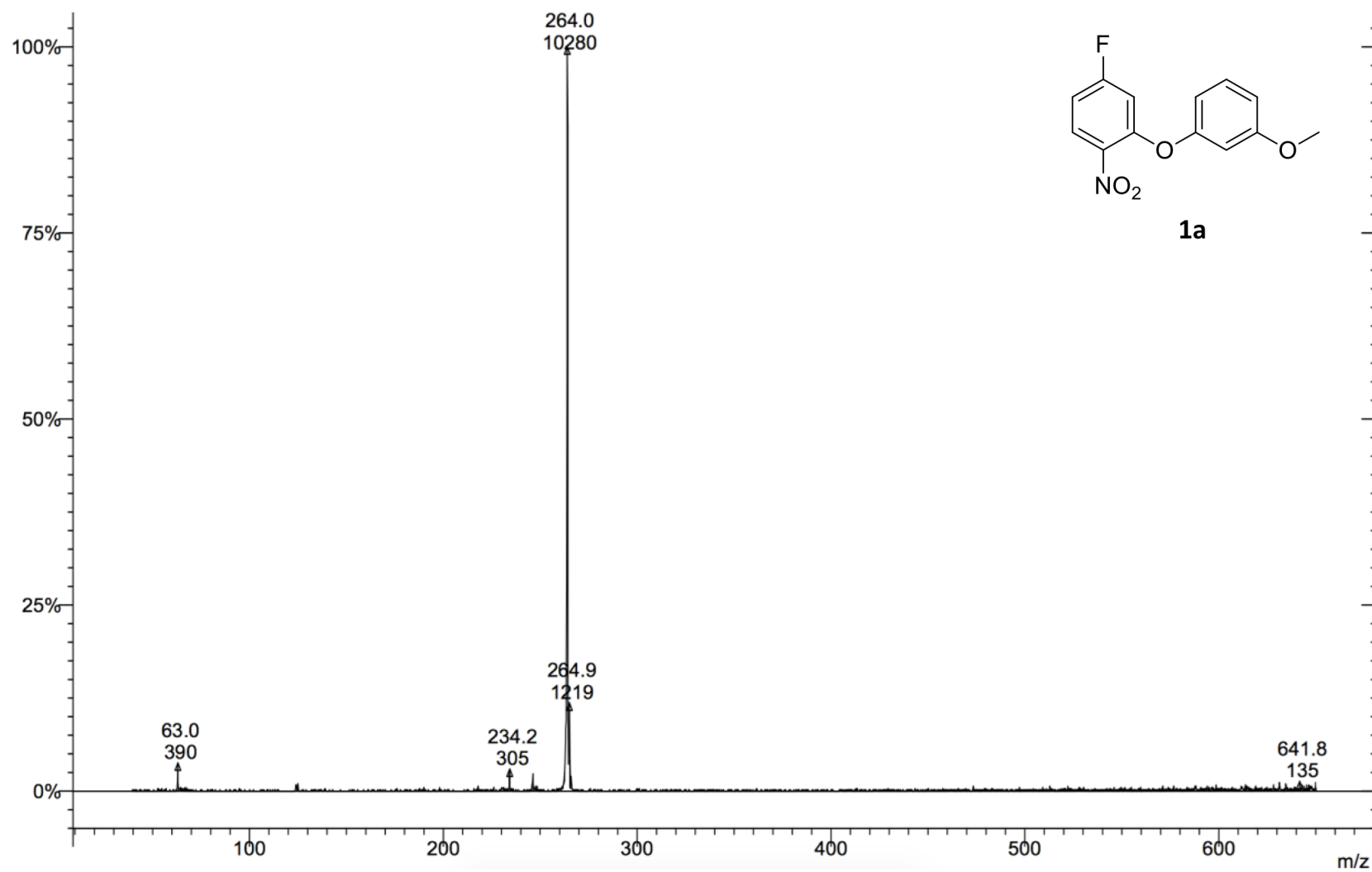


Figure 6. CI Mass spectrum of **1a**.

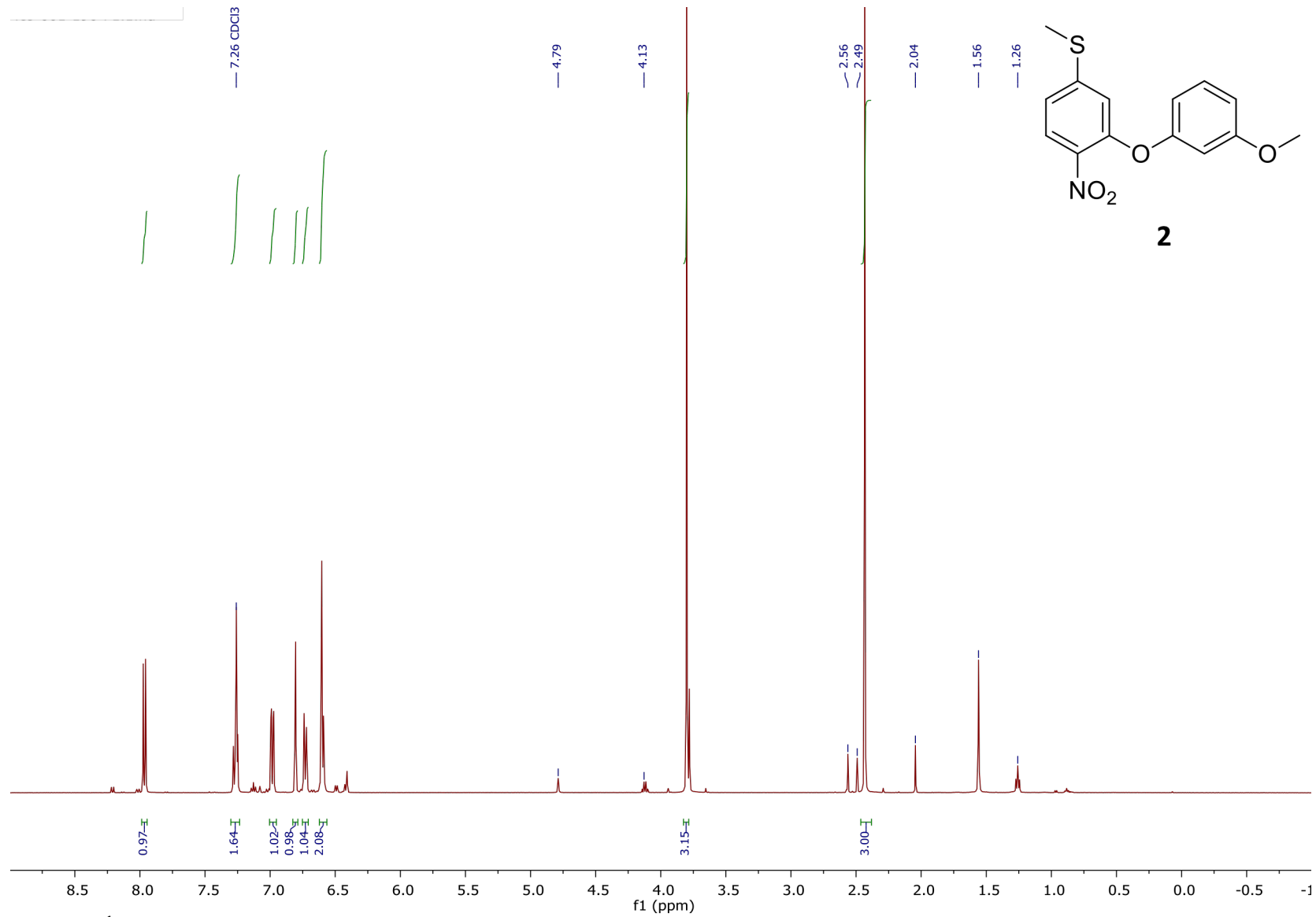


Figure 7. ¹H NMR spectrum of **2**.

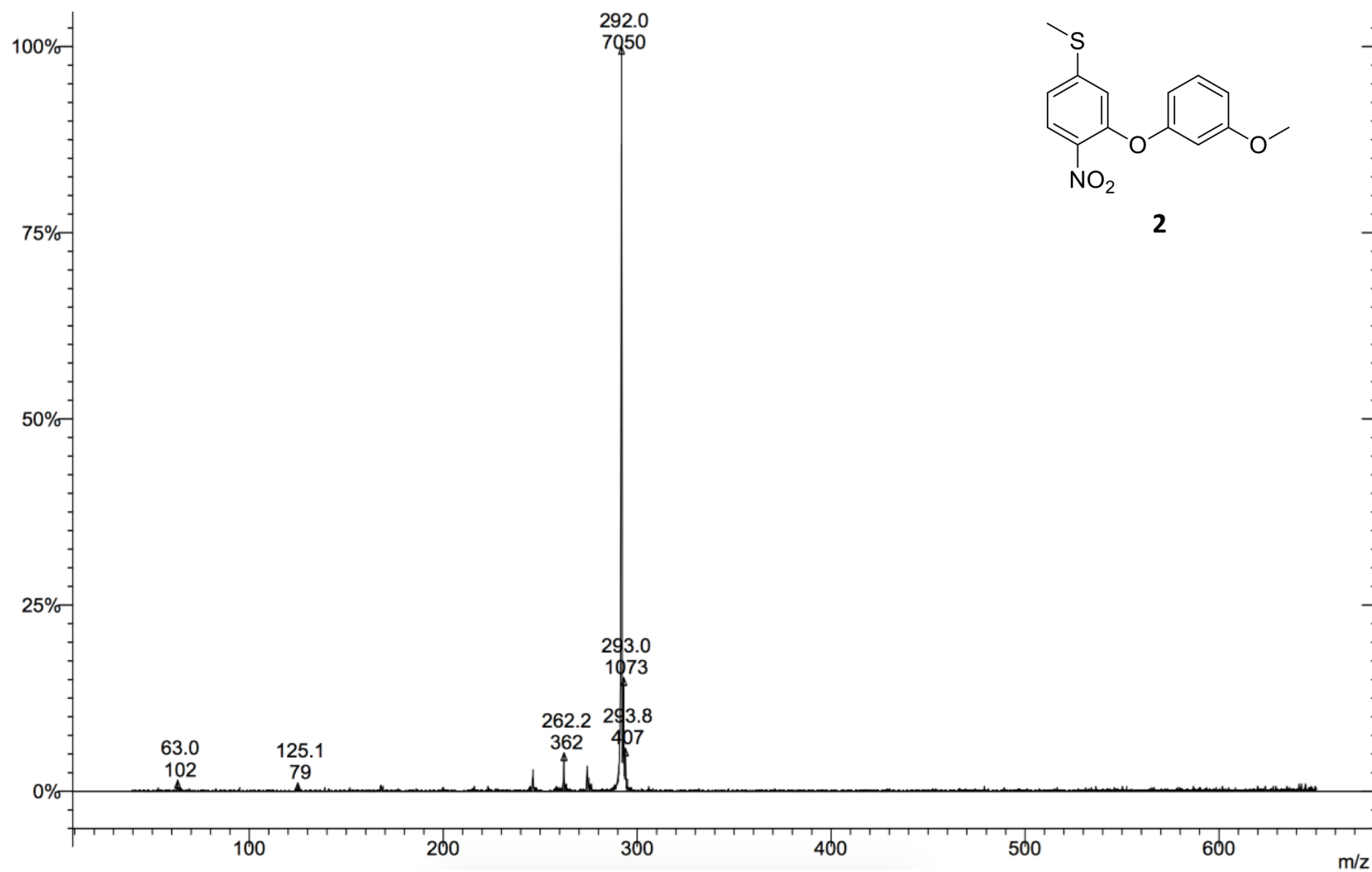


Figure 8. CI Mass spectrum of **2**.

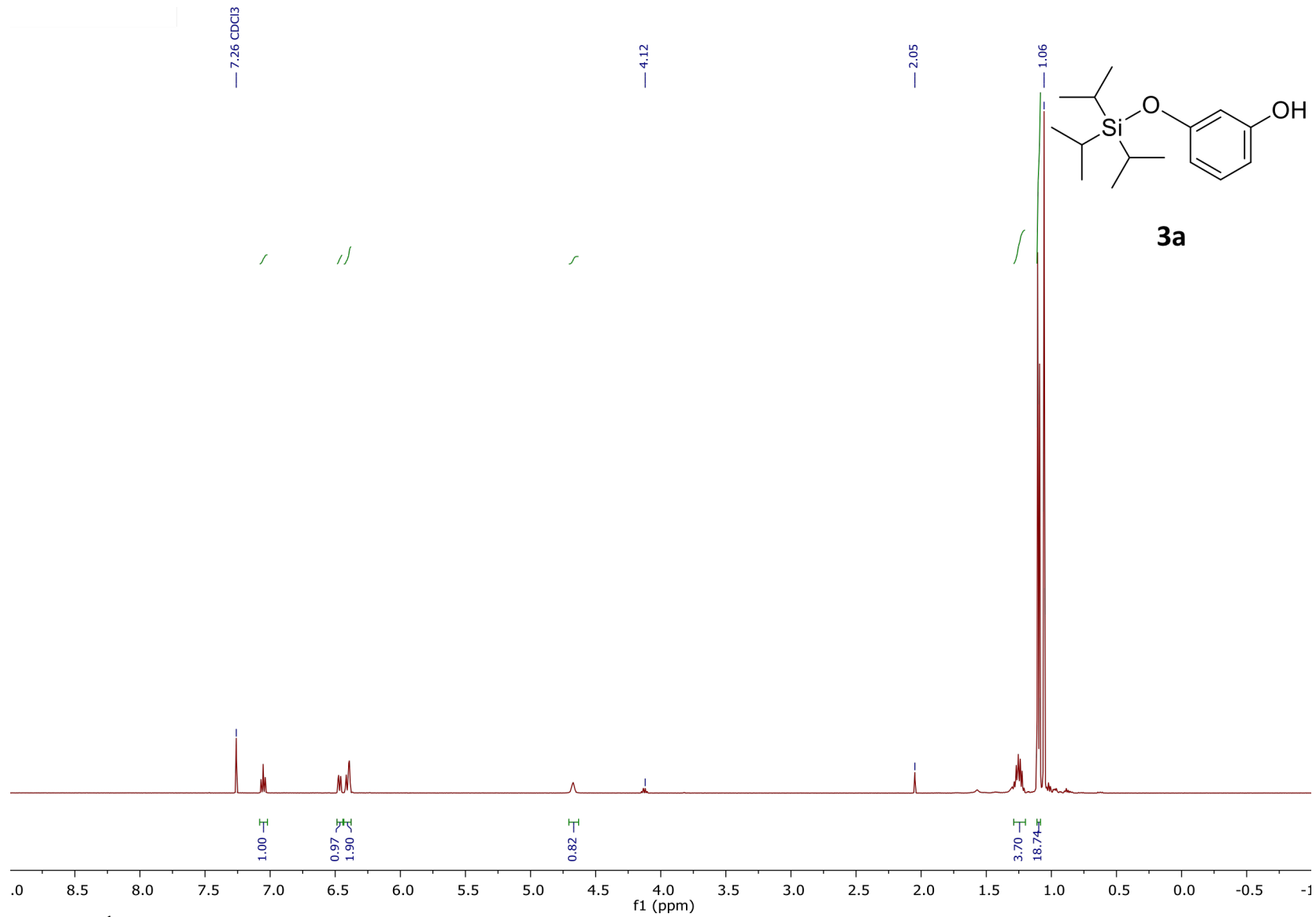


Figure 9. ^1H NMR spectrum of **3a**.

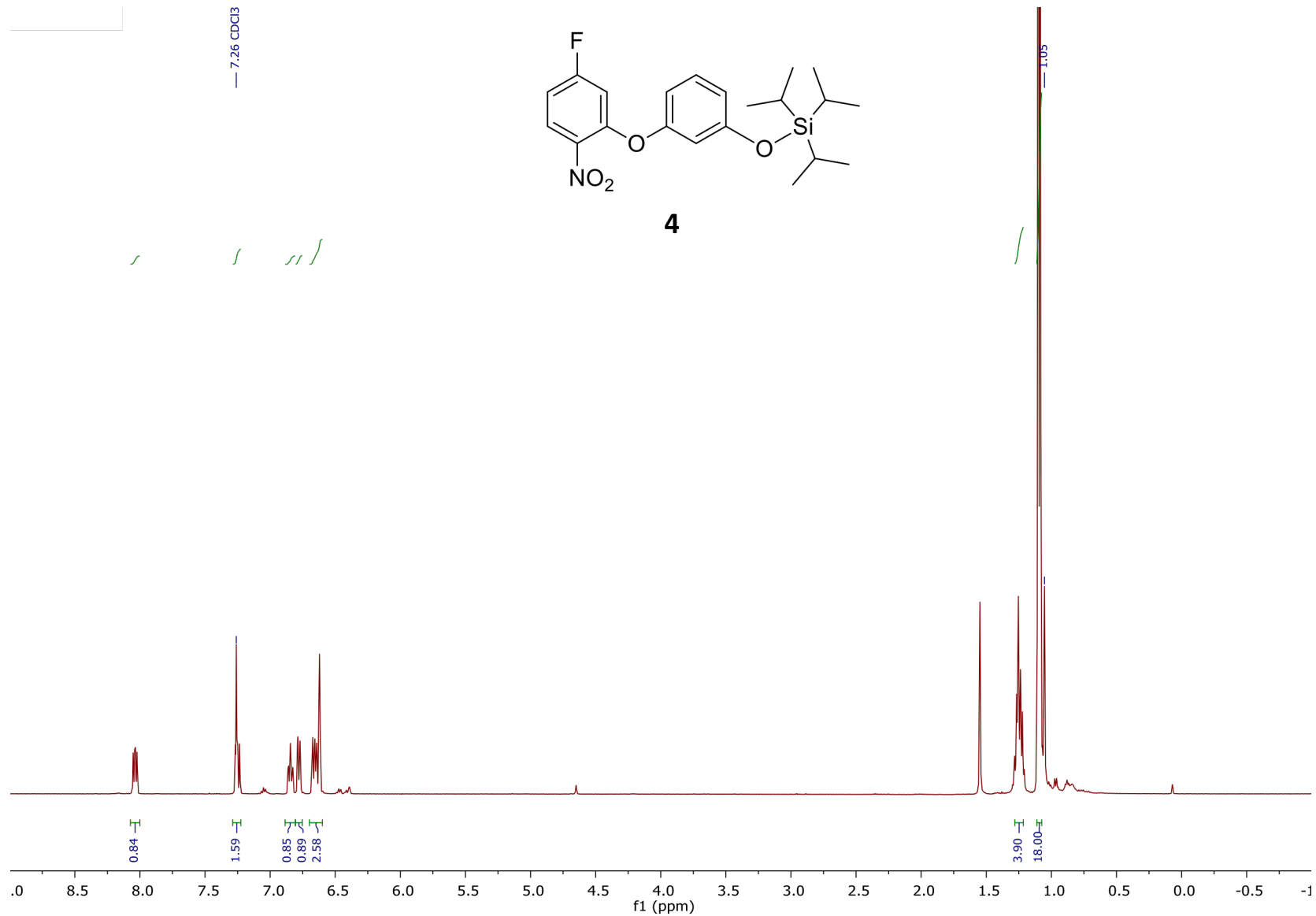


Figure 10. ^1H NMR spectrum of **4**.

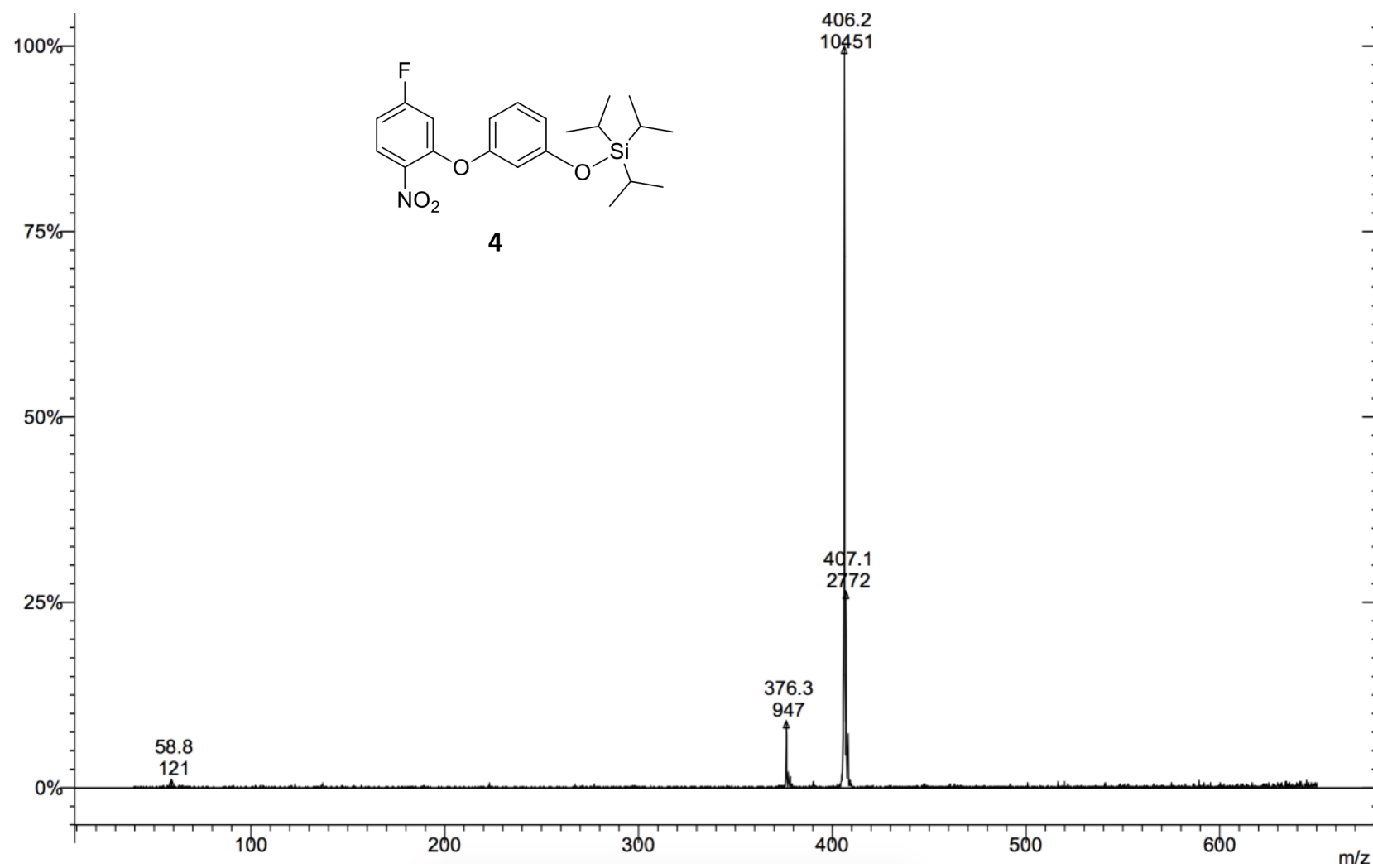


Figure 11. CI Mass spectrum of **4**.

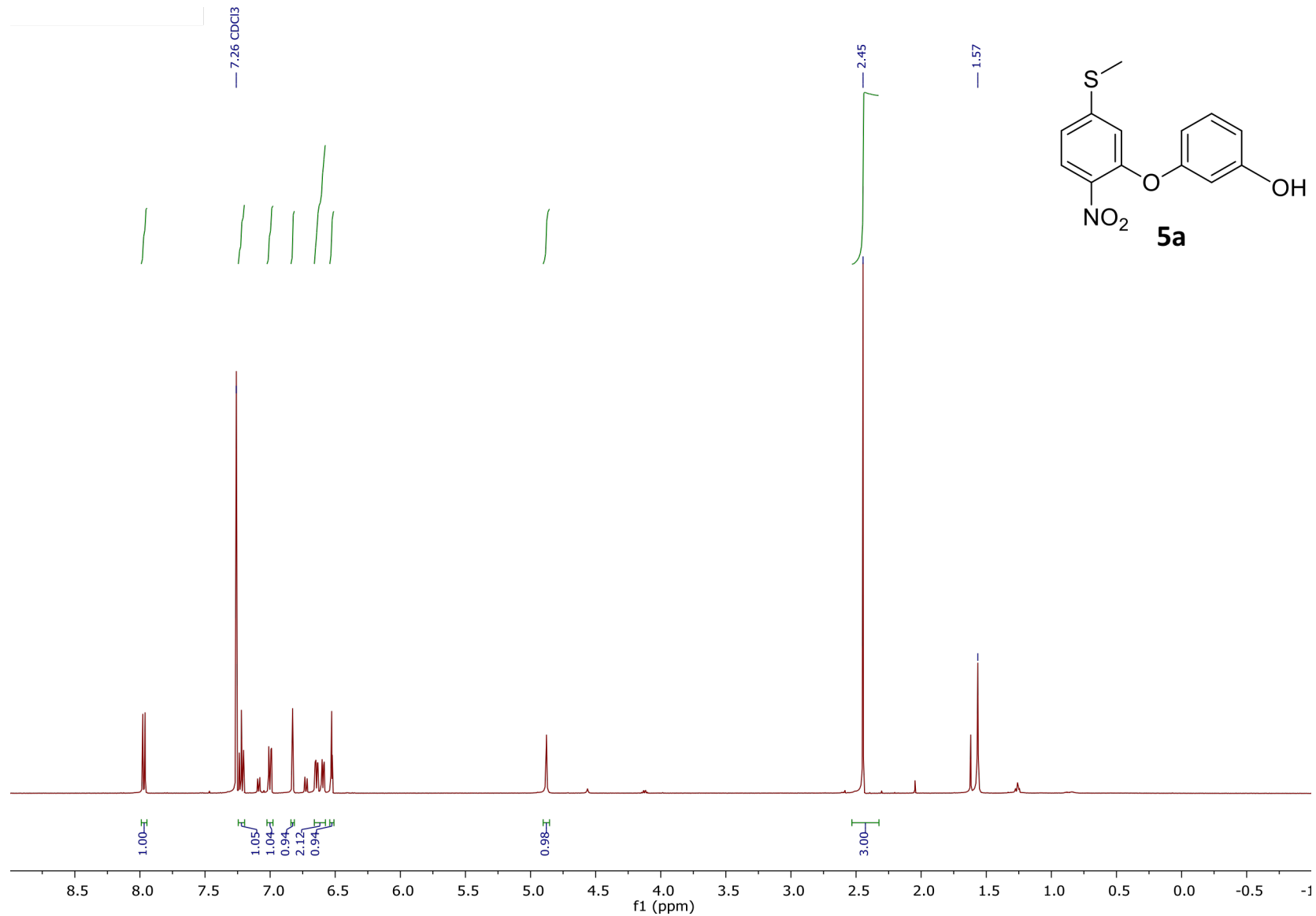


Figure 12. ¹H NMR spectrum of **5a**.

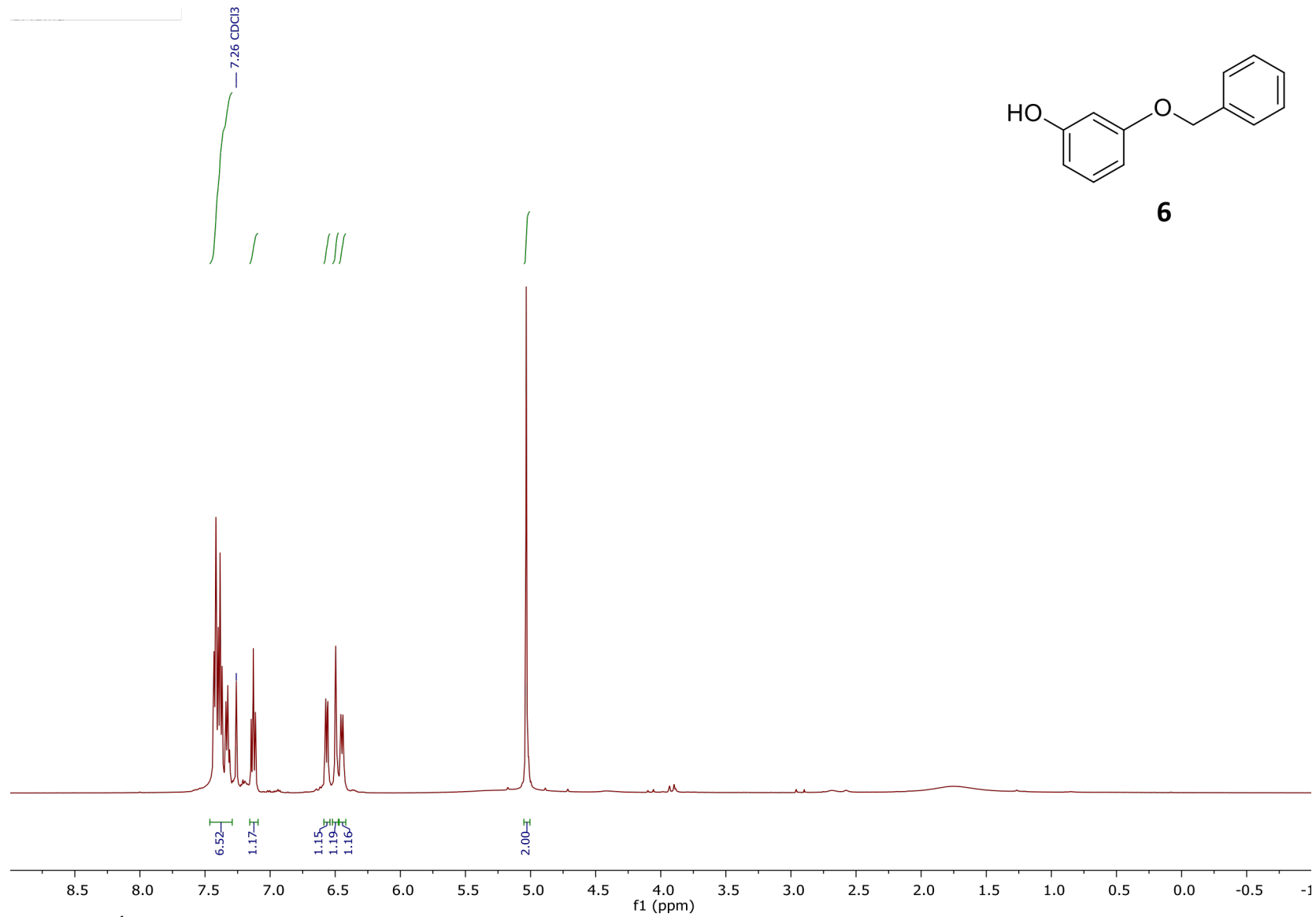


Figure 13. ^1H NMR spectrum of **6**.

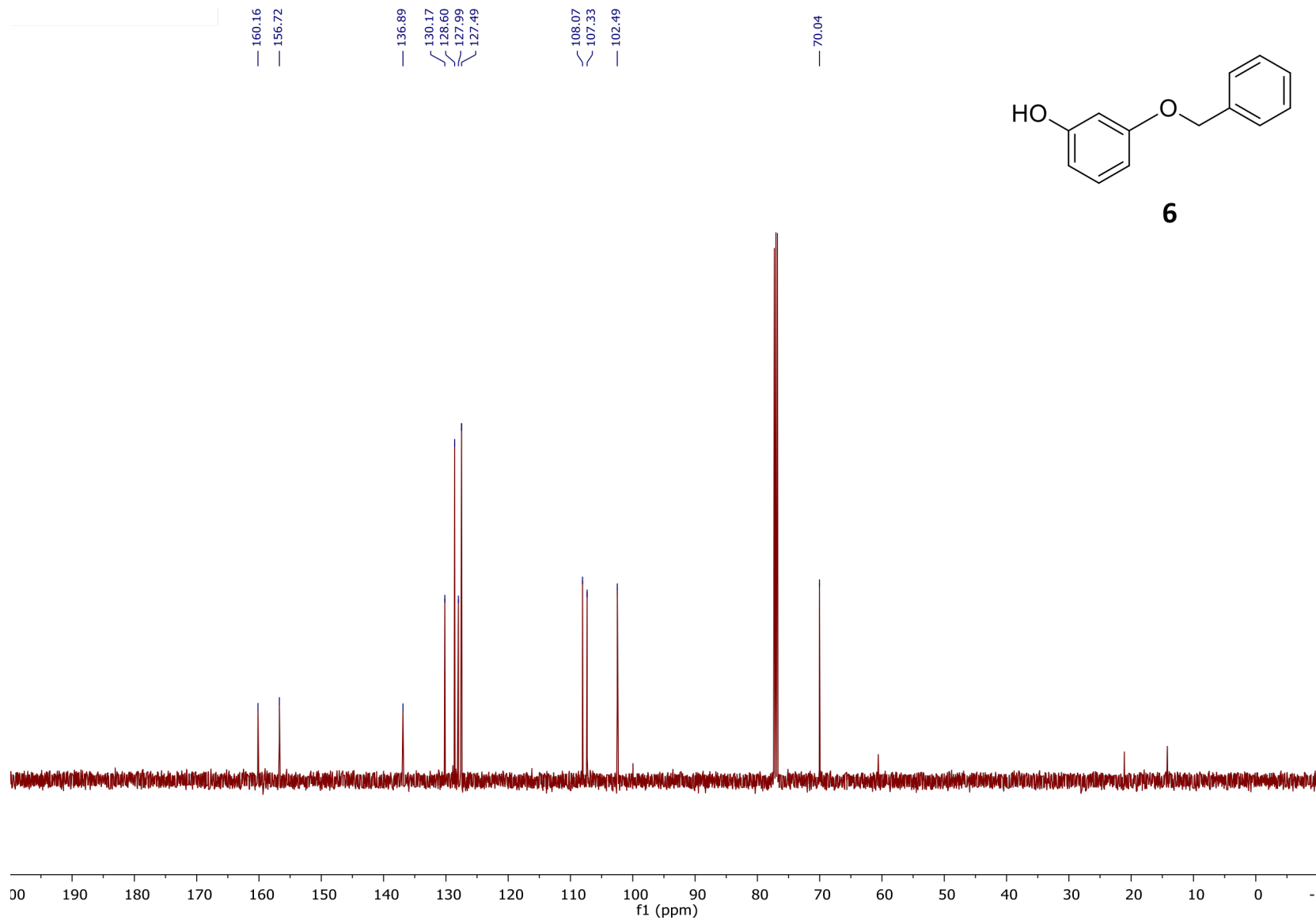


Figure 14. ¹³C NMR spectrum of **6**.

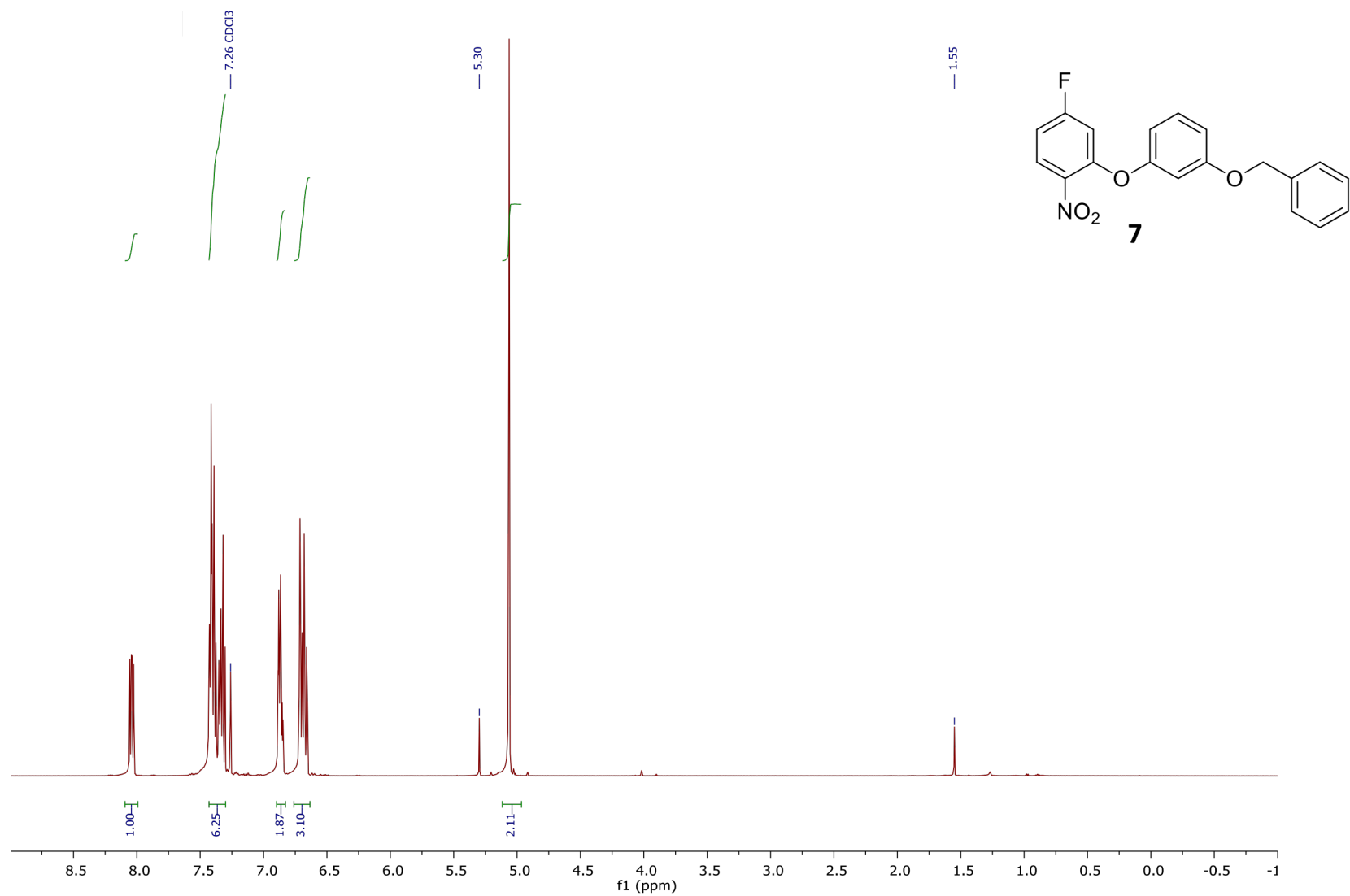


Figure 15. ¹H NMR spectrum of **7**.

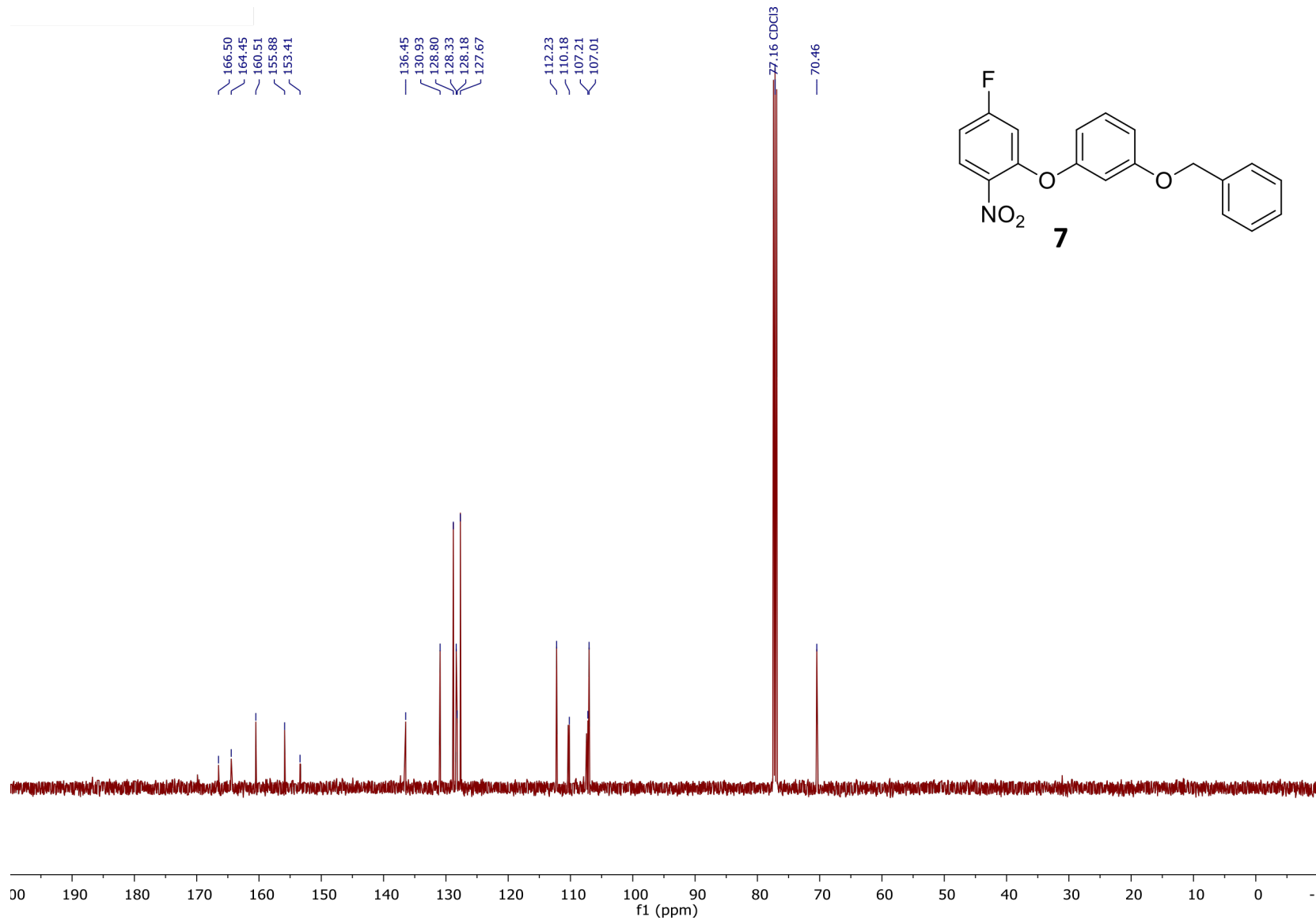


Figure 16. ¹³C NMR spectrum of **7**.

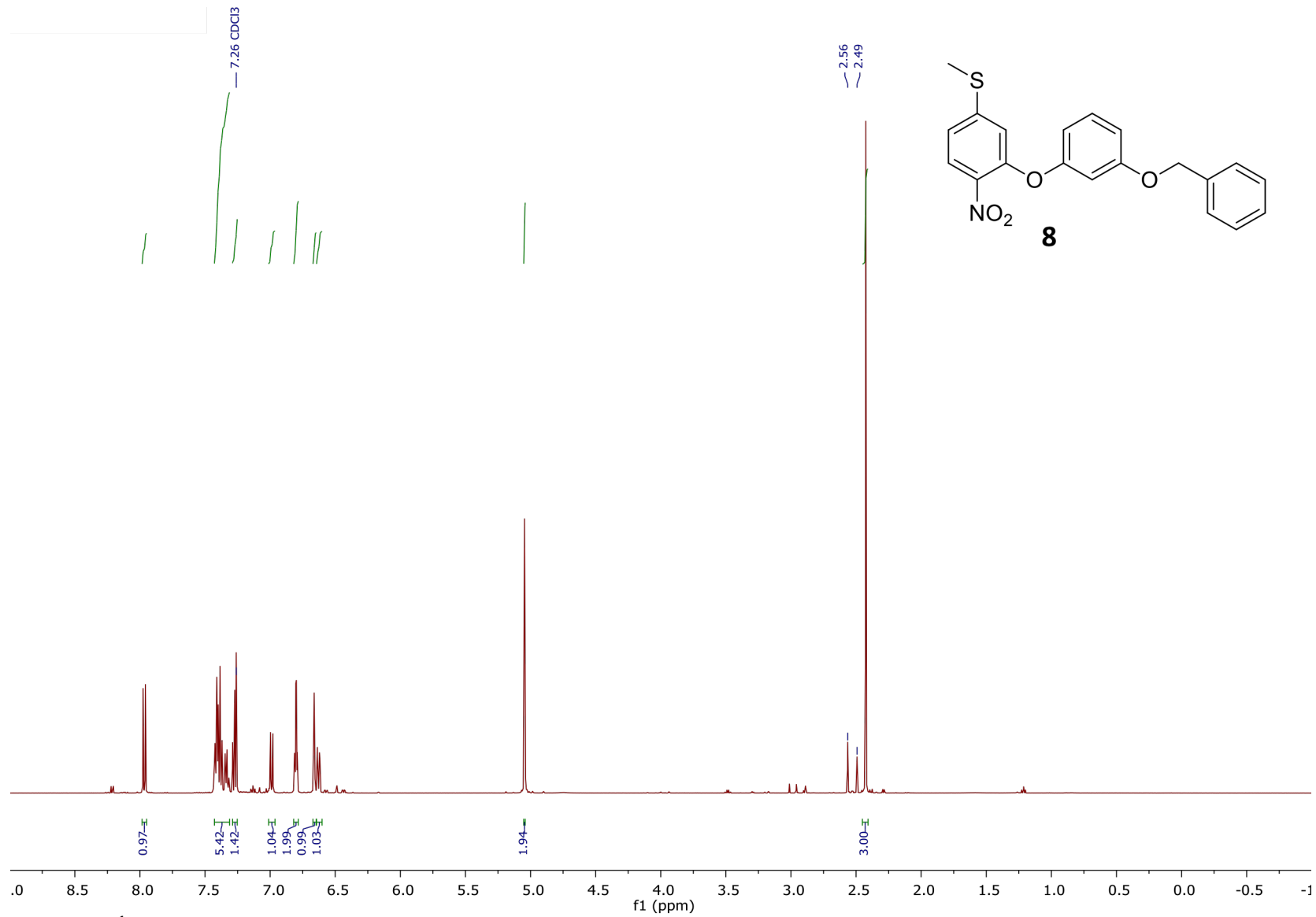


Figure 17. ¹H NMR spectrum of **8**.

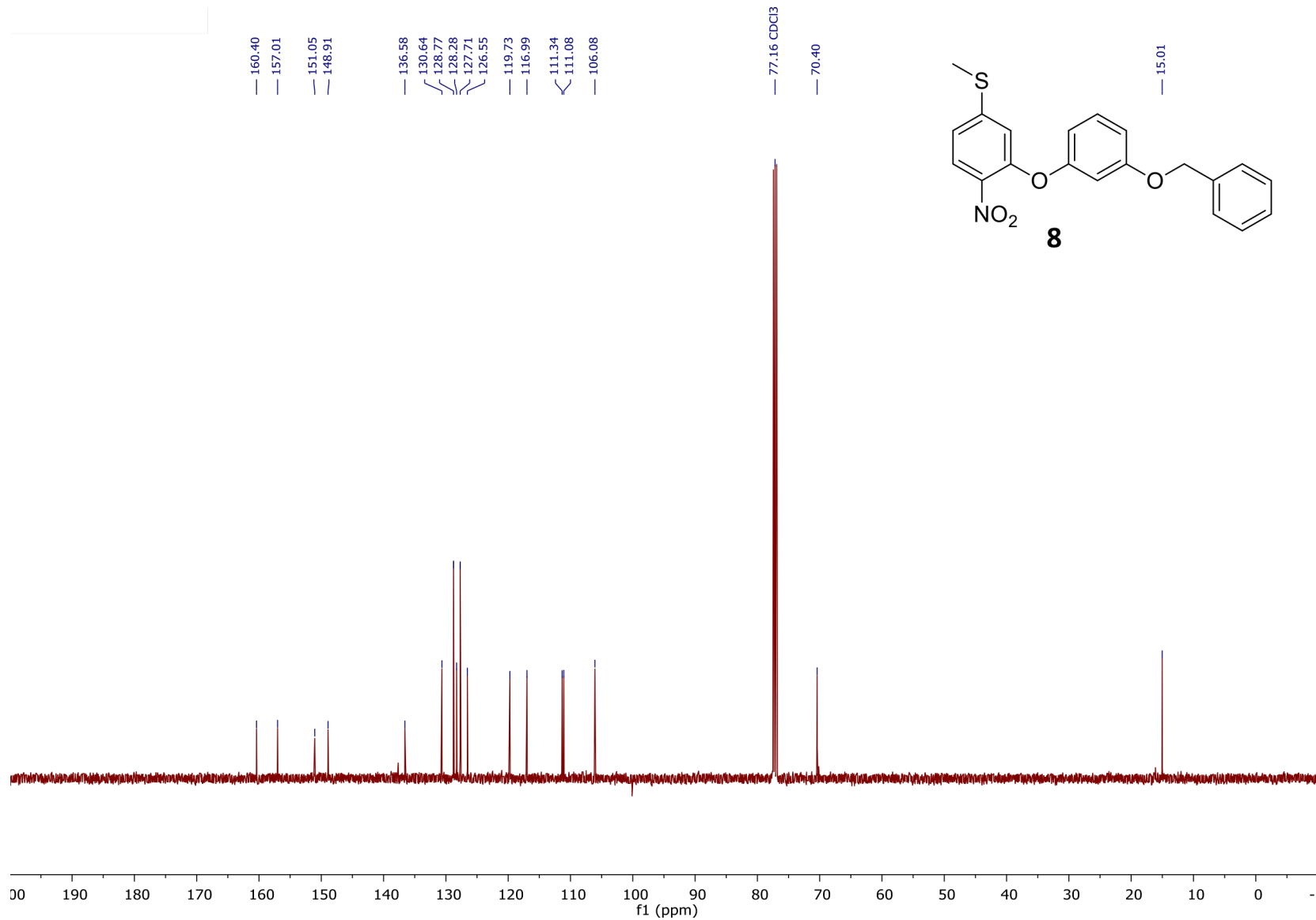


Figure 18. ¹³C NMR spectrum of **8**.

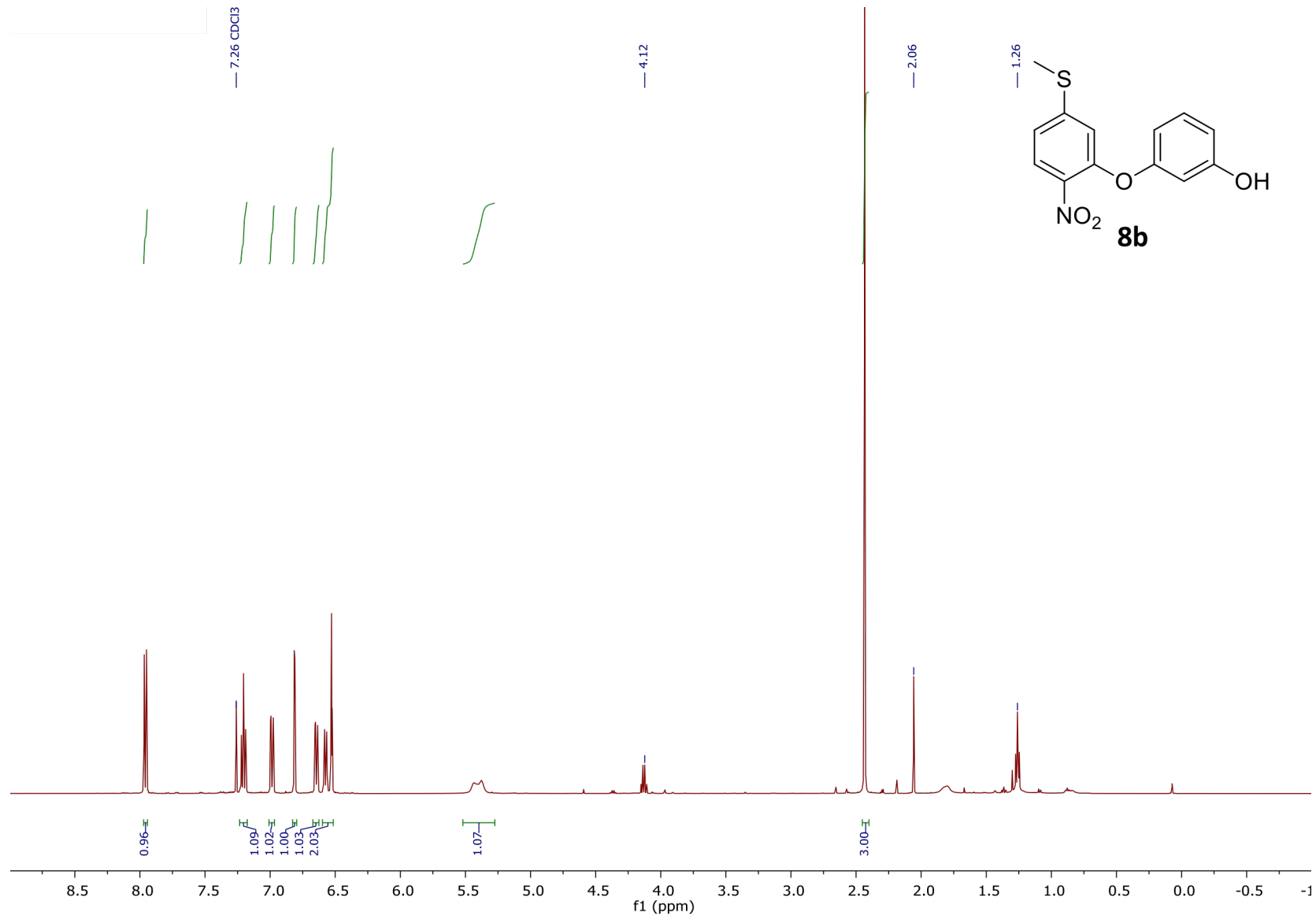


Figure 19. ¹H NMR spectrum of **8b**.

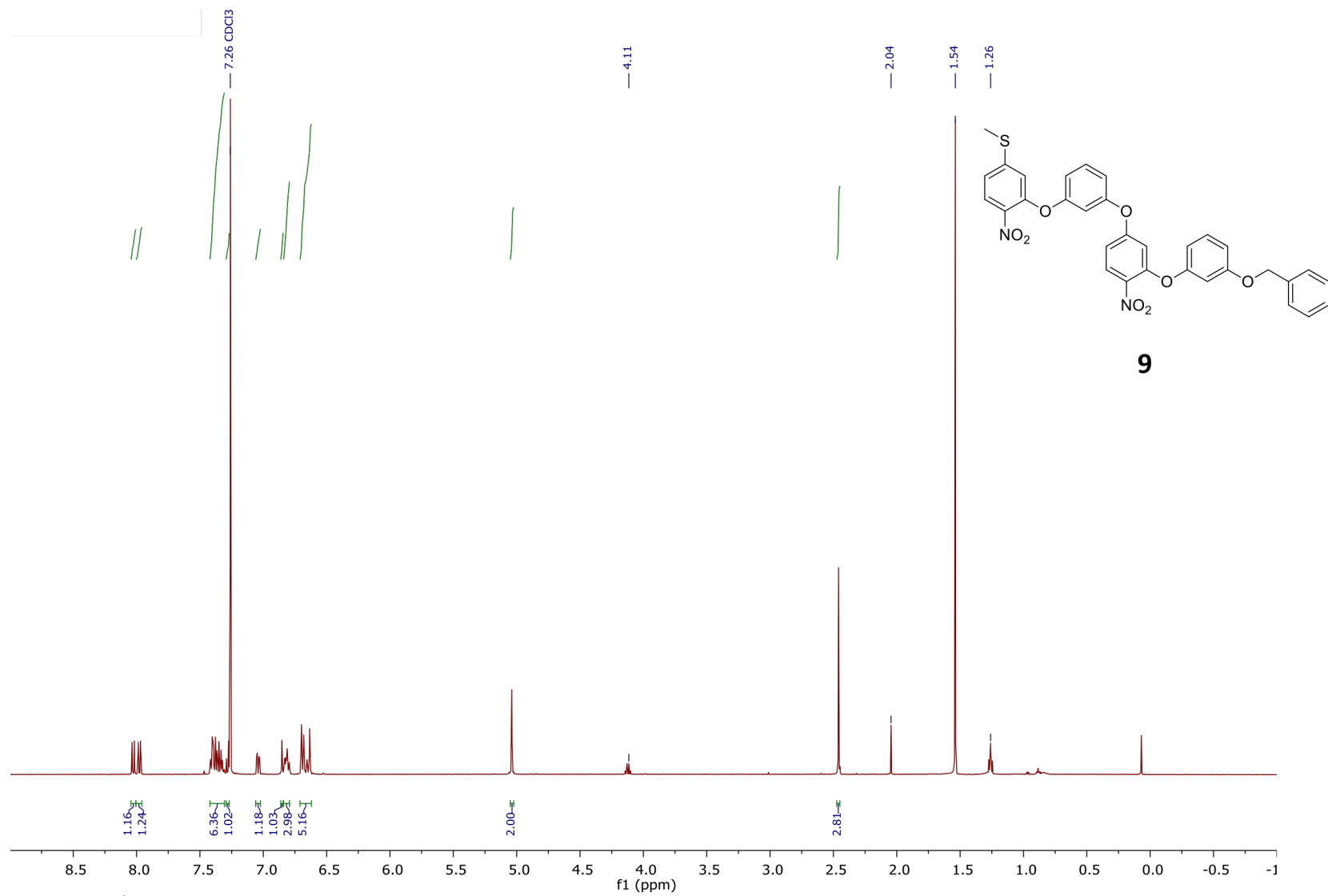


Figure 20. ¹H NMR spectrum of **9**.

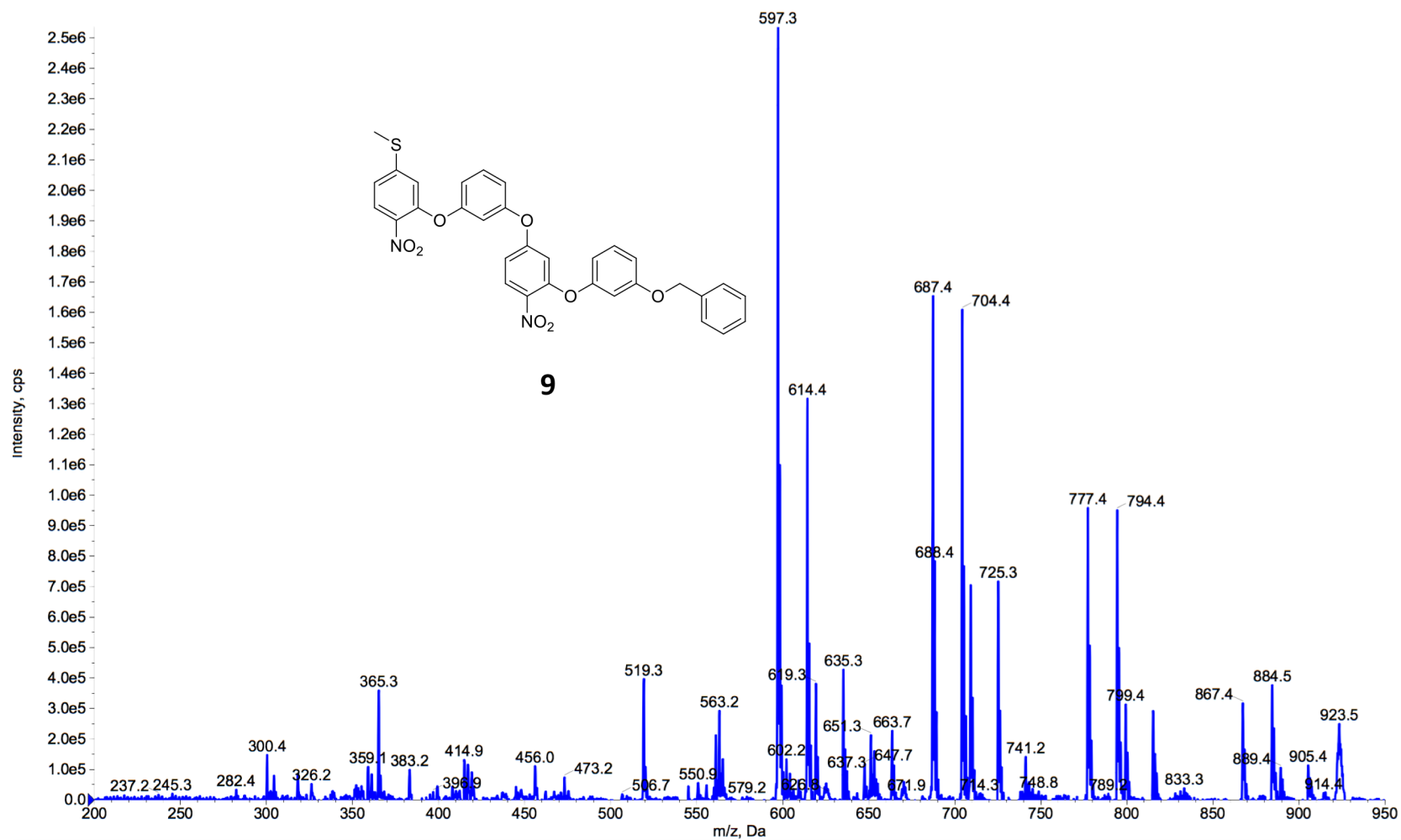


Figure 21. ESI Mass spectrum of 9.

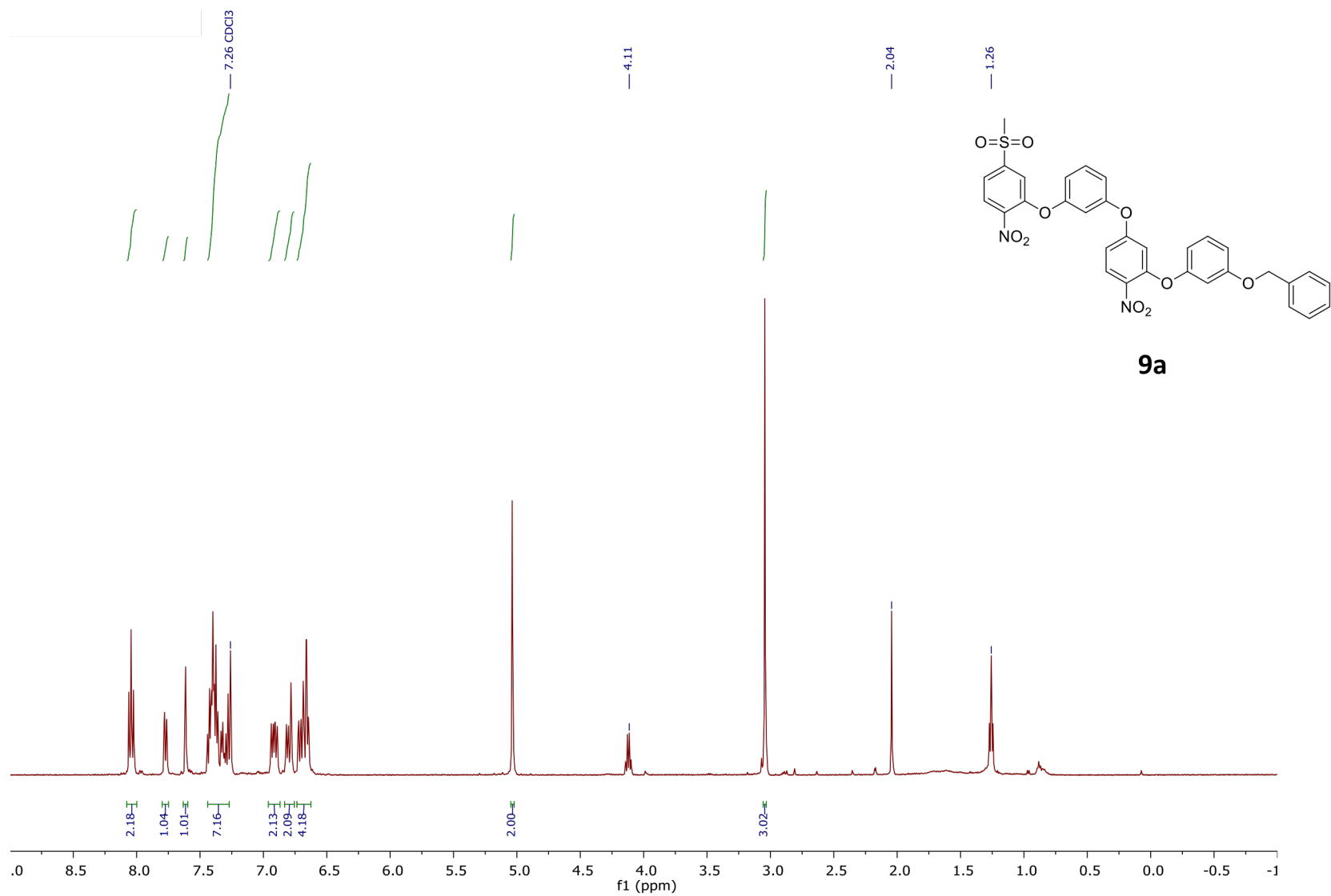


Figure 22. ^1H NMR spectrum of **9a**.

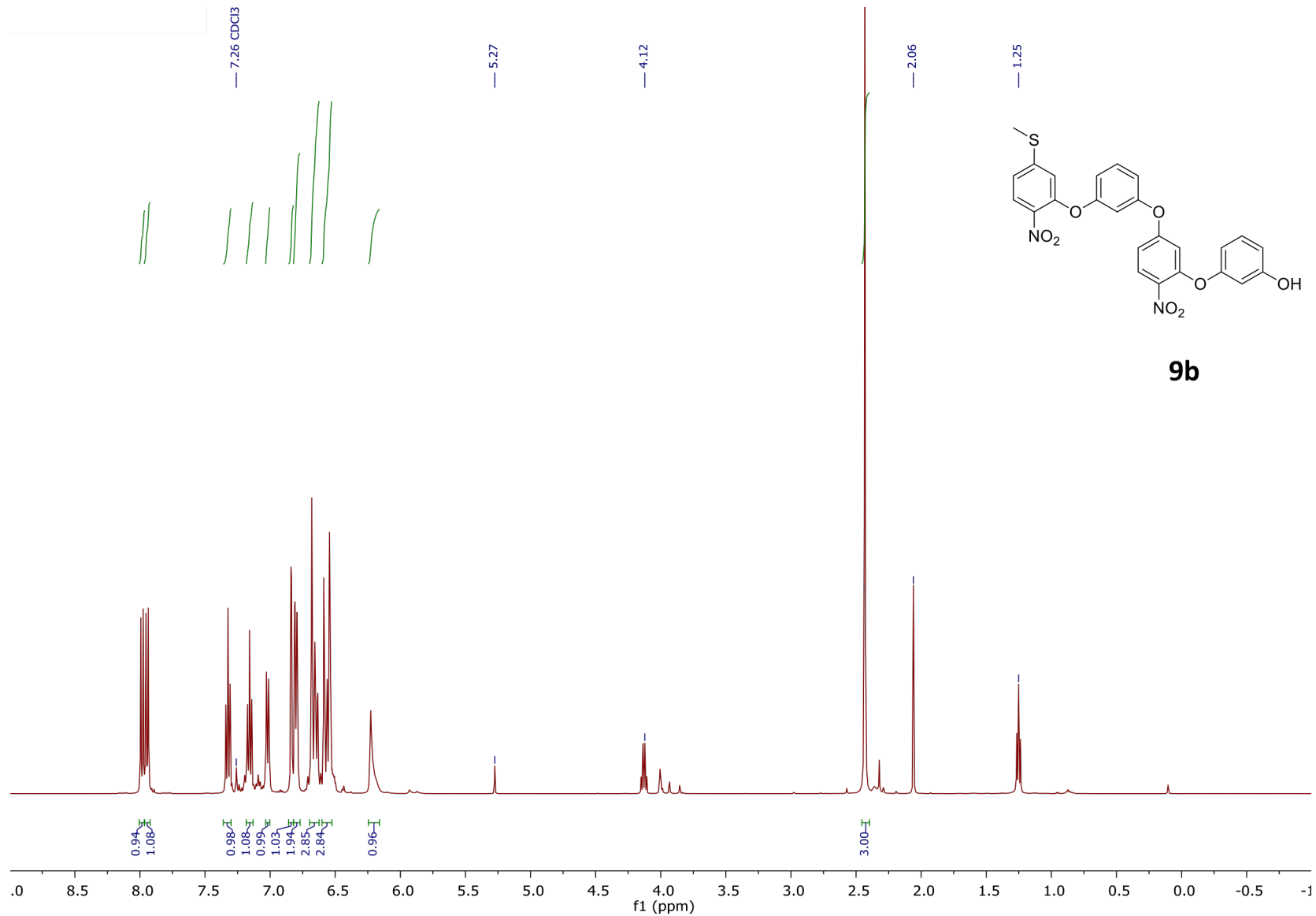


Figure 23. ¹H NMR spectrum of **9b**.

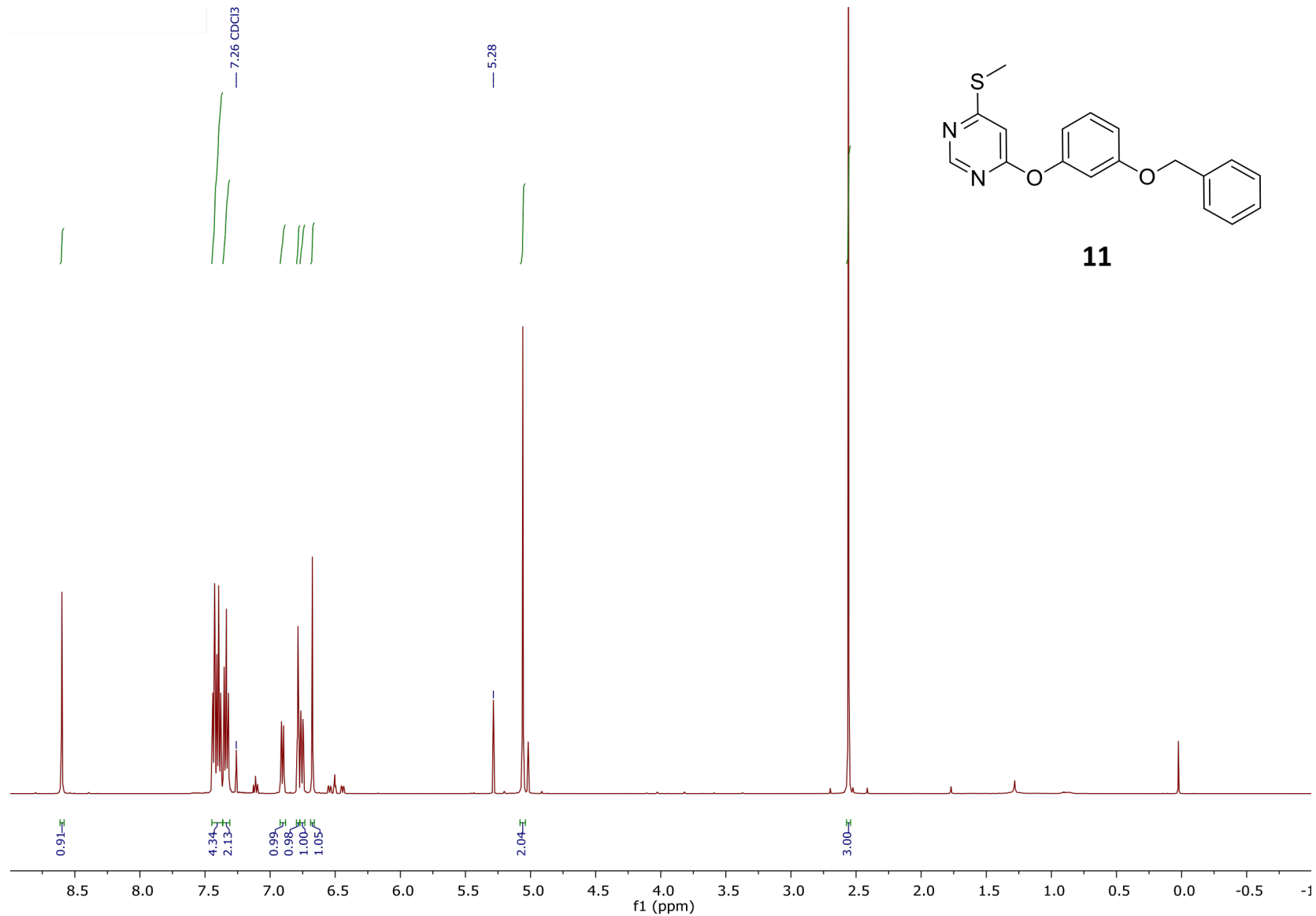


Figure 24. ¹H NMR spectrum of **11**.

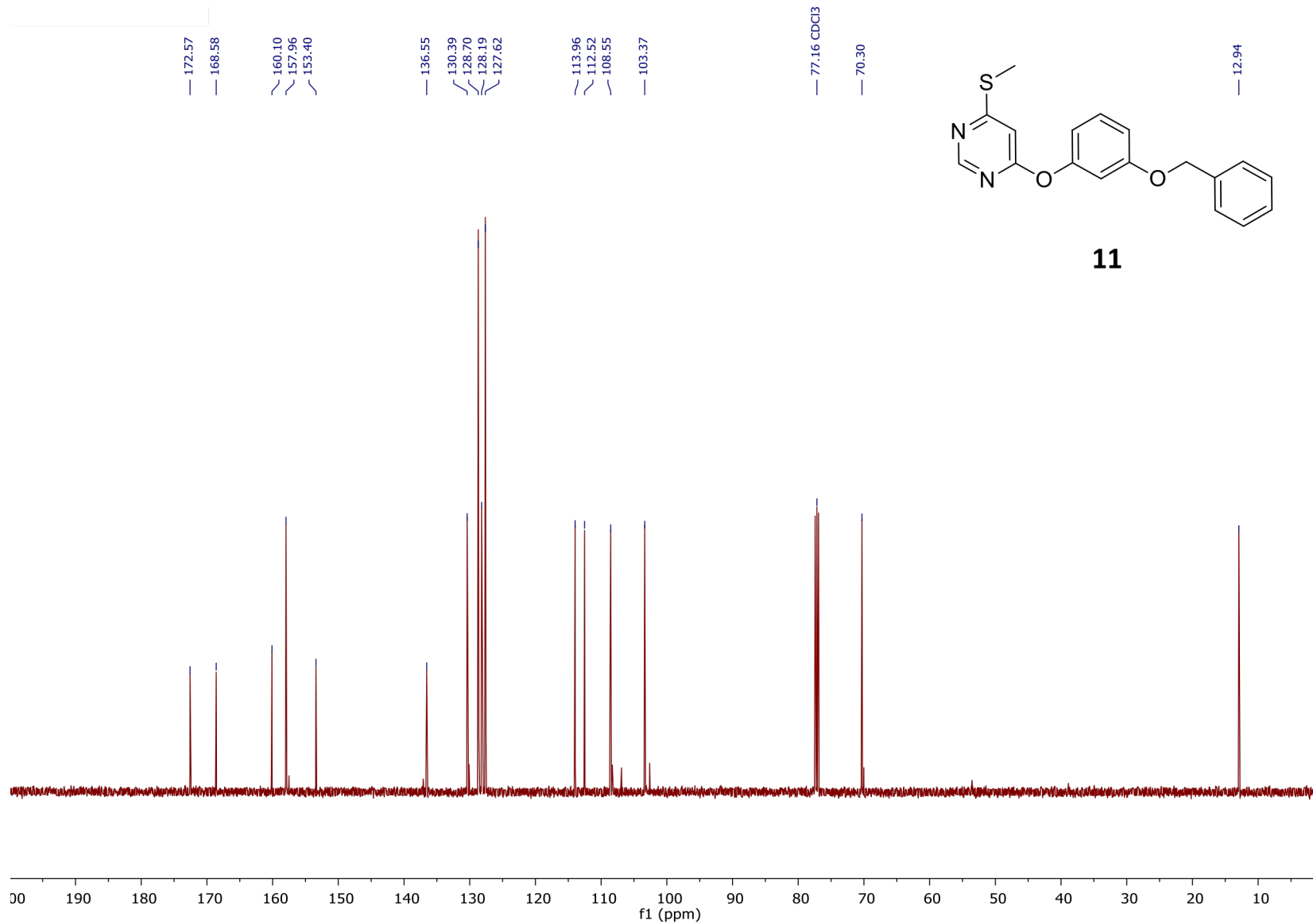


Figure 25. ^{13}C NMR spectrum of **11**.

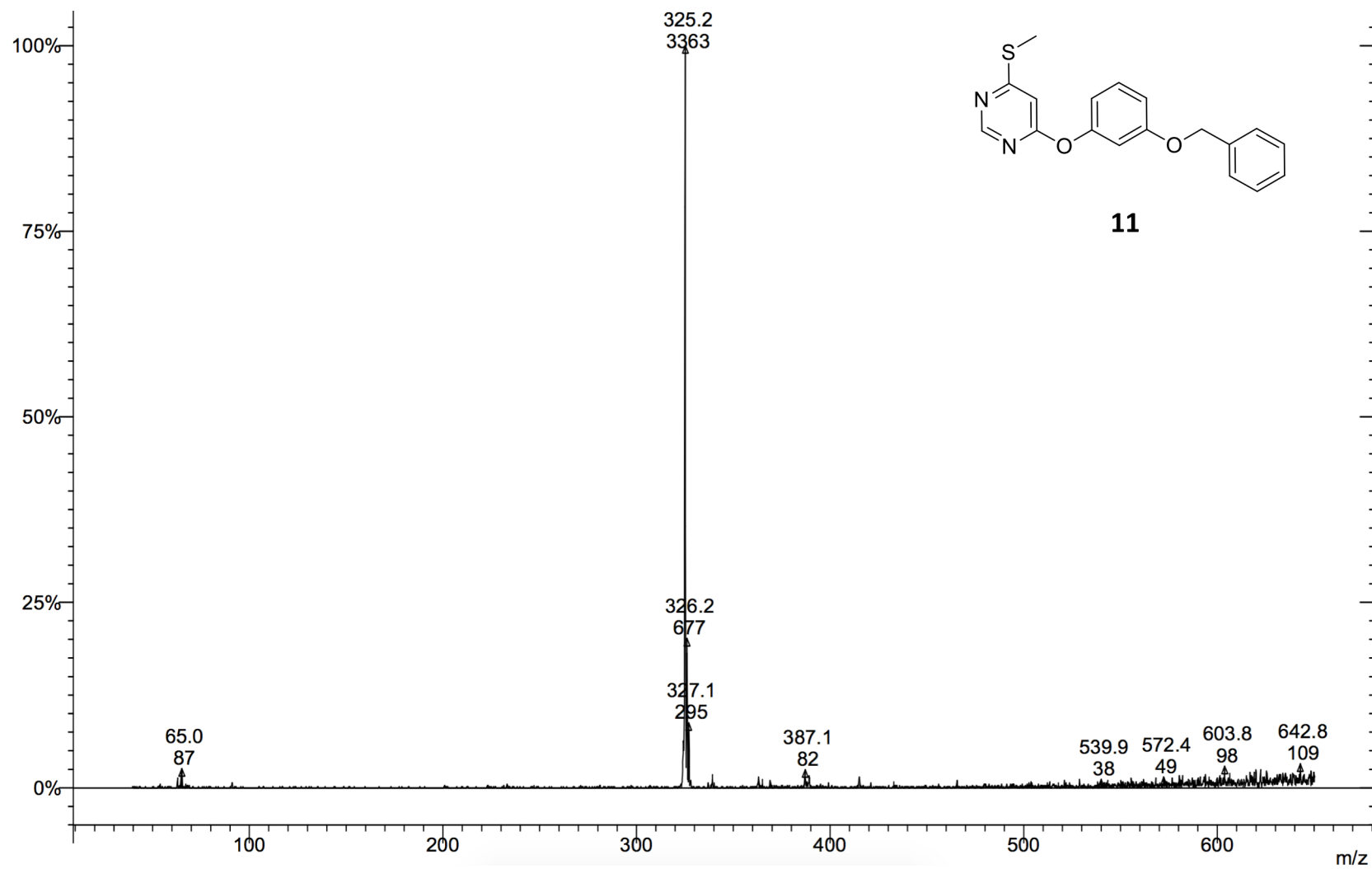


Figure 26. CI Mass spectrum of **11**.

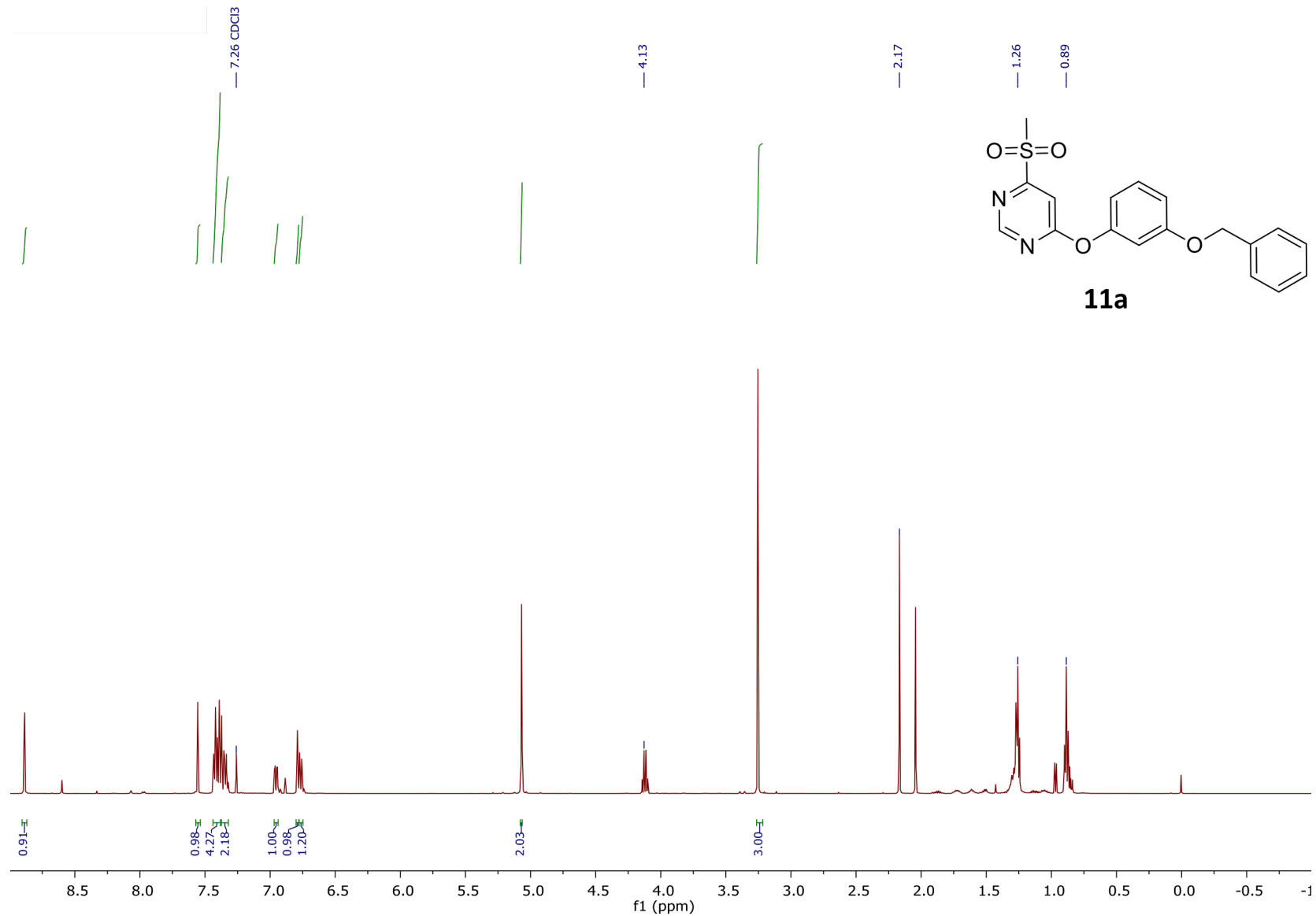


Figure 27. ^1H NMR spectrum of **11a**.

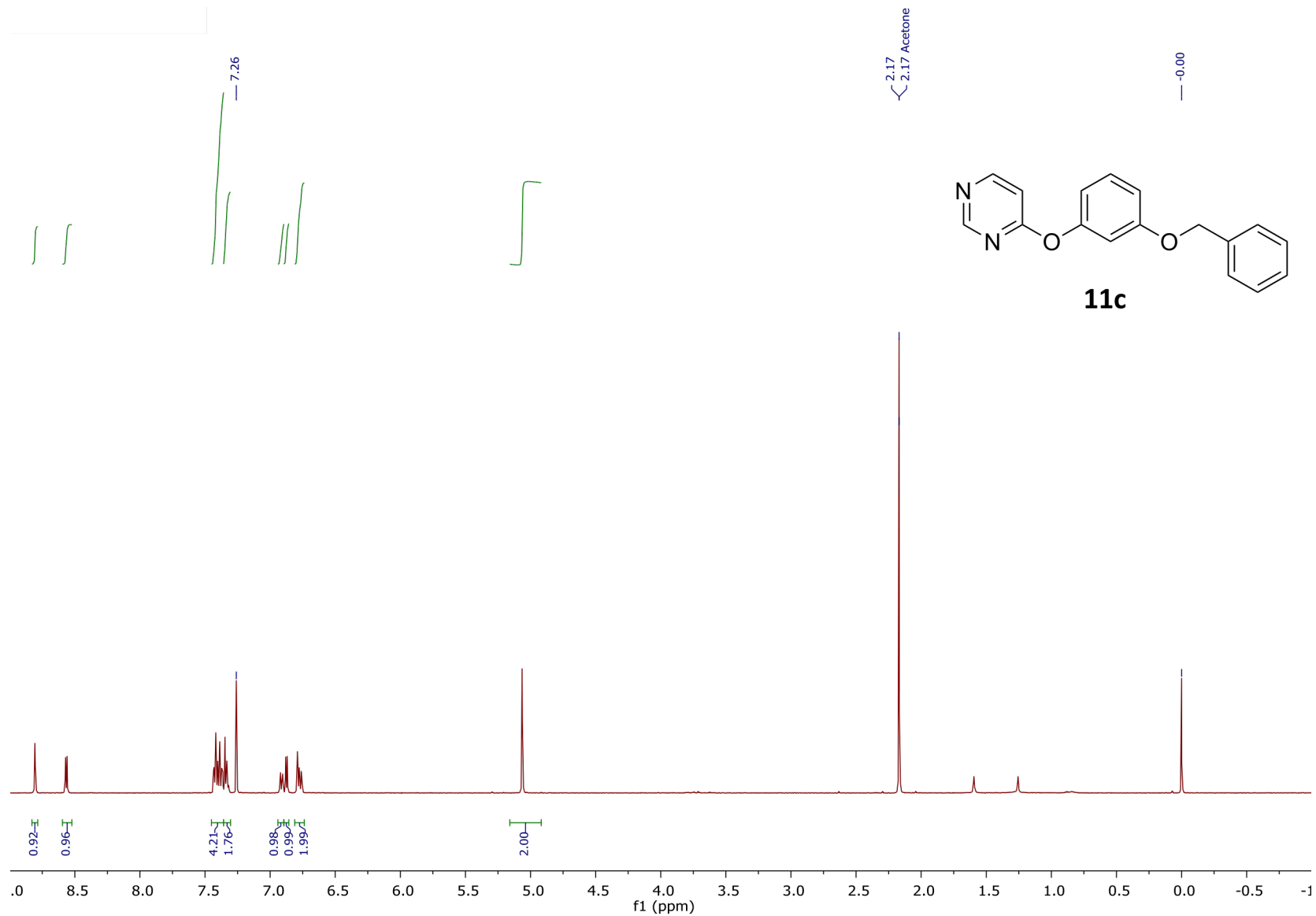


Figure 28. ^1H NMR spectrum of **11c**.

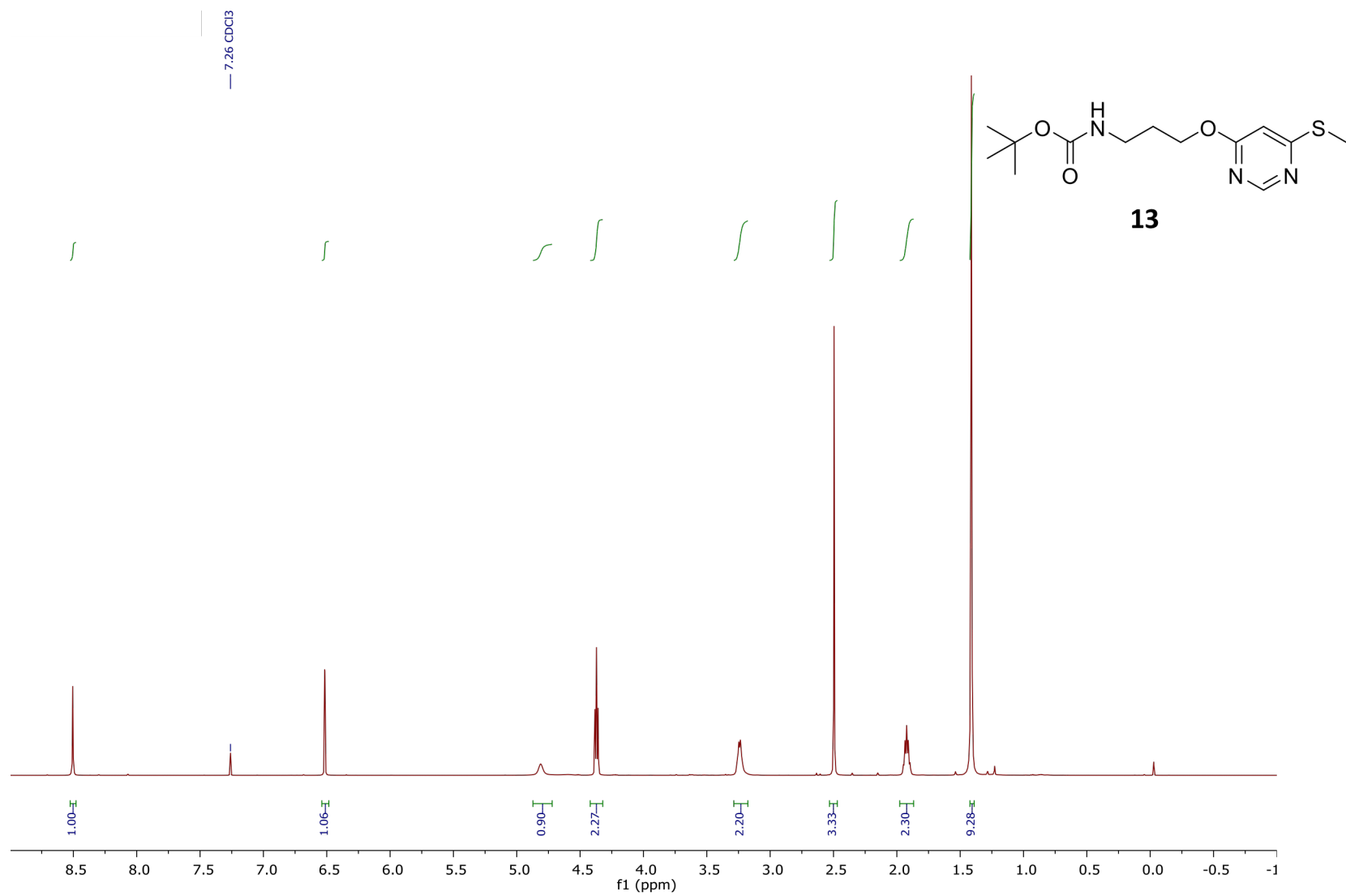


Figure 29. ^1H NMR spectrum of **13**.

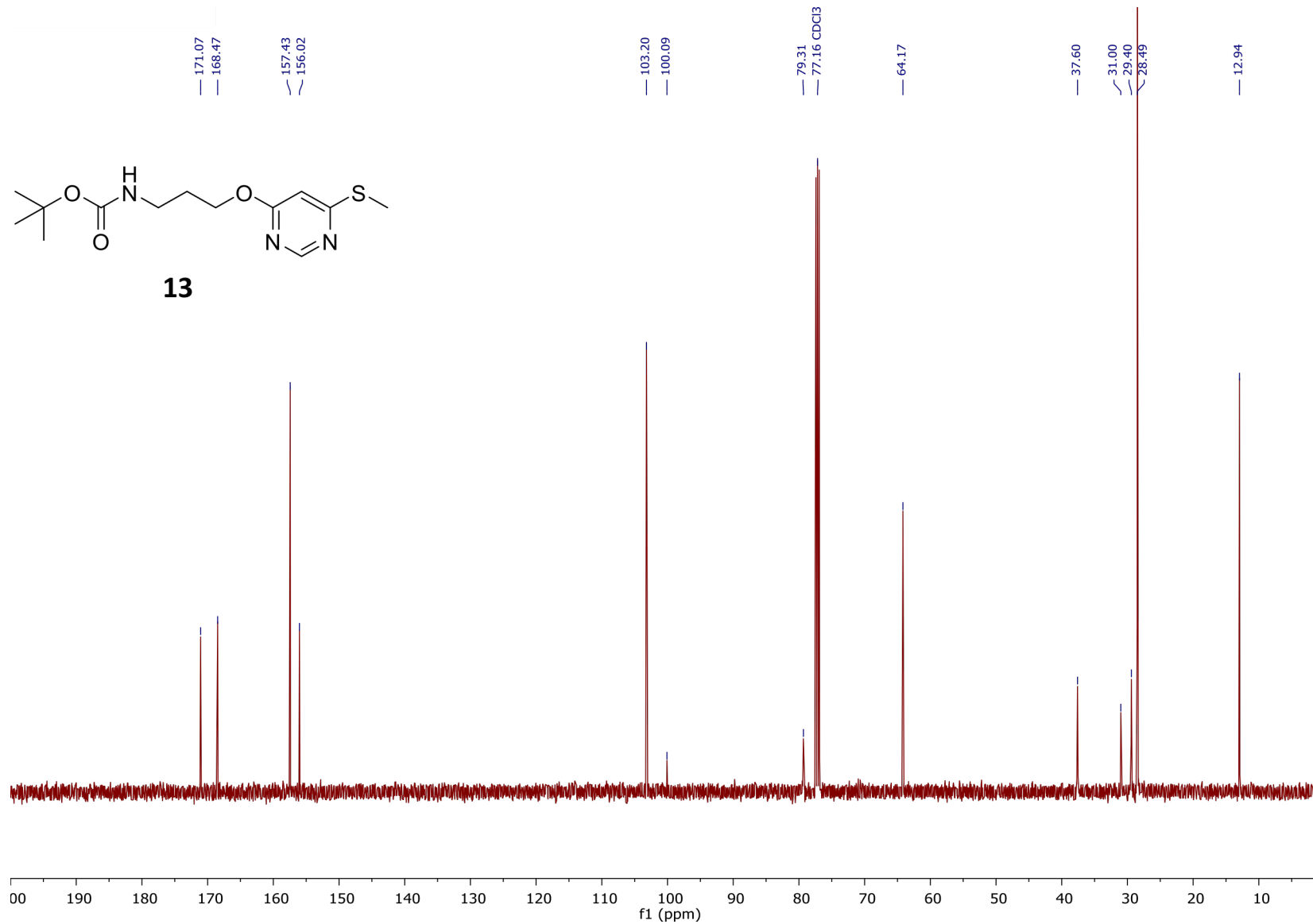


Figure 30. ¹³C NMR spectrum of **13**.

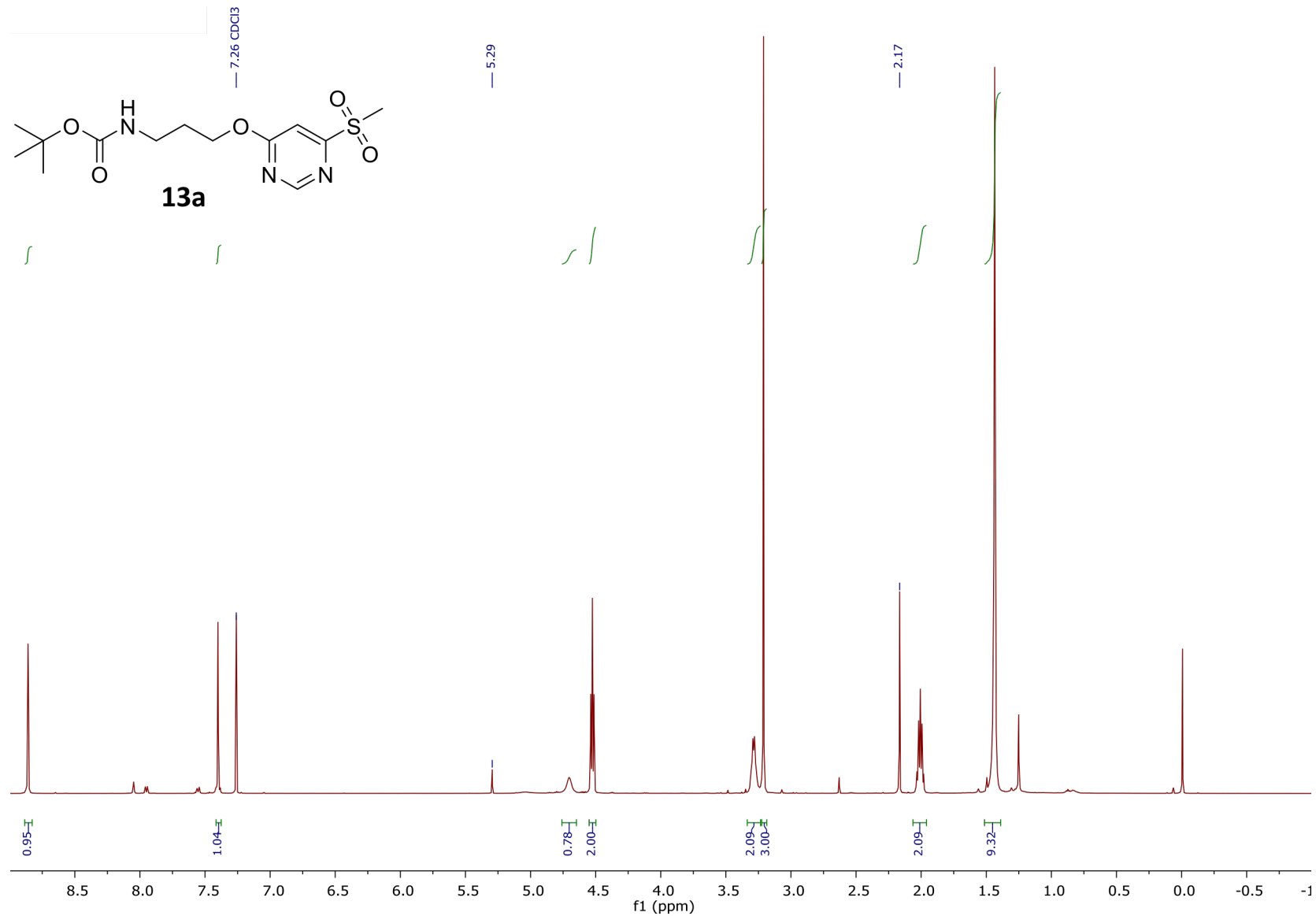


Figure 31. ^1H NMR spectrum of **13a**.

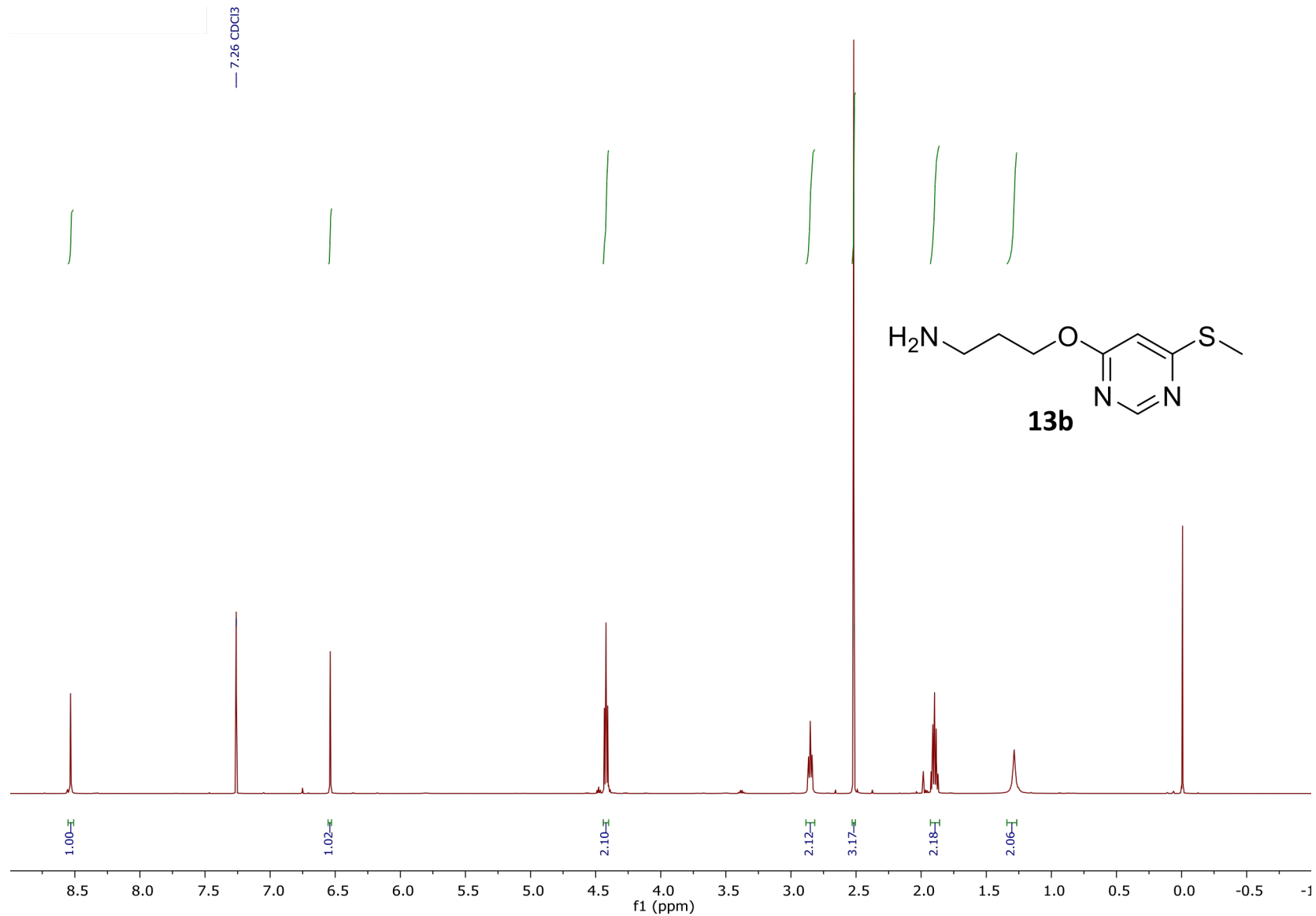


Figure 32. ¹H NMR spectrum of **13b**.

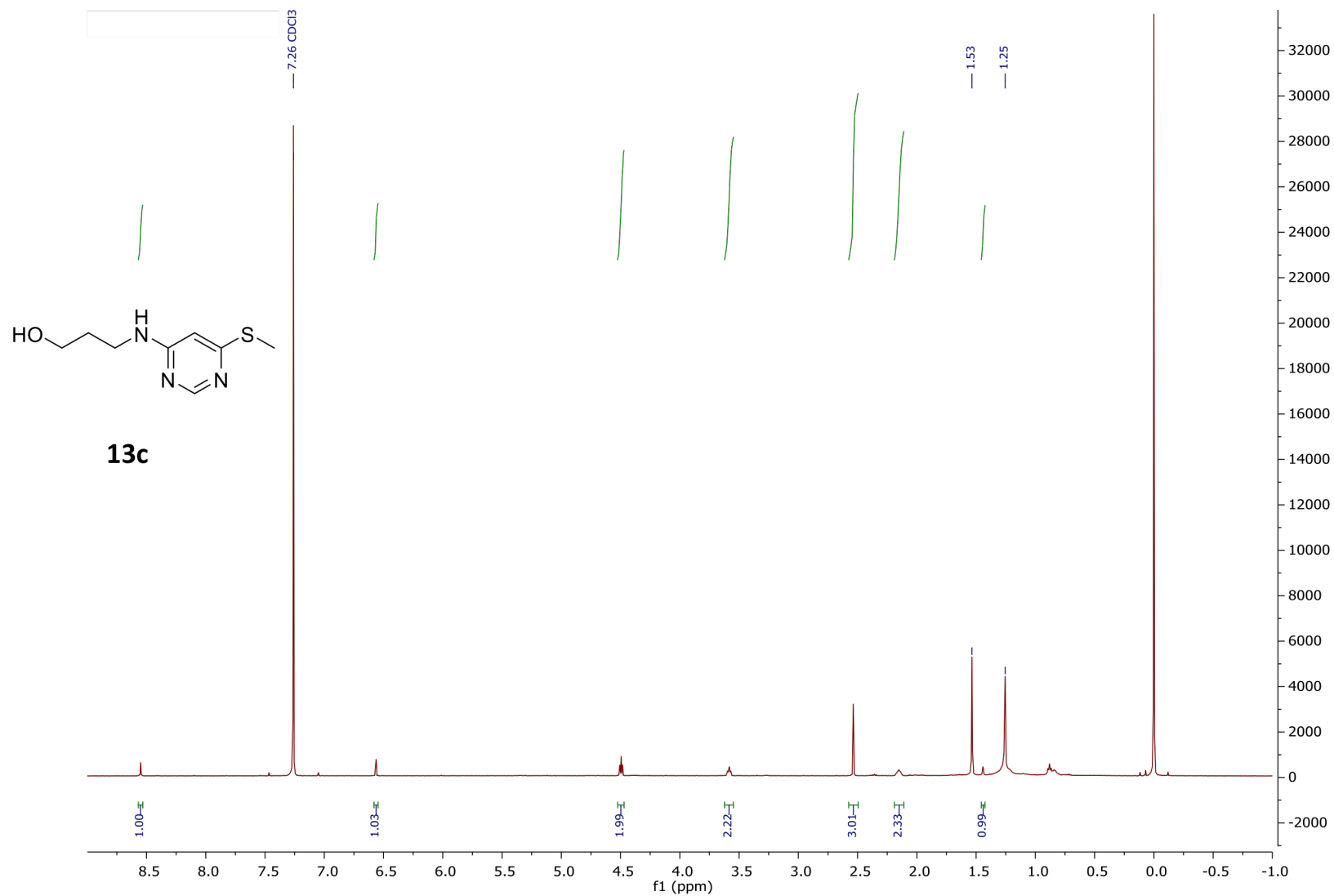


Figure 33. ¹H NMR spectrum of **13c**.

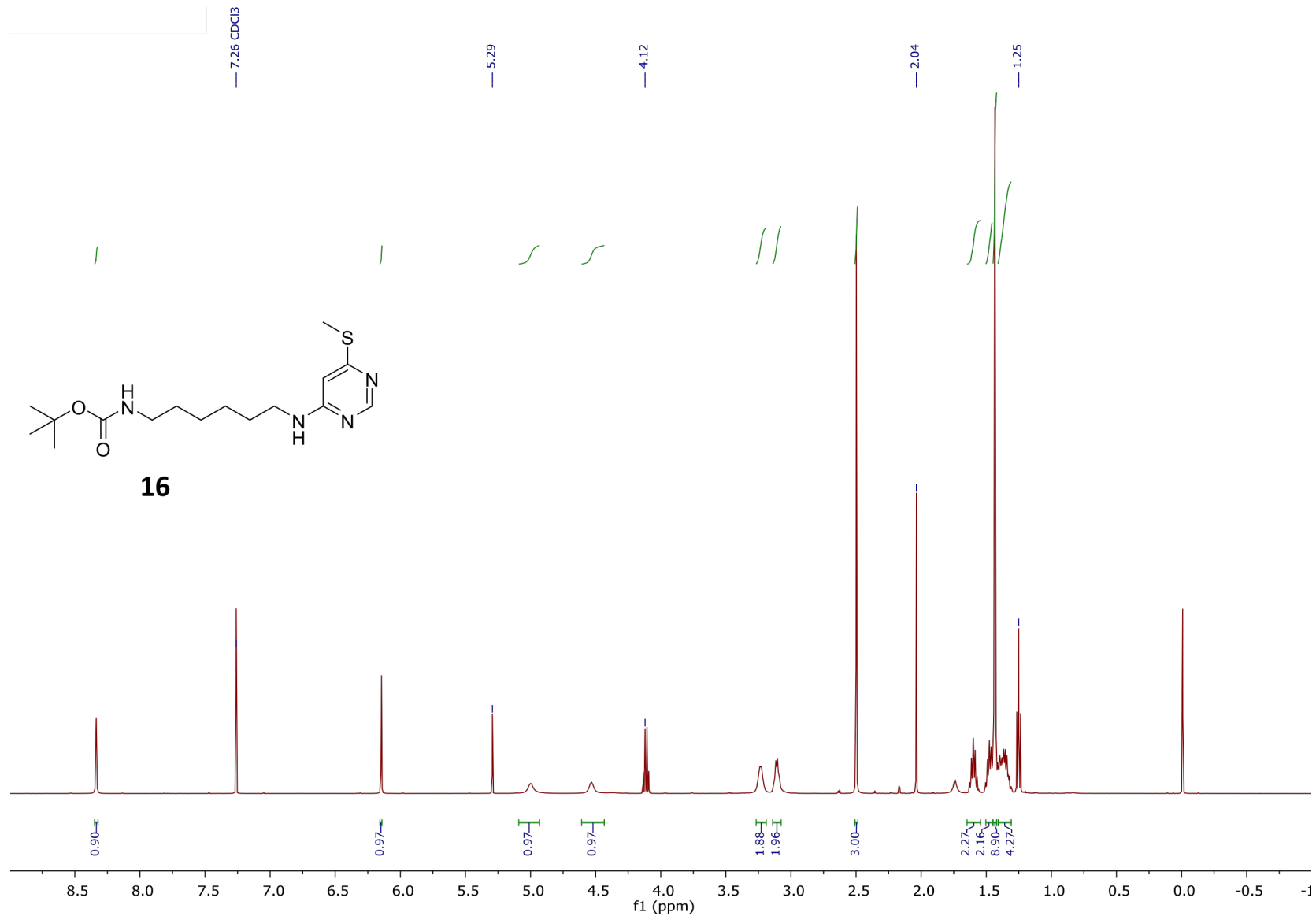


Figure 34. ^1H NMR spectrum of **16**.

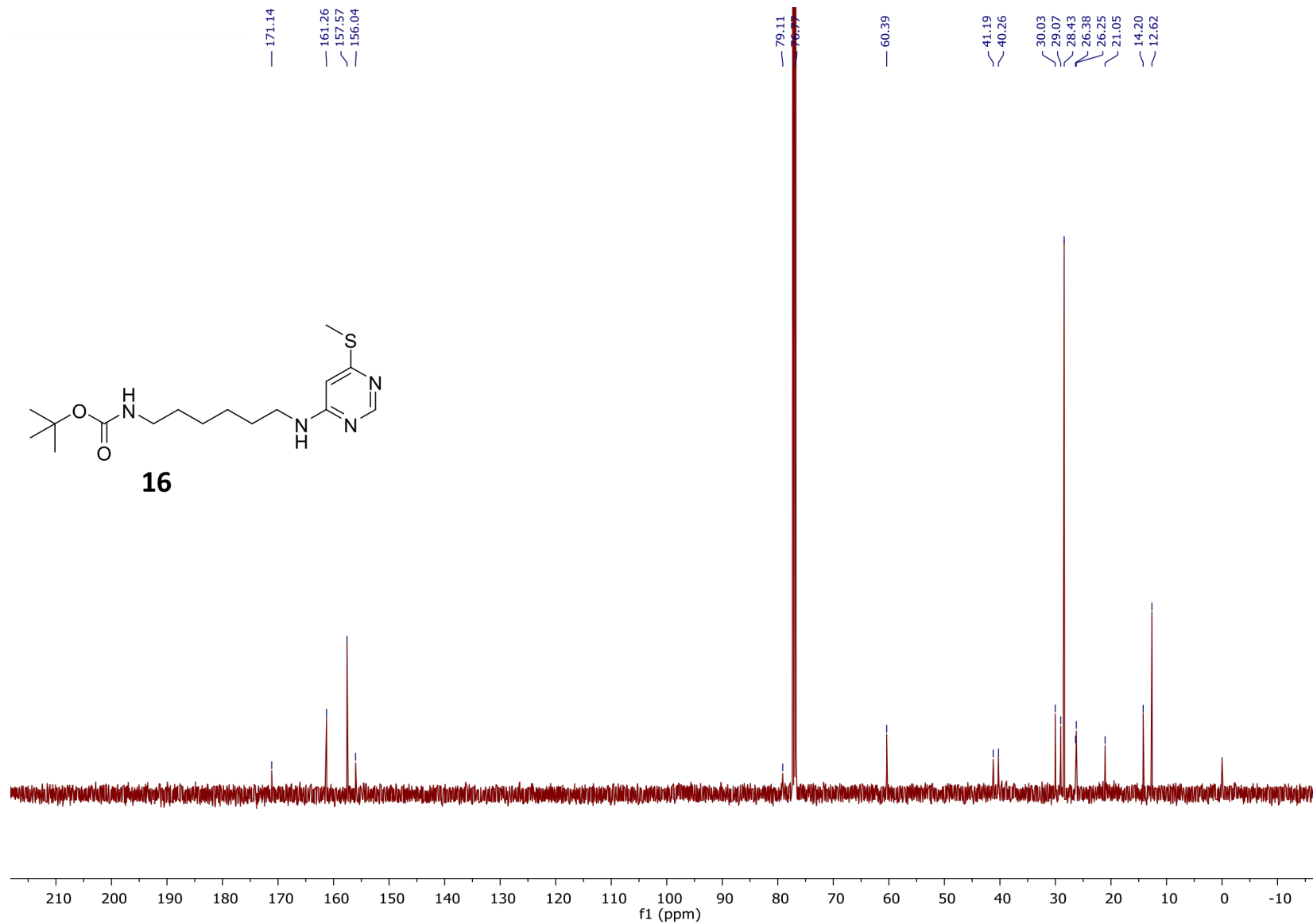


Figure 35. ¹³C NMR spectrum of **16**.

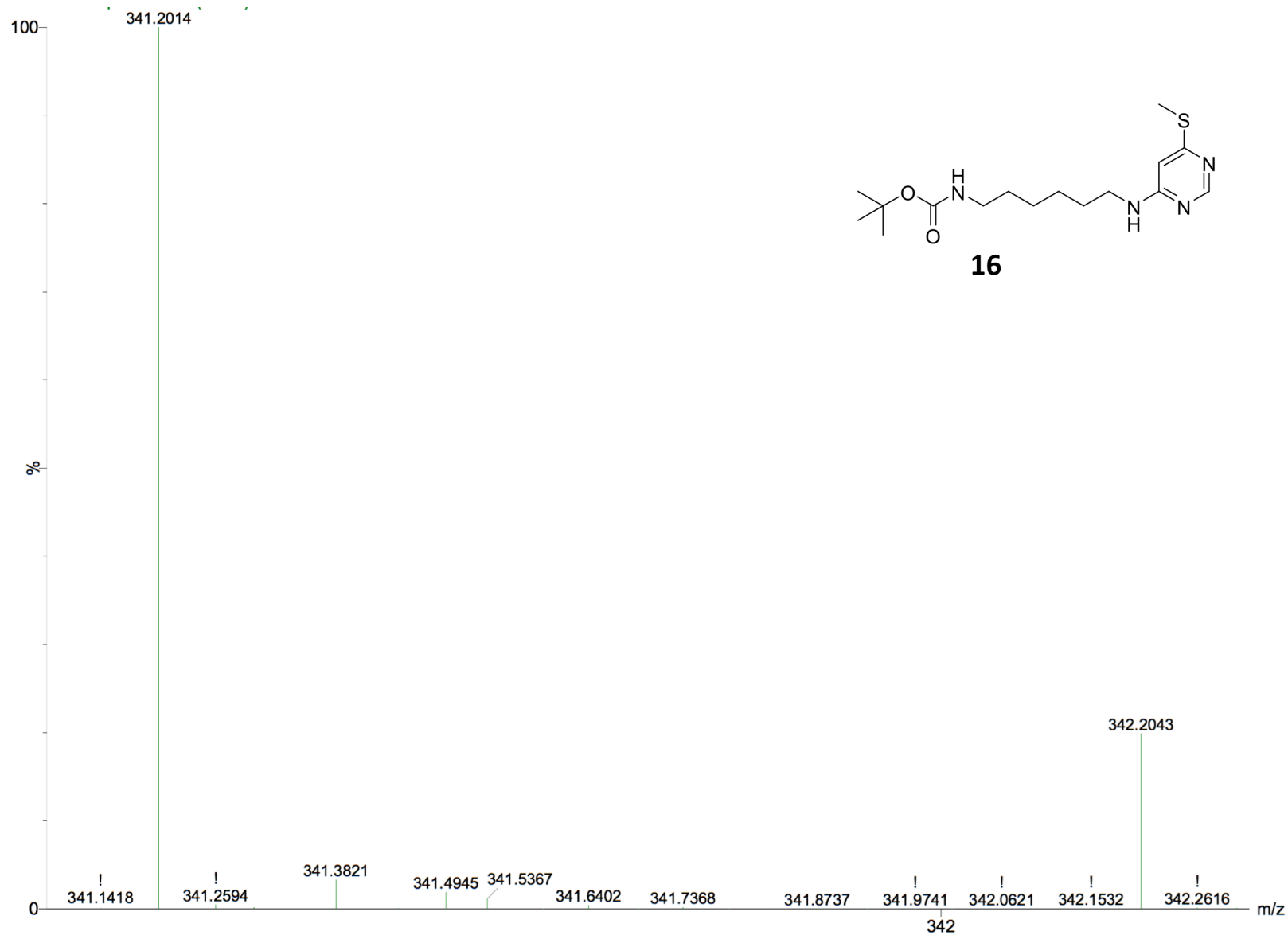


Figure 36. ESI High Resolution Mass spectrum of **16**.

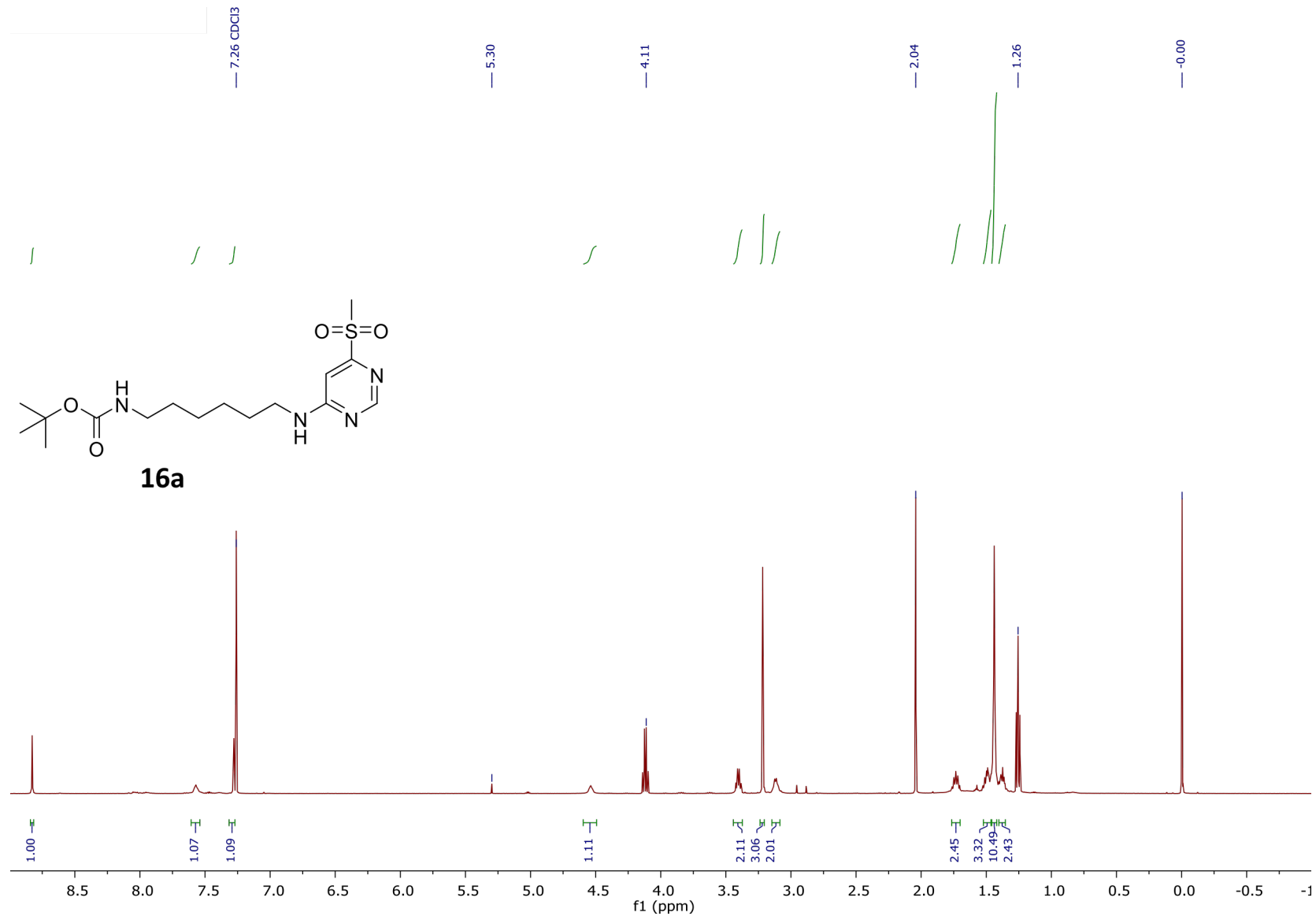


Figure 37. ^1H NMR spectrum of **16a**.